Sulphur metabolism in *Emiliania huxleyi*: Insights from physiological and gene expression studies

Michal Bochenek

A thesis submitted to the School of Environmental Sciences, at the University of East Anglia, for the degree of Doctor of Philosophy, September 2011

Acknowledgements

This page is dedicated to all those who helped me throughout my PhD.

Firstly, I would like to thank my supervisors Gill Malin and Stanislaw Kopriva and my co-supervisor Thomas Bell for the chance I was given to do the project presented here. I sincerely thank them for their enthusiasm while discussing the results and planning new experiments. Also for their continuous support whenever I needed it.

I would like to acknowledge all present and former members of the Malin and Kopriva groups for their help and for creating a great and productive atmosphere in the labs. My very special thanks go to Anna Koprivova (JIC) for introducing me to various molecular approaches and giving me practical advice. Many thanks also to Gareth Lee and Rob Utting (UEA) for their great technical support.

Thanks to everyone in the office for sharing time with me, for company and support over the years and especially for great help I received in the last few days of this thesis.

I cannot finish this acknowledgments page without mentioning Maciek Telszewski and his family. We have crossed paths many times and I hope we will still in the future.

Finally, I want to acknowledge my parents:

Kochani Mamo i Tato, dzięki wam napisałem tę pracę i wam chciałbym ją zadedykować. Dziękuję Wam za wasze ogromne wsparcie przez te ostatnie lata i wiarę w to co robię. Dziękuję również, że mam dom, do kórego zawsze mogę wracać.

The Zuckerman found provided the financial support for this work

Abstract

Sulphur is essential for all living organisms and often a limiting nutrient for the growth of terrestrial plants and freshwater algae, therefore the response to sulphate deficiency has been broadly analysed in these organisms by system biology approaches. On the other hand, with a concentration of 28 mM in today's ocean, sulphate does not limit the growth of marine phytoplankton. Moreover, high sulphate abundance in seawater promotes the biosynthesis of dimethylsulphoniopropionate (DMSP), a unique sulphur compound with implications for plankton biology and ecology, environmental function and the global sulphur cycle. Unfortunately, little is known about the regulation of sulphate uptake and assimilation by marine phytoplankton species. In an effort to advance knowledge of metabolic sulphur pathways in the marine microalgae, this thesis aimed to investigate how sulphate availability regulates physiological, biochemical and molecular changes in the coccolithophore *Emiliania huxleyi* CCMP 1516.

Algal cultures were subjected to artificial variations in ambient sulphur concentration and physiological and biochemical responses were assessed. Next, the global transcriptome response of *E. huxleyi* CCMP 1516 to limited sulphate supply was analysed by RNA sequencing.

Cell abundance and intracellular DMSP concentration decreased with 5 mM sulphate compared to 25 mM controls. Comparative experiments with *E. huxleyi* CCMP 1516, 370 and 373 showed that the magnitude of this response varied amongst strains. Growth and DMSP synthesis were enhanced when sulphur-limited cultures were replenished with sulphate. Low sulphate medium stimulated sulphate uptake and decreased glutathione concentration, but did not affect adenosine 5'-phosphosulphate reductase (APR) activity. Transcriptome data showed 8222 genes were altered in expression, the vast majority up-regulated. Sulphate deficiency induced genes involved in carbohydrate and lipid metabolism, whereas genes involved in amino acid metabolism were frequently down-regulated.

The sulphate deficiency response in *E. huxleyi* shows some similarities to the well described responses of *Arabidopsis* and *Chlamydomonas* but also has many unique features. This dataset allows comparison of the response to sulphate deficiency over a large evolutionary distance and shows that even though *E. huxleyi* is adapted to high sulphate concentration and it retains the ability to re-program its gene expression in response to these conditions.

Contents

List of Figures

List of Tables

Table 1C Table 1C. Summary of the top 100 most up-regulated transcripts in S-limited *Arabidopsis thaliana* with the best BLASTP hits (E-value cutoff of 1E-5) in *Emiliania huxleyi* and *Chlamydomonas reinhardtii* E-value (expectation value) reflecting the number of hits expected to be found by chance. Transcripts induced in all three species are highlighted in bold font. 133

1. Introduction

1.1. The sulphur cycle, climate and marine plankton

1.1.1. Sulphur cycle

The definition of a biogeochemical cycle is the transport and a transformation of matter through all four components of the Earth system: atmosphere, hydrosphere, lithosphere and biosphere. One of the principal global nutrient cycles is that for the element sulphur (S). Figure 1.1 shows the simplified biogeochemical cycle of sulphur; sulphur occurs in a variety oxidation states, ranging from +6 to -2 and as a very reactive element it can be transformed both chemically and biologically. The ocean is a major reservoir of sulphur mainly in the form of dissolved sulphate, gypsum and pyrite minerals (Sievert et al. 2007). Furthermore, the ocean is a main source of dimethylsulphide ($(CH_3)_2S$; DMS) which is mostly derived from dimethylsulphoniopropionate ($(CH_3)_2S^+CH_2CH_2COO^-$; DMSP) and dimethyl sulphoxide ($(CH_3)_2SO_2$; DMSO). DMS is a volatile sulphur compound that is readily transferred from ocean to the atmosphere by sea-to-air gas exchange (Lovelock et al. 1972). The marine production of DMS is thought to contribute ~28 Tg S yr^{-1} (~ 50%) to the global atmosphere (Lana et al. 2011).

Other natural sources of sulphur are volcanic eruptions, weathering of rock and terrestrial vegetation. However, over the recent centuries, human activities have disturbed the natural sulphur cycle. Anthropogenic emissions caused by burning of fossil fuel were assessed by Roelofs et al. (1998) who estimated it at 67 Tg S yr^{-1}, which significantly exceeds the marine biogenic flux. High sulphur emissions rates result in low rainwater pH (as oxidised sulphur readily reacts with water to form sulphuric acid). This wet deposition (acid rain) damages forests, freshwaters, soil and has even been shown proven to cause human illness (Jin and Bierma 2011). The global release of sulphur dioxide ($SO_{2)}$ due to industrial development has also provided large amounts of S to the soil, but from 1970s this deposition significantly declined after the emission limits were forced by environmental law.

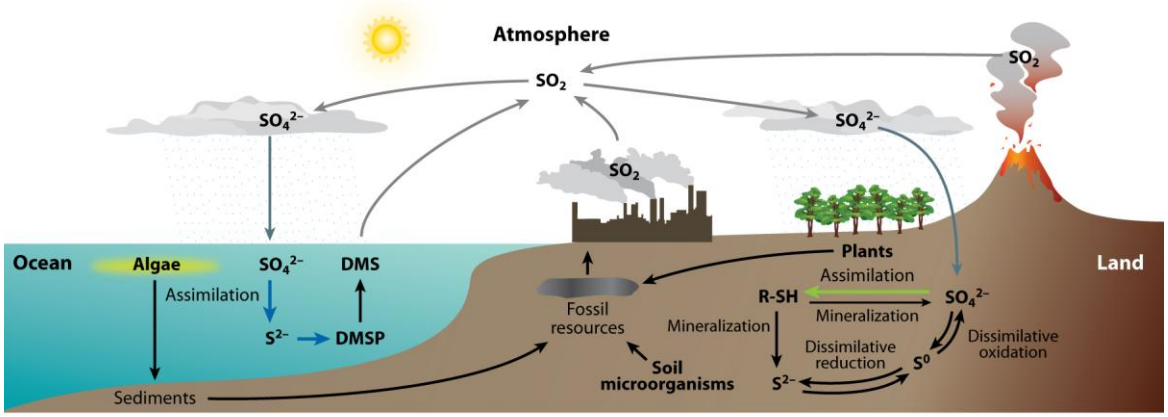

Figure 1.1 The sulphur cycle. The main component of the cycle is sulphate present the water, the soil and the atmosphere. Sulphate assimilation by plants and algae is indicated by green and blue arrows respectively. Dissimilative sulphur reactions are carried out by soil microorganisms that mineralise S-compounds to sulphate. Oceans and volcanoes are the natural sources of the volatile sulphur compounds released to the atmosphere that are subsequently oxidised to sulphate (Takahashi et al. 2011).

1.1.2. Climatic importance of sulphur (CLAW hypothesis)

First published in the 1970s (Lovelock and Margulis 1974), the Gaia theory states that organisms maintain a global homeostasis between biotic and abiotic systems through self-regulating feedback mechanisms. DMS production in the ocean and its consequences for the climate on Earth is an example of Gaia-like regulation.

The year 1987 saw a was breakthrough for the studying DMS(P) since Charlson et al. (1987) proposed the hypothesis that DMS was the one of the Earth's climate regulators. This idea became known as the CLAW hypothesis after the initials of its authors' names. The authors suggest that marine phytoplankton synthesises DMSP and part of this enters the atmosphere in the form of DMS and is oxidised to sulphate particles that can reflect sunlight back into space. These particles can also act as cloud condensation nuclei (CCN) brightening clouds and increasing global albedo. This changes the solar radiation (shading effect) and thereby also the temperature (cooling effect), and in turn this negatively affects algae growth closing the feedback loop. Despite intensive study of the CLAW hypothesis, the complexity of the interrelated processes that are involved and the lack of quantitative, real time measurements do not yet allow to for confirmation of this feedback loop. The gaps in this picture were discussed in a recent paper by Ayers and Cainey (2007) and are summarised briefly here.

First of all, DMS concentration in the water column significantly depends on species composition as well as on bacterial, grazers and virus activity. Secondly, the exact physiological role of DMS(P) remains somewhat elusive, and therefore, our knowledge about how the environment influences emissions is poorly constrained. Wingenter et al. (2007) carried out a mesocosm experiment in Norway and showed that doubling carbon dioxide (CO_2) increases DMS emissions, however measurements from the very similar experiment performed by Vogt et al. (2007) show that doubling or tripling CO_2 did not increase the DMS concentration. This suggests that the biological response to change in CO_2 level is inconsistent. Mesocosm study carried out by Wingenter et al. (2007) did not unambiguously show whether the increase of DMS emission was provoked by a direct response in the phytoplankton community such as increased lyase activity or a speciation change, or an indirect factor such as increased viral lysis or decreased bacterial turnover of DMS.

Another big challenge is estimating DMS flux from seawater to the atmosphere especially during rough weather conditions, which commonly occur but are dangerous for humans to work in at sea. Recently, the direct measurement of gas exchange based on micrometeorological techniques e.g. relaxed eddy accumulation and eddy covariance, have made better evaluation of ocean-atmosphere exchange of DMS possible (Blomquist et al. 2006; Marandino et al. 2008).

Beyond oceanic production and air-sea flux, to verify the CLAW hypothesis and complete cycle of sulphur, one needs to understand atmospheric sulphur chemistry. Anthropogenic activity further complicates these processes through the burning of fossil fuels. Regardless of the true situation, the CLAW hypothesis has inspired scientists from multidisciplinary areas and advanced us in our understanding of the connections within the Earth's systems.

1.1.3. The DMSP/DMS cycle in the marine ecosystems

The ocean ecosystem regulates the production, conversion and emission of DMS(P) through various and complex biological, chemical and physical interactions (Figure 1.2). The fundamental elements of the cycle are the DMSP producers belonging to many phytoplankton groups. This is why a species specific composition is an important factor controlling oceanic DMS concentration. Keller et al. (1989) did a substantial pioneering study where they investigated 123 individual microalgae clones for the production of DMSP. They found a relationship between DMSP concentration and phytoplankton taxonomy. A significant amount of this compound is produced by species belonging to the prymnesiophytes (including coccolithophores) and dinoflagellates, with intracellular concentrations of several hundred mM of DMSP. Generally smaller, but still important amounts of DMSP characterise members of the chrysophytes and diatoms (Keller 1988; Keller et al. 1989; Matrai and Keller 1994). Although some microalgae are not major producers of DMSP on a per cell basis, the ability to form massive blooms may lead to increases in DMS concentration in the ocean.

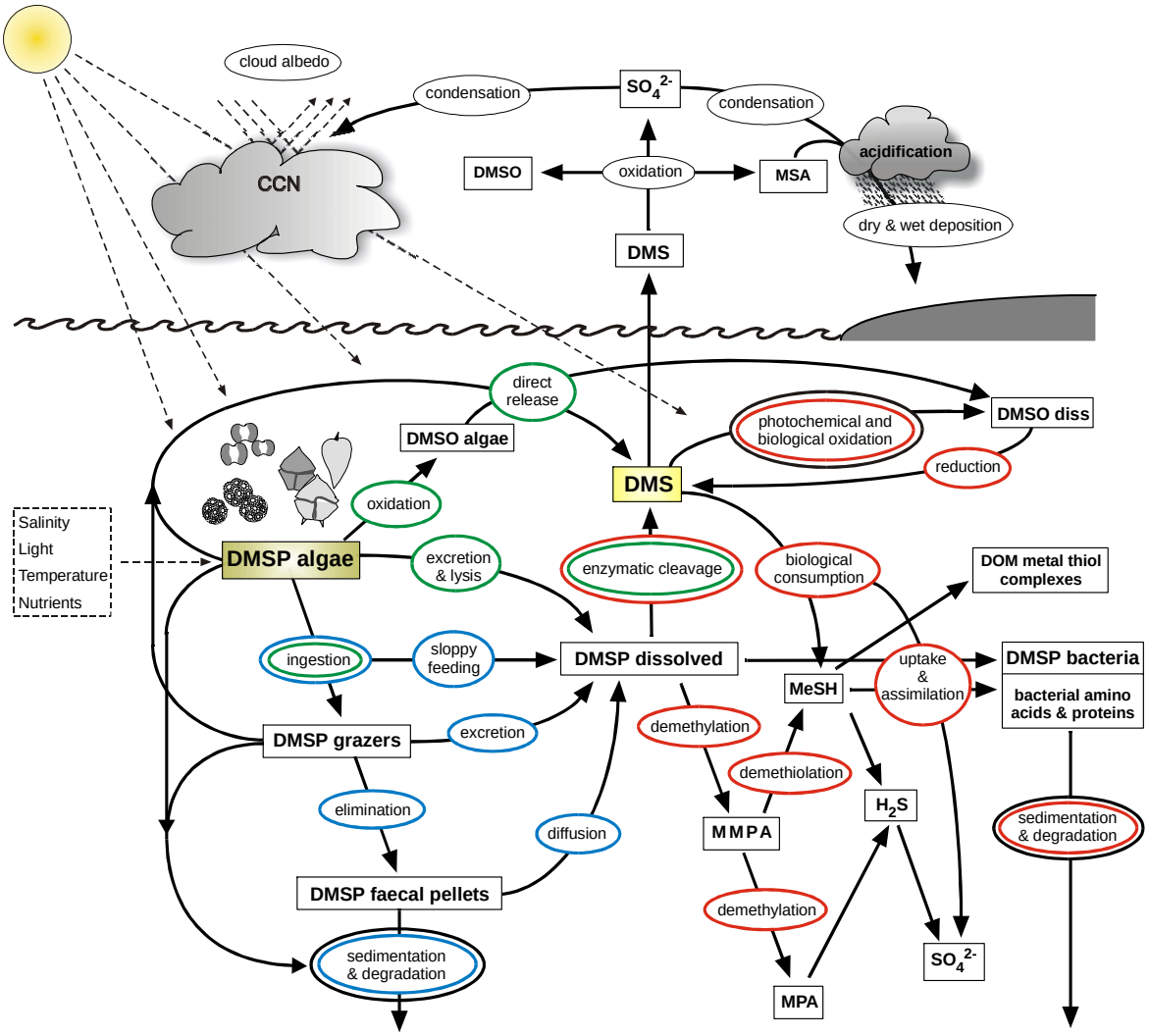

Figure 1.2 Generalised diagram focusing on the production and fate pathways of DMSP and the products of its transformations due to biological and abiotic factors. These factors are indicated in colour as follows: green, phytoplankton; blue, zooplankton; red, bacteria; black, abiotic. Other abbreviations are: CCN, cloud-condensation nuclei; DOM, dissolved organic material; DMSO, dimethyl sulphoxide; MeSH, methanethiol;MPA, mercaptopropionate; MMPA, methylmercaptopropionate; MSA, methanesulphonic acid (Stefels et al. 2007).

DMSP is not simply the precursor of DMS but also plays many physiological roles within algal. DMSP can be a significant component of cellular organic carbon (1-16%) in different phytoplankton groups; for example in the haptophytes class, *Phaeocystis.* DMS and DMSP are also significant carbon sources for bacteria (Matrai and Keller 1994). Moreover, we know that just a small fraction (10-20%) of the DMSP originally produced is ultimately emitted in the form of DMS. The fate of these sulphur compounds is highly regulated by biological and physical processes (Figure 1.2).

At the pH of seawater the chemical half-life of DMSP is about 8 years (Dacey and Blough 1987), therefore biological DMS formation due to enzymatic catalysis by bacteria and algae seems to be the dominant process. Some species have intra- and/or extracellular DMSP-lyase enzymes that may result in enhanced DMS concentrations directly or after DMSP is released into the water (Steinke et al. 1998; Steinke et al. 2000). In its dissolved form, DMSP is consumed and transformed at a high rate by the microbial food web (Figure 1.2). Dissolved DMSP (DMSPd) concentration is usually lower (1-50 nM) and often overestimated (Kiene and Slezak 2006) compared with the particulate pool (1 to >300 mM). However, DMSPd turnover is fast and ranges between 1 and 129 nM d^{-1} (Turner et al. 1988; Kettle et al. 1999; Kiene and Linn 2000). The bacterial community degrades DMSPd not only by enzymatic breakdown to DMS, acrylate and H^+. An alternative to the DMSP-lyase enzyme(s) breakdown process is the catabolism of DMSP to methanethiol (MeSH) via demethylathion/demethiolathion reactions (Kiene 1996). The latter pathway quantitatively dominates over the DMSP lyase pathway (Taylor 1993; Kiene 1996). Kiene et al (1999) have identified that MeSH is a very reactive compound and might be a major sulphur source for the synthesis of amino-acids and proteins in marine bacteria. The authors suggest that, in the ocean, microbial organisms prefer to utilise the trace amounts of available reduced sulphur instead of abundant sulphate in order to save energy.

A proportion of DMS undergoes either photochemical oxidation or biological transformation to form non volatile dimethyl sulphoxide ($(CH_3)_2SO$; DMSO). This compound is still poorly understood, however it is recognised as an effective radical scavenger and widely used in industry and medicine as a drug transporter and cryoprotectant(Hatton et al. 2005). Biologically produced DMS can be converted to DMSO by the dehydrogenase enzyme allowing photoautotrophic bacteria to grow with DMS as the electron donor. On the other hand, DMSO-reductase enzyme catalyses the reverse reaction producing DMS from DMSO (Bentley and Chasteen 2004).

Whilst microbial conversion of DMSP occurs, some fractions of particulate DMSP is transported from surface waters down to the seafloor. For example, Belviso et al. (2006) measured the downward flux in the Malangen fjord, Norway, using sediment traps and found that a significant fraction of the intracellular DMSP standing stock (up to 8% per day) and daily production (up to 56% per day) was lost by sedimentation. However, the magnitude of this loss pathway is likely to vary between different sites depending upon the dominant types of phytoplankton present.

1.2. Sulphur metabolism in photosynthetic organisms

1.2.1. Sulphate uptake

Sulphur is an essential macromolecule for the cell growth as it is a constituent of the amino acids (cysteine and methionine), oligopeptides such as glutathione, vitamins, co-factors and numerous secondary metabolites. Sulphur has important functions in the catalytic or electrochemical processes in the cell.

Sulphate is the major sulphur form acquired and assimilated by bacteria, algae, fungi and plants. Most of the information about its uptake comes from green algae e.g. *Chlamydomonas reinhardtii* (Melis and Chen 2005; Lindberg and Melis 2008) and vascular plants e.g. *Arabidopsis thaliana* (Buchner et al. 2004; Barberon et al. 2008; Takahashi 2010). Figure 1.3 shows the generally accepted pathway of sulphate transport, and assimilatory reduction in plants.

The sulphate ion (SO_4^{2-}) has a negative charge and cannot go passively through the plasma membrane; therefore the uptake is facilitated by H^+-ATPase co-transporters driven by the trans-membrane proton (H^+) gradient. Plant sulphate transporters are predicted to have 12 membrane-spanning domains connected to the C-terminal STAS (sulphate transporters and anti-sigma factor antagonist) domain. For example, *A. thaliana* has 14 genes encoding H^+/SO_4^{2-} co-transporters clustered in 5 functional groups based on sequence similarity, localisation and kinetic properties (Kopriva 2006). In *A. thaliana*, SO_4^{2-} influx from the external environment into the root is assured by high affinity transporters, SULTR 1;1 and SULTR1;2. On the other hand, a low affinity system consisting of SULTR 2;1 SULTR 2;2 and SULTR3;5 transporters, presumably allocates sulphate anions from the roots to the shoots and leaves (Takahashi et al. 2000; Kataoka et al. 2004). Transporters from the SULTR4 group are involved in influx of sulphate from the vacuole to the cytoplasm (Kataoka et al. 2004).

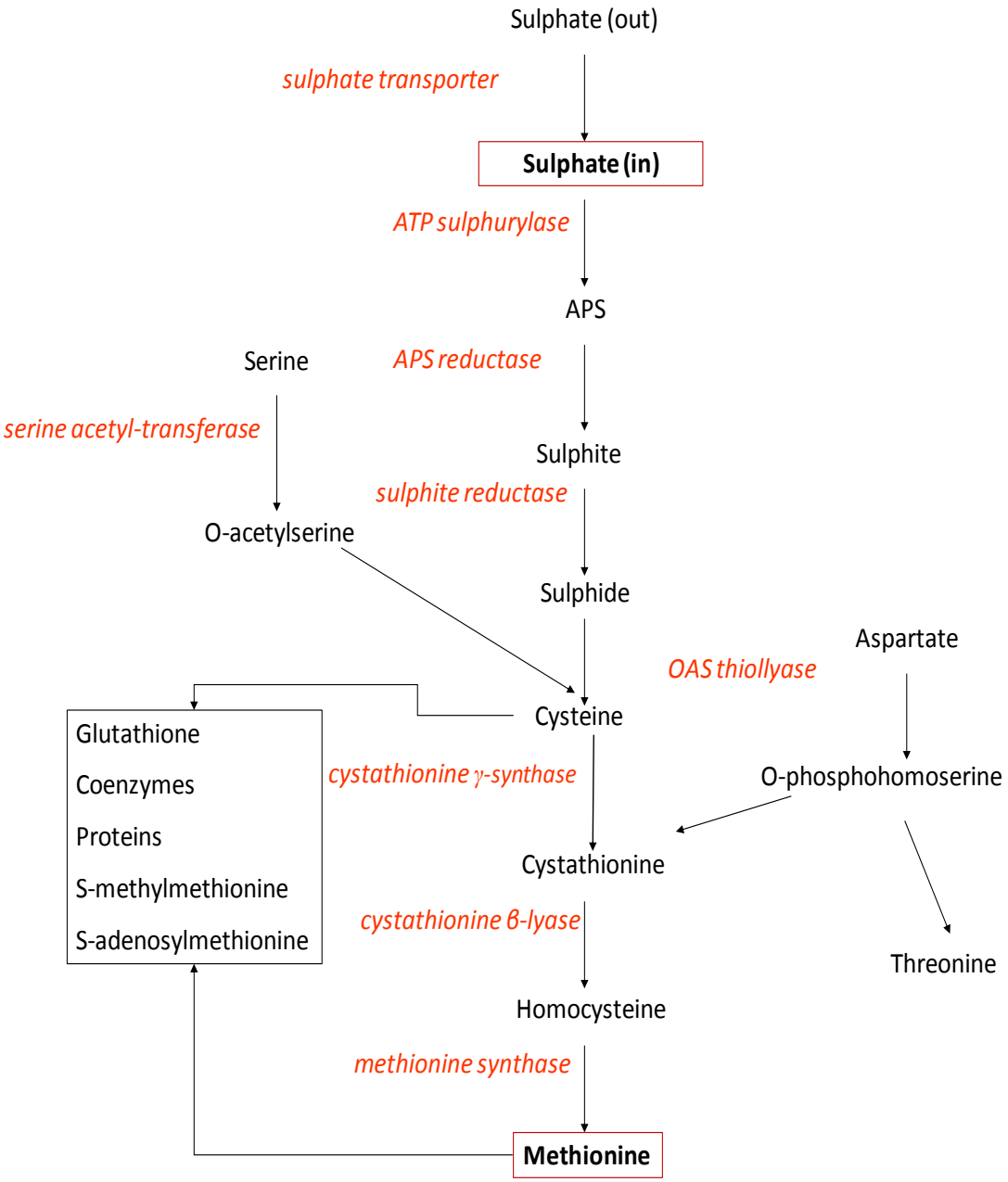

Figure 1.3 Proposed pathway of assimilatory sulphate (SO_4^{2-}) reduction and methionine (Met) synthesis. Adapted from Kopriva and Koprivova (2004).

Algae have a distinct sulphate transport system compared to vascular plants. Analysis of the *C. reinhardtii* genome revealed 3 genes (*SULTR1*, *SULTR2* and *SULTR3*) encoding the H^+/SO_4^{2-} co-transporters that are similar to those found in plant. Another 3 transporters (SLT1, SLT2 and SLT3) belong to the Na^+/ SO_4^{2-} transporter family are found in bacteria and mammals but not in vascular plants. Interestingly, the marine chlorophyte *Ostreococcus tauri* has only 2 Na^+/ SO_4^{2-} transporters which is might be energetically beneficial as sodium concentration in the ocean is high (Pootakham et al. 2010). Apart from a plasma membrane sulphate transport system, C .*reinhardtii* has a chloroplast envelope transport system, SulP, which is similar to the ATP-binding cassette (ABC) transporters of bacteria. This transporter is found in chloroplast genomes of a few basal plants, but not in vascular plants where the plastidic sulphate transporter still awaits discovery (Takahashi et al. 2011).

Plants and algal sulphate transport is highly regulated by sulphur availability. Sulphate uptake affinity and capacity increase within hours of sulphate removal and decrease again upon sulphate restoration. However, we do not know much about sulphate transport regulation in marine microalgae. The high and constant sulphate concentration in the ocean suggests that marine phytoplankton may not require as efficient transport as terrestrial and freshwater organisms.

1.2.2. Sulphate reduction

Sulphate is the most oxidised and stable sulphur compound and it has to be reduced after being transported into plastids to be assimilated. For this reason, in the initial step of assimilatory reduction, sulphate is activated by adenylation to adenosine 5'-phosphosulphate (APS) (Figure 1.3). This reaction is catalysed by ATP sulphurylase (ATPS). In some groups of organisms such as bacteria and fungi a second activation step occurs, where APS is phosphorylated by APS kinase to form adenosine 3'-phosphate 5'-phosphosulphate (PAPS). Patron and co-workers (2008) revealed that plant ATPS genes are more closely related to animal ATPS genes than to those in green algae. Marine microalgae such as diatoms and haptophytes have both types of ATPS genes. *E. huxleyi* and *T. pseudonana* possess a plant-like form fused with APS kinase and inorganic pyrophosphatase which presumably results in much higher APS synthesis rate
(Kopriva et al. 2009; Takahashi et al. 2011). Interestingly, in the dinoflagellate *Heterocapsa triquetra* ATPS is fused with the subsequent enzyme in the pathway, APS reductase (APR), which is another way to improve ATPS efficiency (Kopriva et al. 2009). Activated SO_4^{2-} of

APS molecules are reduced to sulphite (SO_3^{2-}) in the reaction catalysed by APS reductase (APR) (Figure 1.3). In flowering plants and green algae the APR protein consists of an N-terminal reductase domain, that binds [4Fe-4S] cluster cofactors and a C-terminal thioredoxin domain (Gutierrez-Marcos et al. 1996; Kopriva et al. 2002; Kopriva and Koprivova 2004). Marine microalgae have an APR isoform called APR-B. This protein was first identified in the moss *Physcomitrella patens* (Kopriva et al. 2007a) and it is unique in its ability to reduce APS despite lacking the [4Fe-4S] cluster (Kopriva et al. 2007b; Patron et al. 2008). The recently sequenced genomes of *T. pseudonana* and other marine microalgae include genes that encode homologues of APR-B, which probably represents an adaptation to iron limitation in the ocean (Falkowski et al. 1998). Gao et al. (2000) investigated APR and PAPS reductase activity of several marine microalgal species from diverse groups. They showed that APS is the main substrate being reduced and that activity is significantly higher than that found for higher plants.

For further assimilation, SO_3^{2-} generated from APS is reduced by plastidic sulphite reductase (SiR). This enzyme uses reduced ferreodoxin as a reductant and six electrons are needed form sulphide (S^{2-}). The activity of SiR was detected by Schmidt (1973) in cell-free extract from green alga *Chlorella*. *C. reinhardtii* has two genes (*SIR1* and *SIR2*) encoding ferreodoxin-dependent eukaryotic sulphite reductase and *SIR3* gene encoding putative bacterial like enzyme using NADPH as an electron donor. Marine microalgae have these both types of genes. By contrast, in *A. thaliana* SiR is encoded by a single copy gene (Bork et al. 1998).

1.2.3. Cysteine and methionine synthesis

The final step of the assimilatory sulphate reduction pathway is the synthesis of cysteine (Cys) by incorporation of sulphide into *O*-acetylserine (OAS). This reaction is catalysed by *O*-acetylserine(thiol)lyase (OASTL) and follows OAS formation from serine and acetyl-coA catalysed by serine acetyltransferase (SAT). These two enzymes form a complex called cysteine synthase that is important for regulation of Cys synthesis. Plants can synthesise Cys in 3 compartments: cytosol, chloroplasts and mitochondria (Heeg et al. 2008). Multiple genes encoding SAT and OASTL proteins were found in the *T. pseudonana* and *E. huxleyi* genomes suggesting synthesis in different subcellular compartments.

Cys synthesis is the terminal point in sulphur assimilation and the starting point for production of methionine (Met) and various other metabolites containing reduced sulphur.

Met is synthesised in 3 consecutive reactions (Figure 3.1): first cystathionine γ-synthase combines *O*-phosphohomoserine (OPH) with Cys to form cystathionine. Then, the second enzyme, cystathionine β-lyase converts cystathionine to homocysteine (HCys), and in the final step, the thiol group of HCys is methylated in a reaction catalysed by methionine synthase (MS).

1.2.4. DMSP synthesis

Met is an essential amino acid not only for building proteins and cofactors such as S-adenosylmethionine, but also as the precursor of DMSP. In an early study, Green (1962) reported methionine to be the first molecule for the biosynthesis of DMSP n the marine alga *Ulva lactuca*. He showed that methyl group and the sulphur in dimethylsulphoniopropionate came from methionine. Currently, it is believed that biochemical pathway from Met to DMSP evolved in three independent ways (Gage et al. 1997; Stefels 2000). Based on *in vivo* isotope labelling, Gage and co-workers (1997) revealed that the green macroalga, *Enteromorpha intestinalis*, performs DMSP synthesis in four steps (Figure 1.4). A transamination reaction forms 4-methylthio-2-oxybutyrate (MTOB) by removing the NH_3 group from Met. This reaction possibly reflects the elevated levels of DMSP observed under N-limited conditions (Groene 1995). MTOB is subsequently converted to 4-methylthio-2-hydroxybutyrate (MTHB) by MTOB reductase. Whilst the first 2 reactions also occur in non-DMSP producers, the following transformations are unique to DMSP producers (Gage et al. 1997). MTHB is S-methylated by MTHB S-methyltranspherase to generate 4-dimethylsulphonio-2-hydroxybutyrate (DMSHB) and the last step involves oxidative decarboxylation of DMSHB which yields DMSP.

There are far fewer DMSP producers amongst higher plants compared to algae. The strand plant *Wollastonia biflora* is an example of DMSP producing vascular plant (Hanson et al. 1994; Otte et al. 2004). In this species, DMSP synthesis pathway differs from that described for algae. The first step is the formation of S-methyl-methionine (SMM) by methionine S-methylation catalysed by methylmethionine synthetase. Then, SMM undergoes transamination/decarboxylation resulting in DMSP-aldehyde (DMSP-ald) synthesis. Ultimately, the oxidation reaction of DMSP-ald yields DMSP.

The third pathway is thought to be characteristic for the *Poaceae* and was identified in the salt marshes grass *Spartina alterniflora* (Kocsis and Hanson 2000). In this organism, 3-

dimethylsulfoniopropylamine (DMSP-amine) is an intermediate molecule between SMM and DMSP-ald. This distinguishes DMSP production between grasses and higher plants.

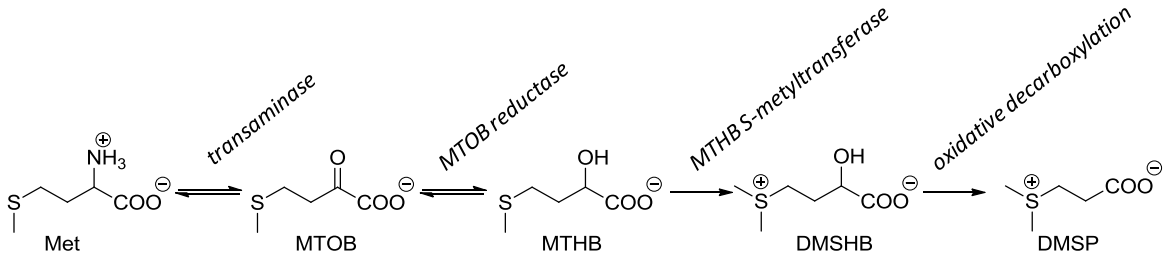

Figure 1.4 The methionine (Met) to dimethylsulphoniopropionate (DMSP) biosynthesis pathway in marine algae established for the green macroalga *Enteromorpha intestinalis* by Gage at al. (1997). DMSHB, 4-dimethylsulfonio-2-hydroxy-butyrate; MTHB, 4-methylthio-2-hydroxybutyrate; MTOB, 4-methylthio-2-oxobutyrate.

1.3. Regulatory mechanisms of sulphur metabolism

1.3.1. Sulphate assimilation under sulphur deficiency stress

Sulphate acquisition and assimilation is a precisely controlled at the metabolic and molecular level according to demand for reduced sulphur. Most of our knowledge is derived from investigations of the model species *A. thaliana* and *C. reinhardtii*.
Sulphate availability seems to be among the most important factor controlling its assimilation rate. Removing sulphate from the environment induced the expression of genes encoding SO_4^{2-} transporters, especially the high-affinity SULTR1;1 and SULTR1;2 (Hirai et al. 2003; Maruyama-Nakashita et al. 2003; Nikiforova et al. 2003). The increase in mRNA abundance under S-starvation was accompanied by accumulation of both transporters and up-regulation of sulphate uptake activity (Yoshimoto et al. 2007). A similar response was demonstrated in *C. reinhardtii* by Yildiz and colleagues (1994). These authors observed that sulphate transport parameters were altered in S-starved algae: the V_{max} increased ~10-fold, whereas the K_M decreased ~ 7-fold. The induction of the high-affinity transport system in this green alga is supported by the recent finding that transcripts encoding three sulphate transporters (SLT1, SLT2 and SULTR2) noticeably increased in response to S-limitation (González-Ballester et al. 2010). An additional sulphate assimilation step induced by S-deprivation is APS reduction both mRNA and enzyme activity affected (Takahashi et al. 1997; Leustek et

al. 2000). Interestingly, in S-starved *C. reinhardtii* 4h after beginning of the treatment APR transcript level started to decline while its activity kept increasing. This suggests that the APR activity is at least partly controlled at the posttranslational level (Ravina et al. 1999). Downstream the S metabolic pathway is also regulated by sulphate availability; under S-limitation conditions the pool of S-metabolites such as sulphate, cysteine and glutathione decreased whereas serine and OAS that are Cys precursors accumulated (Nikiforova et al. 2006).

1.3.2. Transcriptional regulation of sulphate transport and metabolism

Recent advances in functional genomics have led to the identification of the key regulators in sulphate transport and assimilation for plants and green algae (Takahashi et al. 2011) (Figure 1.5).

Maruyama-Nakashita and co-workers (2006) identified a central transcription factor, Sulphur Limitation 1 (SLIM1) that regulates the expression of many genes involved in sulphate assimilation and secondary metabolism (Figure 1.5 A). The authors performed a genetic screen for mutants, with a sulphur-responsive promoter-GFP, that were unable to induce the sulphate transporter gene *SULTR1;2* by S-starvation. SLIM1 belongs to ethylene-insensitive-like (EIL) transcription factors family composed of six members (EIN3 and EIL1 to EIL5). In fact, EIL3 vas verified to be the only member of the family that was able to restore the sulphur limitation in a response-less phenotype *slim1* mutant, therefore it was renamed SLIM1 (Maruyama-Nakashita et al. 2006). SLIM1 is responsible for increase of sulphate uptake and for reduction of synthesis of sulphur-containing secondary metabolites, glucosinolates. It also regulates other components of the signalling pathways, such as microRNA-395 (miR395). Under sulphur-limited conditions SLIM1 induces miR395 in shoots and roots. The miR395 gene is involved in the regulation of sulphate accumulation and its allocation in the plant in such way that it limits expression of SULTR 2;1 to xylem parenchyma which enhance sulphate translocation to the shoot but inhibits shoot to roots transport (Liang et al. 2010; Kawashima et al. 2011).

Sulphur deficiency represses expression of several MYB transcription factors belonging to the R2R3-type MYB family. These factors are another example of sulphur regulation in the plants (Figure 1.5 A). MYB28 and MYB29 are expressed preferentially in leaves and positively regulate the biosynthesis of methionine-derived aliphatic glucosinolates, whereas MYB34 expressed in roots activates the synthesis of indole glucosinolates (Lewandowska

and Sirko 2008). Yatusevich et al. (2010) showed that MYB transcription factors also regulate genes of primary sulphate metabolism and therefore the genes involved in the synthesis of activated sulphate are part of the glucosinolates biosynthesis network. Under S-limitation SLIM1 negatively controls some members of MYB family to restrict sulphur utilisation to primary metabolism (Maruyama-Nakashita et al. 2006). The final addition to the list of transcription factors regulating sulphur metabolism in plants is Long Hypocotyl 5 linking the pathway to light signalling (Lee et al. 2011).

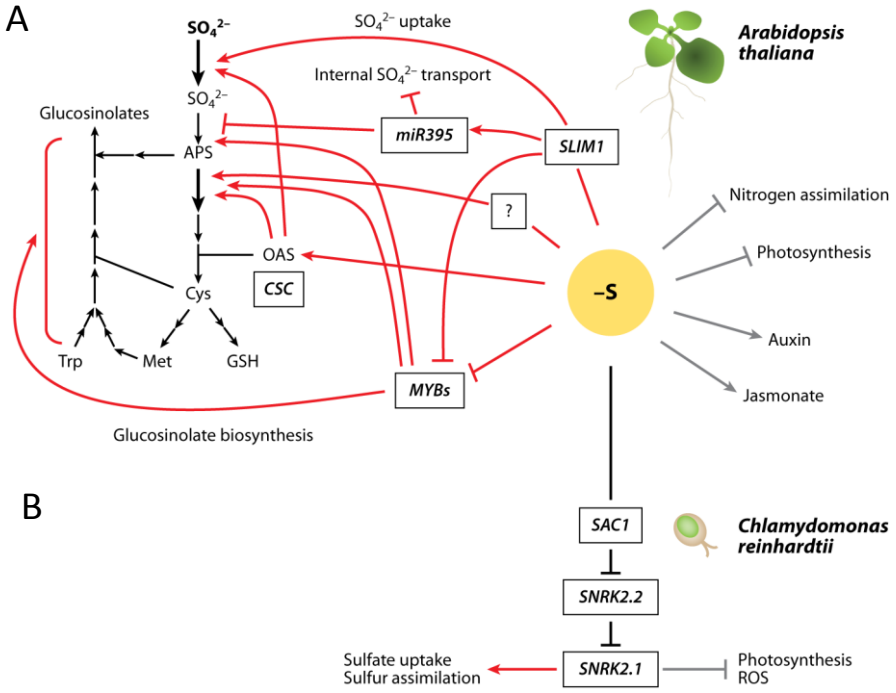

Figure 1.5 Complex regulatory network of pathways driven by S-limitation in: A: the vascular plant *Arabidopsis thaliana* and B: the green alga *Chlamydomonas reinhardtii*. Sulphur transport and metabolism regulations are indicated by red lines, whereas other general pathways modulated by S-limitation are indicated by grey lines (Takahashi et al. 2011).

1.3.3. Sulphur Acclimation1 (SAC1)

Similarly to *A. thaliana*, molecular regulation by S availability has also been studied in *C. reinhardtii* (Figure 1.5 B). Interestingly, the knowledge of sulphur sensing is much more advanced in this alga than in plants. In addition, in contrast to higher plants this green alga is able to secure sulphate supply under S-deprived condition by hydrolysing sulphate esters via the action of arylsulphatase.

The *SAC1* gene encodes for an integral membrane protein associated with an adaptation to low sulphate conditions. Although, SAC1 is homologous to Na^+/SO_4^{2-} transporters (SLC 13 family), it seems to play a role as a sensor of extracellular sulphate level rather than as a transporter (Davies et al. 1996; Moseley et al. 2009). It is also involved in photosynthesis reduction essential when the capacity to assimilate sulphate decreases in the cell (Davies et al.1996). Its regulatory functions were identified by genetic screening of *sac* mutants that were unable to synthesise arylsulphatase under low sulphate conditions and were less efficient in sulphate uptake than wild type cells (Davies et al. 1996). Studies of the *sac1* mutant indicate SAC1 controls not only proteins related to sulphate assimilation but also alters proteins involved in the reconstruction of cell walls and the photosynthetic apparatus when *C. reinhardtii* is S-starved (Takahashi et al. 2001; Ravina et al. 2002; Zhang et al. 2004).

There are two other genes encoding regulatory proteins in response to S-limitation in *C. reinhardtii*. They are the SNRK2 family Ser/Thr protein kinases, SNRK2.1 and SNRK2.2 (also known as SAC3) (Gonzalez-Ballester et al. 2008). SNRK2.1 kinase is essential for the expression of S-responsive genes and for maintaining the viability of S-starved cells (González-Ballester et al. 2010). When cells are replete for sulphate SNRK2.2 inhibits SNRK2.1 and thus represses the acclimation response. However, under sulphur-limitation, SAC1 acts as a negative controller of SNRK2.2 which in turn releases SNRK2.1 (Moseley et al. 2009).

1.4. Physiological roles of sulphur in marine phytoplankton

The fact that DMSP synthesis is limited to just a few taxonomic groups of marine phytoplankton and a few higher plants is very intriguing. The intracellular concentration of this molecule ranges between 50 and 400 mM which correspond to 50 to almost 100% of the total organic sulphur in the cell (Matrai and Keller 1994; Keller et al. 1999). Additionally, various strains within one species can differ substantially in biological DMSP production terms (Steinke et al. 1998). Broad interest in DMSP and DMS has led to suggestions of several hypothetical roles for these compounds in cell metabolism, however, not all of these are fully elucidated. These roles are discussed below.

1.4.1. Compatible solutes (osmo- and cryoprotectors)

Turgor pressure is the difference between the internal (cellular) and external hydrostatic pressures. Marine algae precisely regulate their turgor by accumulation of intracellular inorganic ions, mainly Na^+, K^+, Cl^- (Bisson and Kirst 1995). This is achieved by passive or active ion transport via pores and channels located in the cell membrane. Although, inorganic ion uptake is very efficient and a low energy cost process, the high concentration necessary to balance external hyperosmotic potential may exert a negative effect on cell metabolism. Thus, algae favour the accumulation of compatible solutes, low molecular weight organic compounds, especially under long term hyperosmotic conditions. The main property of these compounds is the ability to modulate osmotic balance without inhibiting individual enzyme activities or overall cellular functions (Brown 1976). Most of these molecules are photosynthetic products e.g. sugars, polyols and heterosides. Other molecules like tertiary sulphonium compounds (DMSP) and quaternary ammonium compounds (glycine betaine) are not direct photosynthetates but they play an important role in some algae, cyanobacteria, bacteria and salt marsh plants (Csonka and Hanson 1991; Stefels 2000; Welsh 2000). In fact, DMSP levels increase in response to high salinity conditions (Vairavamurthy 1985; Dickson and Kirst 1986), whereas salinity down-shock results in DMSP release from the cell (Niki et al. 2007).

Osmolytes that accumulate under hyperosmotic stress can also assist in protein stabilisation provoked by temperature change. Nishiguchi and Somero (1992) demonstrated in their study that DMSP is an effective cryoprotectant of protein structure. This appeared to

be confirmed by the 5-fold higher intracellular DMSP concentration seen in Antarctic green microalgae grown at 0^{o}C compared to 10^{o}C (Karsten et al. 1992).

1.4.2. Antioxidant protection

Various stressors like excess of light energy, starvation or toxins can result in induction of reactive oxygen species (ROS), such as singlet oxygen ($^{1}O_2$), superoxide (O_2^{-}), hydrogen peroxide (H_2O_2) and hydroxyl radicals (•OH) that can damage not only the photosynthetic components but also DNA, proteins and lipids.

Sunda and et al. (2002) proposed that DMSP and its metabolic products, DMS, acrylate, DMSO and methane sulphinic acid (MNSA), may form a cascade of radical scavengers as part of the overall antioxidant system. They observed an increase in DMSP and DMS-production via DMSP lyase activity in microalgae in response to CO_2 and Fe limitation, high Cu^{2+}, H_2O_2 and ultraviolet radiation. Similar up-regulation of DMSP concentration was reported in *T. pseudonana* grown under nutrient limitation (Bucciarelli and Sunda 2003).

DMSP and its derivatives are not the only S-metabolites involved in the ROS removal. The S-containing amino acids Cys and Met are very reactive, especially with $^{1}O_2$ and •OH (Møller et al. 2007). GSH, which is the main non-protein thiol, is also used to remove H_2O_2 and so it is important in redox homeostasis (Noctor and Foyer 1998).

1.4.3. Overflow mechanism

Stefels (2000) proposed a concept that increased production and release of DMSP could represent an overflow mechanism for excess reduced sulphur, and possibly also carbon, under unbalanced growth conditions. She argued that under nitrogen limitation this process could maintain cysteine and methionine concentrations at a sufficiently low level for reductive sulphate assimilation to continue and thus ensure continuation of other metabolic reactions. Indeed, several studies are consistent with this hypothesis. It was observed that algae responded to N-limitation by increasing DMSP concentration (Turner et al. 1988; Grone and Kirst 1992; Bucciarelli and Sunda 2003). If DMSP does function as an overflow compound its intracellular homeostasis should be regulated by the releasing processes rather than production (Stefels et al. 2007). Another possible role for the overflow mechanism

proposed by Stefels (2000) is in protein turnover and amino acid reallocation as an adaptation to new environmental conditions.

1.4.4. DMSP as a chemical defence compound

There are ~10^7 viruses in every millilitre of surface seawater. This means that viruses are the most numerous biological entities in the aquatic systems with ~15 times the total number of bacteria and archaea. Thus marine viruses play an important role in altering community structure and biogeochemical cycling (Danovaro et al. 2011). One of the most significant impacts on phytoplankton communities is algal bloom termination associated with viral lysis (Suttle 1992; Fuhrman 1999; Baudoux et al. 2006). From observation in the laboratory studies, it was reported that viral infection of DMSP producers such as *E. huxleyi* enhances DMSP release to the dissolved pool which can be subsequently converted to DMS mostly by bacterial but also by algal DMSP lyase enzymes (Malin et al. 1998; Niki et al. 2000). On the other hand, Evans et al (2006) observed that DMSP cleavage products: DMS and acrylic acid (AA) inhibited infectivity of the large phycodnavirus –*E. huxleyi* virus 86 (EhV-86). This suggests that the cleavage of DMSP into DMS and AA might have a potential role in reducing the propagation of viral particles within an *E. huxleyi* population. In support of this idea, *E. huxleyi* strains characterised by high DMSP-lyase activity were resistant to virus infection whereas low DMSP-lyase strains did not escape the viral infection (Schroeder et al. 2002).

DMSP and its degradation products were also found to be mediators in marine microbial interactions. Wolfe and Steinke (1996) demonstrated that grazing by the dinoflagellate *Oxyrrhis marina* on *E.huxleyi* triggered DMSP release and its conversion into DMS and presumably also acrylate. These products reacted in turn as a grazing deterrent on the herbivore. It was also shown that *O. marina* preferred to feed on low DMSP lyase activity strains rather than on those with high lyase activity (Wolfe et al. 1997). Furthermore, DMS can attract zooplankton predators that feed on herbivores and thereby reduce the grazing pressure on the microalgae (Steinke et al. 2002).

1.5. *Emiliania huxleyi*

Emiliania huxleyi (Figure 1.6 A), the subject of this thesis, is a coccolithophore belonging to the division Haptophyceae and the class Prymnesiophyceae. Haptophytes are unicellular algae containing chlorophyll a + c that occur mostly in littoral, costal and oceanic waters. Some are capable of forming colonies. The name of this division is associated with the presence of a unique flagella-like organelle, the haptonema (from the Greek *hapsis*-touch). This is considered to play a role in cell attachment or/and prey capture in some species. In many coccolithophores the haptonema is reduced to a vestigial structure (de Vargas 2007). Haptophytes, along with other eukaryotic lineages, the cryptophytes, alveolates and heterokonts (stramenopiles), arose from a secondary endosymbiosis of a heterotrophic eukariote with a red alga. Recently phylogenetic clock analysis based on the slow evolving 18S rDNA nuclear gene and the fast evolving plastid gene *tuf*A, revealed that haptophytes diverged from other chromista ~1200 Ma (Medlin et al. 2008). According to Medlin et al. (1997) the origin of Haptophyceae is much older than the heterokont lineage that comprises diatoms and dated between 170 and 270 Ma. Within the haptophytes, coccolithophores make a distinct clade indicating that calcification evolved only once within the division (Fujiwara et al. 2001; Young and Henriksen 2003). Interestingly, Medlin et al. (2008) suggested that modern coccolithophores originated from a few lineages that survived the major extinction at the Cretaceous/Tertiary (K/T) boundary, whereas this extinction did not affect non-calcifying haptophytes; possibly due to their ability to switch from autotrophy to mixotrophy feeding (Liu et al. 2010). The molecular genetic phylogenies tally with the fossil records showed that calcifying haptophytes originated ~220 Ma ago in the late Triassic waters and they diversified into ~400 morphological species (Bown 1987).

The fossil records of *E. huxleyi* indicate that it is comparatively young coccolithophore morphospecies that appeared ~290 ka ago (Raffi et al. 2006). Since the SSU rDNA and RUBISCO *rbc*L genes are genetically identical in *E. huxleyi* and *Gephyrocapsa oceanica* (Fujiwara et al. 2001), which has a longer fossil record than *E. huxleyi*, it is believed that *E. huxleyi* diverged from *G. oceanica.* At the beginning of its evolution, *E. huxleyi* was a minor species among the coccolithophores but with time it started to dominate spreading from low latitudes (~85 ka) to middle latitudes (~70 ka) and high latitudes (~60 ka) of the North Atlantic.

Today, *E. huxleyi* is the most abundant and cosmopolitan coccolithophore in the ocean (Brown and Yoder 1994) and ofte makes up more than 50% of the coccolithophore flora (Okada and Honjo 1973). Being temperature and salinity tolerant *E. huxleyi* is a cosmopolitan species that lives in the entire photic zone, especially in nutrient-rich subpolar waters, the borders of the subtropical oceanic gyres as well as in equatorial and costal upwelling regions (Okada and Honjo 1975; Winter et al. 1994; Flores et al. 2010). Because of its high environmental tolerance, *E. huxleyi* can form massive blooms (Figure1.6 B) sometimes covering very large areas; e.g. a bloom in the Bering Sea covered an area of 2 x 10^5 km^2 with cell concentration reaching almost 3 x 10^6 cells L^{-1} (Sukhanova and Flint 1998). As a result *E.huxleyi* can have a significant impact on the local environment. As a producer of calcium carbonate ($CaCO_3$, calcite) coccoliths *E.huxleyi* is responsible for a large proportion of carbon cycling via CO_2 consumption during photosynthesis and CO_2 generation during calcification (Westbroek et al. 1993). Moreover, this microalga contributes to the export of calcite to the seabed via settling of coccoliths after bloom termination (Baumann 2004). Aside from global carbon cycling, *E. huxleyi* is a key DMSP producer and is important for the sulphur cycle. This process is described in greater detail above (see section 1.1.1).

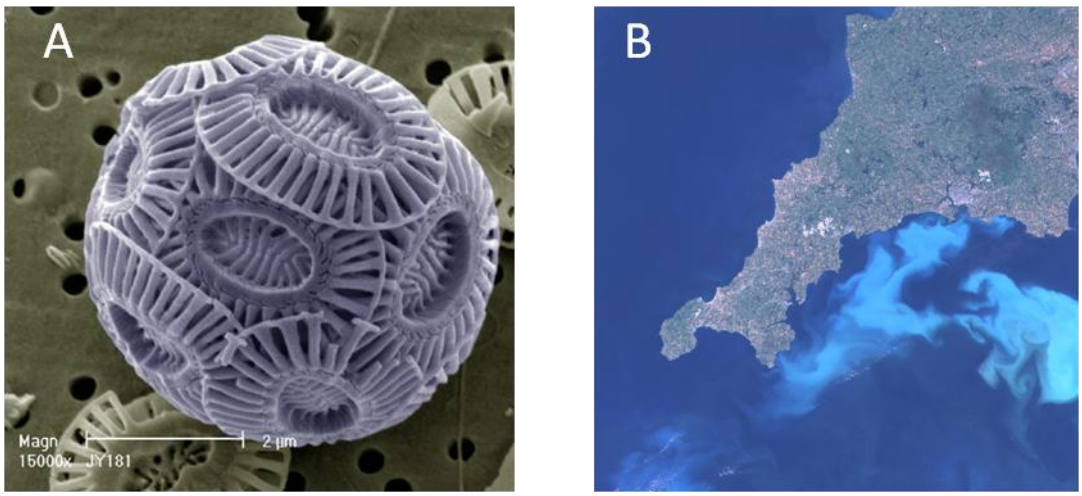

Figure 1.6 A, scanning electron microscope micrograph of *Emiliania huxleyi* with formed calcified platelets (coccoliths). Photography was taken from Jeremy R Young, The Natural History Museum, London (http://protozoa.uga.edu/portal/coccolithophores.html). B, Satellite picture of *E. huxleyi* bloom in the English Channel, coast of Plymouth (Cornwall). Photography was taken from (NASA http://visibleearth.nasa.gov).

Another interesting feature of *Emiliania* and other coccolithophores is its life cycle consisting of the coccolith-bearing non-motile stage that is diploid (2N) and haploid (1N) scale-bearing flagellated phase; both forms can reproduce asexually (Green et al. 1996; Paasche 2001). Coccolithophores are able to alternate from asexual to sexual reproduction by meiosis and syngamy (Billard and Inouye 2004). This haplodiploic character of the life cycle was confirmed by Green et al (1996) using flow cytometric techniques. The heteromorphic life cycle is the most important biological feature differentiating the prymnesiophytes from other groups of microalgae (de Vargas 2007). In diatoms (2N life cycle) only the gametes are haploid, whereas in dinoflagellates (1N life cycle) diploid cells are limited to zygotes. Recently, Frada and co-workers (2008) demonstrated that viral attack triggers a shift of the *E. huxleyi* population from 2N cells that initially dominate in the bloom to 1N phase cells that are more virus-resistant. By this 'escape' mechanism haploid *E. huxleyi* cell can mate and return to the diploid cell type and possibly repopulate a new *E.huxleyi* bloom.

All these *E.huxleyi* characteristics and the environmental importance of this species led to the *E. huxleyi* CCMP1516 genome sequencing project. The draft version of the genome has been released by the Department of Energy Joint Genome Institute (JGI) and thus introduces great opportunities for the advanced molecular study of this fascinating organism.

1.6. The motivations for this research project

Multidisciplinary studies from many fields of the science that gradually link together are critical to describe the broad range of elements and processes that shape the Earth's ecosystems. Thanks to the contribution from many disciplines we better understand how, when and why these various components act together, although many gaps remain to be discovered.

Diverse research on sulphur, one of the most versatile elements, is a good example of how the contributions from various research fields increasingly allow us to recognise how the environment functions. On the biological level, sulphur is a very important element due to its reactivity in different oxidation and reduction states. Sulphur is incorporated into amino acids, oligopeptides, vitamins, cofactors, lipids and polysaccharides. Additionally many oceanic phytoplankton species have an extra demand for sulphur due to the production of another S-metabolite - DMSP. On the other hand, DMSP is the precursor of DMS the compound with the important role in climate regulation. Recognition of metabolic and molecular processes occurring at the cellular level are essential in order to obtain deep understanding of the biological, physical and chemical relationships between marine ecosystems and climate.

Most of the information about sulphur metabolism relates to organisms that are potentially exposed to S starvation like higher plants or freshwater algae. The high sulphate concentration in seawater means that marine microplankton does not experience S-deprivation and as a results sulphur assimilation and metabolism is rather poorly studied in these organisms. The aim of the research described in this thesis was to advance knowledge of metabolic sulphur pathways in the coccolithophore *Emiliania huxleyi* (CCMP 1516). To understand how sulphur metabolism varies, we subjected cultures to artificial variations in ambient sulphur concentration and assessed the physiological and molecular responses. In addition to illuminating the sulphur metabolism in marine organism, the results obtained during the project have further potential for future comparative studies between phylogenetically and ecologically distant organisms.

2. Materials and Methods

This chapter describes general methods and techniques that have been used for the laboratory experiments. It covers the standardised preparation and maintenance of *Emiliania huxleyi* cultures as well as measurements of various growth parameters. The principle sulphur metabolism-related methods are also described. In addition, the thesis contains relevant and specific 'Materials and Methods' sections in Chapter 3, 4 and 5.

2.1. Algal culture

2.1.1. Culture growth conditions

E. huxleyi strains CCMP1516, CCMP370 and CCMP373 were obtained from the Provasoli-Guillard National Center for Culture of Marine Phytoplankton (CCMP). They were originally isolated from the North Pacific, the North Sea and Sargasso Sea, respectively. Stock cultures were maintained in the LGMAC (Laboratory for Global Marine and Atmospheric Cycles) Marine Trace Gas Biology Laboratory. *E. huxleyi* was grown in 100 mL conical flasks with 50 mL (ESAW) medium (see Section 2.1.2). Cultures were kept in a MLR-351 Plant Growth Chamber (Sanyo E & E Europe BV, Loughborough, U.K.) at 15^{o}C under a light:dark cycle of 14:10 h and an irradiance of 180 µE m^{-2} s^{-1} (Scalar PAR Irradiance Sensor QSL 2101, Biospherical Instruments Inc., San Diego, U.S.A). Both stock and experimental cultures were incubated under the same temperature and light regimes. With these culture conditions *E. huxleyi* usually produced no coccoliths. In order to keep cells in suspension, the culture flasks were gently swirled by hand on a daily basis. New stock cultures were established every 10 days by transferring an inoculum from the exponentially growth culture into fresh media. To maintain sterile conditions and avoid contamination aseptic procedures were applied. All culture media and glassware were autoclaved at 120^{o}C for 30 min. All culture transfers and culture sub-sampling were carried out in a Class II Microbiological Safety Cabinet (Class II, Walker, Glossop, U.K.). In addition, the interior of the cabinet was wiped with 70% ethanol before use and the neck of the glassware was flamed with gas burner before and after manipulation. To examine the axenicity of the cultures we used nucleic acid staining with 4',6-diamidino-2-phenylindole (DAPI) followed by epifluorescence microscopy (see Section 2.1.4).

2.1.2. Medium preparation

All cultures of *E.huxleyi* were grown in Enriched Seawater, Artificial Water (ESAW) medium, which allowed us to control the sulphur concentration and ionic strength. The recipe was originally designed by Harrison et al.(1980) for coastal and open ocean phytoplankton and was modified by Berges et al. (2001). The seawater base is composed of anhydrous salts and hydrated salts (Table 2.1) that were prepared separately to prevent precipitates formation. One litre of ESAW was made by dissolving anhydrous and hydrated salts in 600 mL and 300 mL of distilled water, respectively. Next, the solutions were autoclaved, cooled down, aseptically combined and made up to a final volume of 1 L with sterile distilled water. The pH of the prepared synthetic seawater should be ~8.2 and it was always checked before using the medium.

Solutions of macronutrients, iron, trace metals and vitamins (Table 2.2) were prepared separately and stored in 4^{o}C with the exception of vitamin solution which was stored in -20^{o}C. Since these 4 solutions could encourage bacterial growth in the medium, the seawater base was enriched with syringe filter sterilised 1mL L^{-1} aliquots of each solution just before cells inoculation.

Table 2.1 Composition of ESAW media with the final molar concentrations.

Compound	Stock solution ($g\ L^{-1}\ dH_2O$)	Quantity in 1L ESAW	Final concentration in the ESAW medium (M)
Anhydrous salts:			
NaCl		21.194 g	3.63×10^{-1}
Na_2SO_4		3.550 g	2.50×10^{-2}
KCl		0.599 g	8.03×10^{-3}
$NaHCO_3$		0.174 g	2.07×10^{-3}
KBr		0.0863 g	7.25×10^{-4}
H_3BO_3		0.0230 g	3.72×10^{-4}
NaF		0.0028 g	6.67×10^{-5}
Hydrated salts:			
$MgCl_2.6H_2O$		9.592 g	4.71×10^{-2}
$CaCl_2.2H_2O$		1.344 g	9.14×10^{-3}
$SrCl_2.6H_2O$		0.0218 g	8.18×10^{-5}
Macronutrients:			
$NaNO_3$	46.670	1 mL	5.49×10^{-4}
$NaH_2PO_4.H_2O$	3.094	1 mL	2.24×10^{-5}
$Na_2SiO_3.9H_2O$	15.000	1 mL	5.30×10^{-7}
Iron solution		1 mL	
Trace metals solution		1 mL	
Vitamins solution		1 mL	

Table 2.2 Composition of the solutions added to the seawater base with the final molar concentration in the ESAW.

Compound	Stock solution ($g\ L^{-1}$ dH2O)	Quantity used	Final concentration in the ESAW medium (M)
Iron solution:			
$Na_2EDTA.\ 2H_2O$		2.44 g	6.56×10^{-6}
$FeCl_3.\ 6H_2O$		1.77 g	6.55×10^{-6}
Trace metal solution:			
$Na_2EDTA.2H_2O$		3.090 g	8.30×10^{-6}
$ZnSO_4.7H_2O$		0.073 g	2.54×10^{-7}
$CoSO_4.7H_2O$		0.016 g	5.69×10^{-8}
$MnSO_4.\ 4H_2O$		0.540 g	2.42×10^{-6}
$Na_2MoO_4.2H_2O$	1.480	1 mL	6.12×10^{-9}
Na_2SeO_3	0.173	1 mL	1.00×10^{-9}
$NiCl_2.6H_2O$	1.490	1 mL	6.27×10^{-9}
Vitamins solution:			
Thiamine HCl		0.1 g	2.96×10^{-7}
Biotin	1 g	1 mL	4.09×10^{-9}
B12	2 g	1 mL	1.48×10^{-9}

2.1.3. Cell characteristics in culture

The growth of cultures was examined using a Coulter particle counter (Beckman Multisizer 3 Coulter Counter, High Wycombe, UK) with a 100 µm aperture tube. This instrument allowed rapid and precise measure of the *E. huxleyi* growth parameters: cell diameter (µm), cell density (cells mL^{-1}) and cell volume (μm^3 mL^{-1}). The Coulter principle is based on the change in the electric field when a particle (e.g. microalgal cell) from a sample passes through an aperture. The cell suspension has to be diluted such that only one cell passes through the aperture at a time to prevent coincidence. The number of electric pulses is then equal to the number of particles and the amplitude of a pulse is proportional to the volume of the particle. The electric signal is processed and translated to give the particle characteristics and the instrument gives a cell diameter derived from the primary volume measurement assuming that the particle is spherical. To measure the change in *E. huxleyi* parameters during the time course, 100 or 500 µL (depending on the cell density) of culture sample was diluted with filtered seawater to 10 mL of final volume. Seawater background was subtracted from the measured sample.

2.1.4. Testing of *E. huxleyi* culture axenicity by DAPI staining

The stain 4',6-diamidino-2-phenylindole (DAPI) binds to DNA forming a fluorescent complex and was used to detect possible bacterial contamination of microalgal cultures. A sample for DAPI staining was prepared by withdrawing 1-4 mL from the culture and fixing it with 3 µL mL^{-1} of Lugol's iodine (aqueous KI 10 % w/v and iodine 5 % w/v) and 50 µL mL^{-1} of neutralised formalin (20 % aqueous formaldehyde with 100 g L^{-1} hexamine). The mixture was distained with a drop of 3% w/v sodium thiosulphate (stored in 4^{o}C). All 3 solutions were syringe filtered prior addition to the samples. Then, 10 µL mL^{-1} of DAPI solution (Sigma-Aldrich, 1 mg mL^{-1} stock solution, stored at -20^{o}C) was added and the sample was dark-incubated for 15 min. The DAPI stained sample was filtered under vacuum onto a 0.2 µm pore black polycarbonate filter placed on a 0.45 µm pore cellulose nitrate backing filter and washed with sterile seawater. Next the polycarbonate filter was laid on microscope slide bearing a drop of immersion oil. Another drop of immersion oil and a coverslip was put over the filter.

The presence of bacteria was checked by examining the filters under UV light using a fluorescence microscope (Olympus BX40, Essex, UK). Bacteria appeared as small bright dots in the background of large algal cells (Figure 2.1).

2.1.5. Purification of *E. huxleyi* cultures

Although, the rigorous aseptic conditions were applied to avoid contamination of *E. huxleyi*, occasional bacterial infections were unavoidable. In such cases cultures were treated with a cocktail of antibiotics (Jan Strauss, University of East Anglia, personal communication). All the antibiotic stock solutions were prepared by dissolving the solid form in a suitable solvent and passing the solution through a 0.2 µm syringe filter. Aliquots of the stock solutions were stored at -20^{o}C.

The antibiotic treatment was carried out by transferring cells in the mid-exponential growth into fresh medium containing the antibiotic mixture (Table 2.3). Next, cultures were re-grown to the exponential phase. These incubated cells were then inoculated into fresh medium, this time without antibiotics, and the culture was allowed to re-grow again to exponential phase. The effectiveness of the antibiotics treatment was checked by DAPI staining (Figure 2.1).

Table 2.3 Composition of antibiotics mixture added to non-axenic *E. huxleyi* cultures.

Antibiotic	Stock concentration (mg mL^{-1})	Type of solvent	Working concentration (µg mL^{-1})
Ampicilin	15	Milli-Q water	50
Gentamicin	1	Milli-Q water	10
Streptomycin	25	Milli-Q water	25
Chloramphenicol	34	100% ethanol	1
Ciprofloxacin	1	0.1M HCl	10

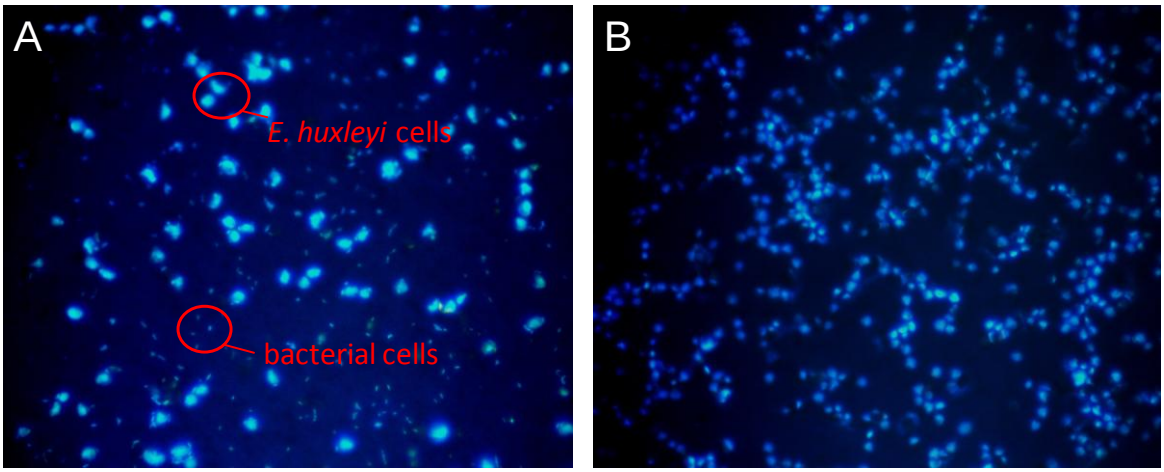

Fig. 2.1 DAPI stained cultures of *E.huxleyi* before (A) and after (B) treatment with antibiotics. No bacteria attached to the cells nor free-living bacteria were observed in the antibiotic-treated cultures.

2.2. DMSP measurements

2.2.1. Sample preparation

The content of particulate dimethylsulphoniopropionate (DMSPp) in *E. huxleyi* was analysed as dimethyl sulphide (DMS) using headspace gas chromatography (GC). The method was adapted from the Steinke et al. (2000) procedure primarily designed for DMSP lyase activity measurements. Depending on the cell density, between 2 and 3 mL of culture was gently filtered by hand vacuum pump (< 10 cm Hg) through 25mm Whatman GF/F filters (nominal pore size 0.7 µm. Whatman UK Ltd., Maidstone, U.K.). These filters were then transferred into 4 mL vials containing 3 mL of 0.5 M NaOH and the vials were immediately closed using a gas-tight screw thread cap with a Teflon faced septum (Alltech, Stamford, UK). Cold alkali hydrolysis of DMSP yields DMS with a 1:1 ratio. Volatile DMS was released to the headspace of the vial. To assure complete DMSP to DMS conversion the samples have been incubated for at least 24 h in darkness at room temperature before they were analysed on the GC.

2.2.2. Gas chromatography- headspace measurement

Following conversion to DMS, DMSPp was quantified using the GC (GC-2010, Shimadzu UK Ltd., Milton Keynes, UK) equipped with a 30 m x 0.53 mm CP-SIL 5CB column (Varian, Oxford, UK) and a flame photometric detector (FPD). The carrier gas was helium with a flow rate 35 mL min^{-1} and the air and hydrogen flame gases had flow rates of 60 and 70 mL min^{-1}, respectively. The temperatures settings were: 200^{o}C, 120^{o}C and 250^{o}C for the injector, column and detector, respectively.
The headspace method was used to measure gaseous DMS in the headspace of 4 mL vials. To achieve equilibrium between DMS in the headspace and in the aqueous phase, prior to GC analysis, vials were incubated for 1 h at 30^{o}C. Fifty µL headspace was withdrawn by the autosampler (Multipurpose Sampler MPS Gerstel, Mülheim an der Ruhr, Germany) equipped with the 100 µL gas-tight syringe and injected into GC for DMS quantification.

2.2.3. Calibration

The GC was calibrated using a duplicate series of known concentration (1-25 µM) of DMSP standards prepared in identical vials to those used for experimental samples. In each case the appropriate volume (4-10 µL) of DMSP stock solution was placed on the septum inside the cap and very carefully and rapidly inverted to seal a vial containing 3 mL of 500 mM NaOH. In this way the DMSP did not come into contact with the NaOH until the vial was closed and shaken. The calibration was obtained by relating detection signal as the square root of the peak area (y) to DMSP concentration (x). The linear relationship $y=ax+b$, where a is the slope and b the intercept, was used to quantify the DMSPp concentration in each sample. DMSP concentrations in the samples were always in excess of that in the lowest calibration standard.

2.3. APS reductase Activity (APR)

Adenosine 5'-phosphosulphate (APS) reductase (APR) activity was measured as the the formation of [^{35}S] sulphite from [^{35}S] APS and dithioerythritol (DTE) (Brunold 1990) with a modification of a procedure described by Kopriva et al. (1999). The culture was concentrated by centrifuging for 10 min at 10000 x g. The supernatant was removed and the pellets were re-suspended in 1.5 mL of fresh culture medium and centrifuged at 10000 x g for 5 min. The pellets from the second centrifugation step were snap frozen in liquid nitrogen and stored at -80^{o}C until analysis.

A crude extract was generated by sonication (Soniprep 150, MSE, London, UK) of the frozen pellet in 500 µL extraction buffer (50 mM Na/KPO_4 adjusted to pH 8; 30mM Na_2SO_3; 0.5 mM, adenosine 5'monophosphate (AMP) and 10 mM DTE, dithioerythritol). The extracts were centrifuged for 30 s at 400 rpm to remove cell debris. To measure activity, 20 µL of supernatant was added to 240 µL of reaction assay mixture (Table 2.3) in a 1.5 mL tube without lid and incubated for 30 min at 37^{o}C. After incubation, 100 µL of 1M Na_2SO_3 was added and the tubes were transferred into 20 mL scintillation vials filled with 1 mL of 1 M triethanolamine solution. Two hundred µL 1 M H_2SO_4 was added to the tubes, the vials were closed immediately and incubated overnight at room temperature. The acidification of the reaction mix causes the [^{35}S]sulphite to form gaseous [^{35}S]SO_2 which is trapped in the triethanolamine solution. The next day the tubes were removed from the vials, their bottoms washed with 200 µL water and 2.5 mL scintillation ncoctail Optisafe 3 (Perkin Elmer) were added. Sulphur radioactivity was determined in a scintillation counter (Wallac 1409 Liquid Scintillation Counter).

Table 2.4 Composition of the APR reaction assay mixture.

Component	Concentration	Volume (µl)
2-amino-2-(hydroxymethyl)-1,3-propanediol (Tris) - HCl, adjusted to pH 9	1 M	25
Magnesium sulphate ($MgSO_4$)	2 M	100
Dithioerythritol (DTE)	200 mM	10
Adenosine [^{35}S]5'phosphosulphate (APS), specific activity 1kBq /10 µL	3.75 mM	5
H_2O		100

Total protein concentration in the extract was measured with a Bio-Rad protein assay kit (Bio-Rad Laboratories, München, Germany) based on the method of Bradford (1976). The cell extracts (100-200 µL) was diluted with distilled water to 800 µL and then 200 µL of Bio-Rad protein assay was added to give a final volume of 1 mL. The mixture was incubated for 15 min at room temperature and the protein level was determined by measuring absorbance at 595 mm using uv-vis spectrophotometer (Lambda Bio, Bucks, UK). Bovine serum albumin was used as the protein standard.
The APR activity (nmol min^{-1} mg $protein^{-1}$) was calculated according to the formula:

$$\mathrm{APR_{activity}} = \frac{37.5 \times \mathrm{cpm}}{\mathrm{cpm_{APS}} \times \mathrm{C_{prot}} \times \mathrm{V_E} \times \mathrm{T}}$$

where:

cpm_{APS} = specific activity (counts per minute, cpm) of APS reductase activity (APR)
C_{prot} = protein concentration in extract (mg mL^{-1})
V_E = volume of extract in the assay (mL)
T = time of incubation (min)

2.4. HPLC analysis of low molecular weight thiols

Algal cells were collected by gentle (< 5 psi) filtration of 15 to 25 mL (depending on density of culture) through a 25 mm diameter GF/F filter, which was then snap frozen in liquid nitrogen and stored at -80^{o}C until extraction and analysis. Thiol extraction was carried out according to Dupont et al. (2004). Briefly, the filters were placed into a grinding chamber containing 2 mL of 10 mM methanesulphonic acid (MSA) and incubated at70^{o}C for 2 min, chilled on ice and then homogenised with a Wheaton Overhead Stirrer. The resultant cellular homogenate was then centrifuged for 10 min at 16060 x g and 4°C. Then 800 µL of supernatant was taken and adjusted to pH 9 by adding 84 µL of 100 mM tetraborate buffer supplemented with 10 mM diethylenetriaminepentaacetic acid (DTPA). The analysis of cysteine (Cys) and glutathione (GSH) was performed following the method of Koprivova et al. (2008). In order to reduce disulfides, 50 µL of pH 9 extract was incubated in the dark at 37°C for 15 min with 1 µL of 100 mM dithiothreitol (DTT). Afterwards, 35 µL water, 10 µL of 1 M Tris pH 8 and 5 µL of 100 mM monobromobrimane (Thiolyte® MB, Calbiochem) were added and the derivatisation reaction was allowed to proceed in dark at 37°C for 15 min.

The reaction was stopped by adding 100 µL of 9 % acetic acid. Analyses were performed on a Waters 2695 HPLC (Waters Ltd., Elstree, U.K.) equipped with a reverse-phase column (Spherisorb^{TM} ODS2, 250 x 4.6 mm, 5 µm, Waters). Monobromobrimane derivates were quantified by fluorescence detection (474 detector, Waters) with excitation at a wavelength of 390 nm and emission at 480 nm. The optimal separation of thiols was achieved using a linear eluting gradient program (Table 2.4)
Standards of GSH and Cys were analysed to verify retention times and to develop standard curves for peak area calibrations.The calibration curve and retention times were established by plotting peak areas *vs.* GSH and Cys standards (0.025, 0.0625, and 0.125 nmol).

Table 2.5 Elution gradient programme for optimised GSH and Cys analysis. Solution A was 10% (v/v) methanol, 0.25% (v/v) acetic acid (pH adjusted to 3.9) and solution B was 90% (v/v) methanol, 0.25% (v/v) acetic acid (pH adjusted to 3.9). The flow rate of the solvent pump was kept constant at 1 mL min^{-1}.

Mobile phase A (%)	Mobile phase B (%)	Time (min)
96	4	0
86	14	2
84	16	22
0	100	28
96	4	34

2.5. Statistical analysis

All data were submitted to statistical analysis of standard deviation and t-test using Microsoft Excel unless otherwise stated. Only differences with p-value < 0.05 were considered significant.

3. Physiological and biochemical responses of *E. huxleyi* to sulphur availability

3.1. Introduction

Sulphur is an essential mineral nutrient, therefore, its deficiency has severe consequences for photosynthetic organisms as described in detail in Chapter 1. Since sulphur is important for crop yield and quality, sulphur metabolism has attracted considerable attention (for review see Takahashi et al. 2011). However, published investigations have focused on higher plants and freshwater green algae and, accordingly, rather little is known about sulphur metabolism in marine phytoplankton. The rationale for the low interest is the fact that, unlike nitrogen or phosphorus, sulphate is present in high concentration in the ocean (~28 mM) and so is not considered to limit growth. On the other hand, isotopic measurements indicate that sulphate concentration in the ocean fluctuated across the geological history of the Earth and this may have influenced algal evolution (Gill et al. 2007; Gill et al. 2011). Indeed, coccolithophorids along with diatoms and dinoflagellates, flourished in the oceans between Palaeozoic and Mesozoic when sulphate concentration varied from 13 to 27 mM (Ratti et al. 2011). This may suggest that these taxa achieved evolutionary success in the ocean because of the high sulphate concentration. Since the ocean is S-replete, many marine algae synthesise significant amounts of S-metabolites including DMSP. Indeed, Matrai and Keller (1994) reported that DMSP may account for between 50 to 100% of the total organic sulphur in some marine microalgae, though the 100% value must be an overestimate (see Chapter 1). This has implications for the global sulphur cycle through the DMSP breakdown product, DMS, some of which is liberated to the atmosphere. As *Emiliania huxleyi* accumulates high levels of DMSP, we examined the physiological and biochemical responses of this phytoplankton species to sulphur availability.

Initially we tested the response of *E. huxleyi* to a range of sulphate concentrations using a chemically defined seawater medium. This allowed us to established S-limited conditions for further experiments. We also compared the effect of sulphate depletion in three different strains of *E. huxleyi*. Further experiments were designed based on previously published data on the physiological and metabolic reaction to sulphur limitation in plants and/or chlorophytes. Thus, we investigated the effect of sulphate availability on sulphate uptake, 5'-adenylsulphate reductase (APR) activity and thiol concentrations.

The results described in this chapter were also the foundation for a molecular study using RNA sequencing of S-limited versus S-replete *E.huxleyi*, and they helped us to draw a meaningful analysis of the transcriptomic results discussed in Chapter 5.

3.2. Materials and Methods

3.2.1. *E. huxleyi* response to sulphur limitation

Three biological replicate batch cultures of *E. huxleyi* were grown in 250 mL conical flasks containing 150 mL of ESAW medium containing 25, 10, 5 or 1 mM Na_2SO_4. The ionic strength was kept constant in all media by increasing concentration of NaCl and cultures were grown as described in Chapter 2. The experiment commenced when media were inoculated with exponentially growing stock culture (ESAW, 25 mM Na_2SO_4) to give an initial cell density of ~4 x 10^4 cells mL^{-1}. Culture growth parameters (cell number, culture biovolume and cell volume) were measured on a daily basis, whereas samples for intracellular DMSP and maximum efficiency of PS II (Fv/Fm) measurements were taken every other day.

3.2.2. Comparison of growth and DMSP synthesis between *E. huxleyi* strains: CCMP 1516, 370 and 373

Triplicate batch cultures of *Emiliania huxleyi* strains CCMP 1516, 370 and 373 were grown in 500 mL conical flasks with 250 mL of 25 or 5 mM SO_4^{2-} medium. Cultures were inoculated with exponentially growing stock culture to give an initial cell density of ~1 x 10^4 cells mL^{-1}. Cell growth was monitored on a daily basis and samples for intracellular DMSP were taken every other day starting from day 3.

3.2.3. Sulphate uptake

To measure sulphate uptake, triplicate *E. huxleyi* cultures were grown in 500 mL conical flasks 250 mL ESAW medium containing 25 mM (control) and 5 mM SO_4^{2-}. When cultures entered exponential phase, 50 mL (control) or 100 mL (5mM SO_4^{2-}) of each culture was filtered onto a 47-mm diameter, 1.2 µm filter (Millipore™ Membrane Filter), and then washed with S-free medium to remove sulphate. The cells were re-suspended in 50 mL tubes with 10 mL ESAW medium containing 25 mM or 5 mM sulphate. The cell density and volume was determined in each tube. [^{35}S]sulphate was added to the cultures to a specific activity of 192 kBq mL^{-1} (Hartman Analytic) and the cells were incubated for 60 min in the light. After the incubation, the cells were collected by filtration, washed extensively with S-free medium and placed into 20 mL scintillation vials. To dissolve the filters and disrupt the cells, 5 mL of tissue solubiliser (Solene®-350, PerkinElmer, www.perkinelmer.co.uk) was added and the vials were kept overnight at room temperature. The next day 10 mL of scintillation cocktail Optisafe 3 (Perkin Elmer) was added and [^{35}S] radioactivity was determined in a scintillation counter (Wallac 1409, Perkin Elmer).

3.2.4. Collection of samples for APS reductase activity time course

E. huxleyi batch cultures were grown in 500 mL conical flasks with 250 mL of 25 mM or 5 mM SO_4^{2-} medium. Cultures were inoculated with exponentially growing stock culture to give an initial cell density of ~5 x 10^4 cells mL^{-1} and cell growth was monitored daily. Samples for APR activity and DMSP analysis were collected at 5 time points representing the different culture growth phases. For enzyme assays cells were harvested with a 2-step centrifugation. Firstly, 25 mL aliquots were centrifuged for 10 min at 10000 x g and 4^{o}C, and then the cell pellets were re-suspended in 1.5 mL of ESAW medium and centrifuged for 10 min at 10000 x g and 4^{o}C. The samples were snap-frozen in liquid nitrogen and stored at -80^{o}C prior to APR activity analysis (see Chapter 2).

3.2.5. Collection of samples for measurements of thiols time course.

To measure cysteine (Cys) and glutathione (GSH) in *Emiliania huxleyi*, triplicate batch cultures were grown in 1 L conical flasks with 500 mL of 25 mM or 5 mM SO_4^{2-} medium. Cultures were inoculated with an exponentially growing stock culture to give an initial cell density of ~5 x 10^4 cells mL^{-1}. Samples were taken at 3 time points representing the mid-, late-exponential and stationary phases of culture growth. Depending on the cell concentration, between 15 and 30 mL of culture was filtered onto a 25 mm diameter GF/F filter, snap-frozen in liquid nitrogen and stored in -80^oC prior to extraction and analysis (see Chapter 2).

3.2.6. *E.huxleyi* growth and DMSP production in response to S-compounds resupply

Sulphate resupply

Sulphate was added back to S-limited (5 mM SO_4^{2-}) cultures of *E. huxleyi* using two different approaches. Figure 3.1 shows the scheme for the first approach. Briefly, *E. huxleyi* batch cultures were grown in 2 L conical flasks with 1.2 L of 25 or 5 mM SO_4^{2-} ESAW medium. Cultures were inoculated with exponentially growing stock. After *E. huxleyi* had been grown in control and S-limited media for 10 days, cultures were split into 3 duplicate sets of 250 mL each. From the S-limited cultures, one set was resupplied with 20mM SO_4^{2-} and the other set was left without extra sulphate. The third set derived from the S-replete culture. All 3 sets were balanced in terms of ionic strength by adding NaCl to the S-limited cultures. Aliquots of dissolved Na_2SO_4 and NaCl were sterilised using a disposable syringe filter (0.2 µm). The culture growth and intracellular DMSP were measured every 24h before and after sulphate restoration.

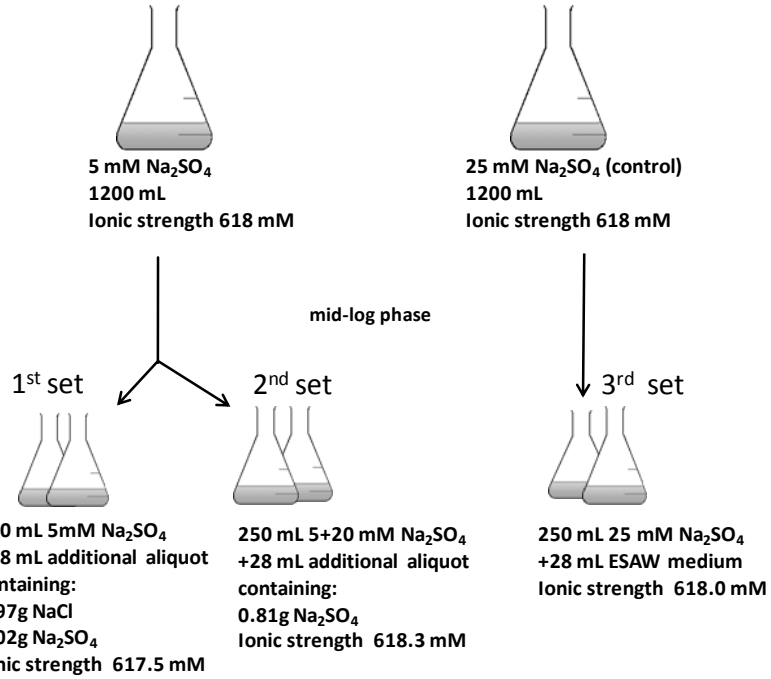

Figure 3.1 Experimental design used in sulphate replenishment experiment (1st approach).

In the second approach, triplicate batch cultures were grown in 500 mL conical flasks with 200 mL of 25 or 5 mM SO_4^{2-} medium. All cultures were inoculated with exponentially growing stock culture grown in standard ESAW medium. The experiment commenced when cultures were in exponential phase and there was a significant difference in cell density and intracellular DMSP between the control and low-S cultures. At this point, 20 mM SO_4^{2-} was added into one set of S-limited cultures. The S-limited and S-replete cultures were again adjusted with NaCl to have the same ionic strength. Samples were taken every 24 h to measure growth parameters, intracellular DMSP and APR activity.

Cysteine and methionine resupply

Triplicate *E. huxleyi* batch cultures were grown in 250 mL conical flask with 150 mL of 25 or 5 mM SO_4^{2-} medium. The experiment was carried out in the same manner as the one described above. S-compounds added to S-limited cultures were sterile aliquots of L-cysteine or L-methionine (Sigma-Aldrich, UK) used at a final concentration of 0.2 and 1mM for Cys or 0.1 and 0.5 mM for Met.

Equimolar S-compounds resupply

To test the response of S-limited *E. huxleyi* culture to addition of equimolar concentrations of different S-compounds a final concentration of 5 mM sulphate, L-cysteine or L-methionine was used. The experiment was carried out with the approach described above

3.2.7. Salinity down-shock

Water of two different salinities was prepared by diluting standard ESAW medium to 80% and 70% with Milli-Q water. In order to maintain the same sulphur and pH status in all 3 salinities, the concentration of sodium sulphate (Na_2SO_4) and sodium bicarbonate ($NaHCO_3$) was adjusted in the media (to standard ESAW concentration) and the autoclaving procedure was replaced by filter sterilisation. Triplicate cultures (250 mL conical flask, 50 mL medium) were inoculated with exponentially growing stock culture to give an initial cell density of ~$5x10^4$ cells mL^{-1} Cell growth was monitored daily, whereas samples for intracellular DMSP were taken at 3 time points of the culture growth: day 4, 7 and 8 representing log, linear and stationary growth phases, respectively.

3.3. Results

3.3.1. *E. huxleyi* response to sulphur limitation

The effect of sulphate availability on *E. huxleyi* growth and capacity for noncyclic photosynthetic electron flow (Fv/Fm) was examined over 13 days in batch cultures grown in ESAW media containing various sulphate concentrations: 25 (control), 10, 5 and 1 mM (Figure 3.2; Table 3.1). The data show that lowering sulphate concentration down to 10 mM had only a marginal effect on the cell growth (Fig 3.2, A). The specific growth rate measured around day 6 in the logarithmic growth phase was 0.62 (±0.03) and 0.58 (±0.02) d^{-1} in the control and 10mM SO_4^{2-} cultures, respectively. This indicated that even 2.5-fold reduction in sulphate did not inhibit cell division. In contrast, at 5 mM of SO_4^{2-} the growth rate was reduced by ~50% (0.30 ±0.04 d^{-1}). When sulphate concentration was further lowered to 1 mM, the *E. huxleyi* culture was unable to grow (Figure 3.2, A). The decrease in the specific growth rate of the culture exposed to the low sulphate concentration was paralleled with an increase in overall volume of the cell (Figure 3.2, B). The average cell volume was the same at 25 and 10mM SO_4^{2-} and decreased throughout the time course to ~50% of the initial values. Contrary to this, we observed that *E. huxleyi* grown at 5 and 1mM SO_4^{2-} had significantly bigger cell volumes than cells grown at the higher sulphate concentration. Moreover, in the 1 mM SO_4^{2-} culture the cell size increased sharply over the time course attained ~6-fold bigger volume than control but did not divide. Surprisingly, Fv\Fm (the apparent efficiency of photosystem II) measured in dark-adapted samples (Figure 3.2, C) did not show a clear response to low sulphate conditions, the exception being 1mM SO_4^{2-} where there was an initial drop to 0.41 (±0.01) and then the Fv\Fm recovered to within the range recorded for the cultures grown with higher sulphate concentration.

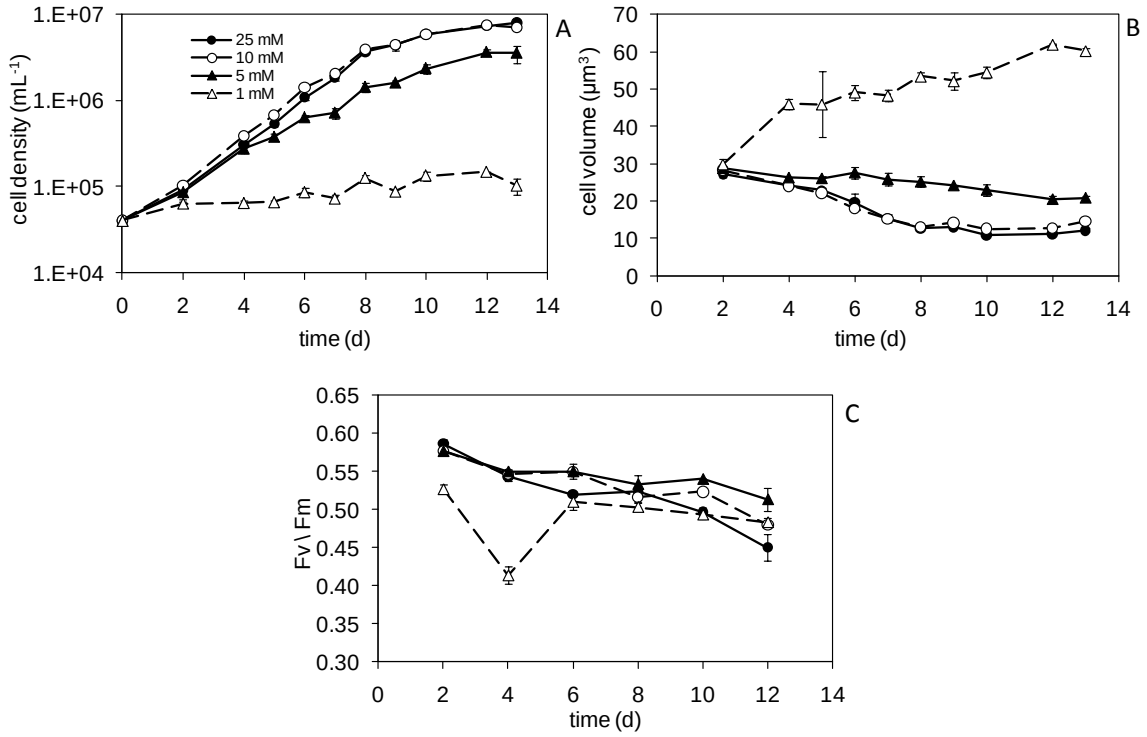

Figure 3.2 Cell density (A), cell volume (B) and efficiency of photosystem II (C) from batch cultures of *Emiliania huxleyi* grown at 4 different sulphate concentrations. Results are shown as means ±standard deviation from 3 biological replicates. In this and subsequent figures error bars are sometimes invisible when they fall within the symbol.

Table3.1. Specific growth rate (d^{-1}), cell volume, photosynthetic efficiency and intracellular DMSP during *E.huxleyi* exponential growth at 25, 10, 5 and 1mM sulphate. Values in brackets are standard deviation of biological triplicate.

$[SO_4^{2-}]$	Growth rate (d^{-1})	Cell volume (μm^3)	Photosynthetic efficiency (Fv\Fm)	DMSP (mM)
25 mM	0.62 (± 0.03)	19.61 (± 2.27)	0.52 (± 0.00)	256 (± 35)
10 mM	0.58 (± 0.02)	17.89 (± 0.60)	0.55 (± 0.00)	184 (± 4)
5 mM	0.30 (± 0.04)	27.64 (± 1.64)	0.55 (± 0.01)	113 (± 4)
1 mM	0.05 (± 0.02)	49.17 (± 1.98)	0.51 (± 0.01)	65 (± 1)

Intracellular DMSP was also measured in the *E. huxleyi* cultures grown under the various sulphate conditions. DMSP concentration was normalised to cell number and cell volume (Figure 3.3). Given that cell volume changed with the S status of the medium and also depended on the growth phase, the data can only be properly compared when DMSP content is calculated on a cell volume basis. For this reason, in the subsequent experiments only DMSP data expressed per cell volume is shown.

Under control growth conditions intracellular DMSP was relatively stable and at a high level (~250 mM, Table 3.1). On the other hand, cells that grew under low sulphate showed a notable reduction in DMSP content. In all S-limited cultures we observed a continuous decrease in DMSP concentration until day 8 when it dropped to about 68, 28 and 20% of the control value at 10, 5 and 1 mM SO_4^{2-}, respectively. It is noteworthy that at10 mM SO_4^{2-} DMSP production was altered but cell growth was not affected, whereas cultivation at 5 and 1 mM of SO_4^{2-} decreased both cell growth and DMSP accumulation. This experiment indicated that a 5 fold reduction in sulphate in the medium results in reduction in growth rate and apparent DMSP biosynthesis, whilst the cell density was high enough to allow cell harvesting. Thus 5 mM SO_4^{2-} was chosen as the low-S condition for the subsequent experiments.

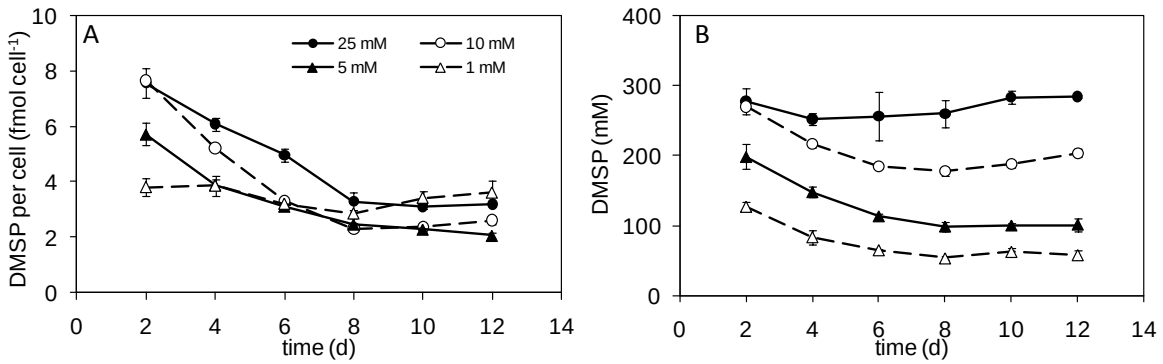

Figure 3.3 DMSP concentration normalised to cell number (A) and cell volume (B) for batch cultures of *Emiliania huxleyi* grown under 4 different sulphate concentrations. Results are shown as means ±standard deviation from 3 biological replicates.

3.3.2. Comparison of the growth and DMSP concentration *E. huxleyi* strains: CCMP 1516, 370 and 373

Cultures of *E. huxleyi* strains CCMP 370, 373 and 1516 (used in this experiment as the control) were grown in ESAW medium containing 25 and 5 mM SO_4^{2-}. These strains were chosen for the experiment based on the work carried out by Steinke et al. (1998), who demonstrated variation in intracellular DMSP level and DMSP lyase activity among 6 *E. huxleyi* strains. CCMP 370 was characterised as a high intracellular DMSP content /low DMSP lyase activity strain, whereas 373 had high intracellular DMSP content/ high DMSP lyase activity. The data obtained here show that these 3 strains did not respond uniformly to sulphate depletion (Figure 3.4). The specific growth rates measured in the exponential phase (days 2 and 7) of the S-limited cultures were 0.47 (± 0.03), 0.71 (±0.05) and 0.73 (± 0.00) d^{-1} for *E. huxleyi* strains 1516, 370 and 373, respectively. It should be noted that the cell abundance decreased in S-limited strains 1516 and 370, whereas the growth of strain 373 was unaffected by SO_4^{2-} limitation. Similar to previous experiments, in strain 1516, the growth rate of low-S cells was not significantly different (Student's t-test; $p>0.05$) from the control until day 7. After that day growth decreased markedly with cell density reaching ~50% of the control (Figure 3.4). On the other hand, the response of strain 370 to SO_4^{2-} reduction was already observed after day 1 with the growth rate in exponential phase significantly different (Student's t-test, $p<0.05$) from the control.

Intracellular DMSP concentration was measured in all the *E. huxleyi* strains every other day between days 3 and 14 and showed a similar trend in all strains (Figure 3.4). As with cell density, DMSP concentration in 1516 and 370 exhibited a decrease in the low sulphate medium. In the exponential phase DMSP decrease was slightly less marked in 1516 (by ~35%) than in 370 (by~50%). In *E. huxleyi* 373, lowering sulphate concentration in the medium had no apparent effect on DMSP production during exponential growth, though a small decrease in DMSP level of ~20% was seen when S-limited cells entered late exponential/early stationary growth (Figure 3.4). In doing this experiment we demonstrated that in *E. huxleyi* the reaction to reduction in sulphur availability, in terms of growth and DMSP concentration was strain specific.

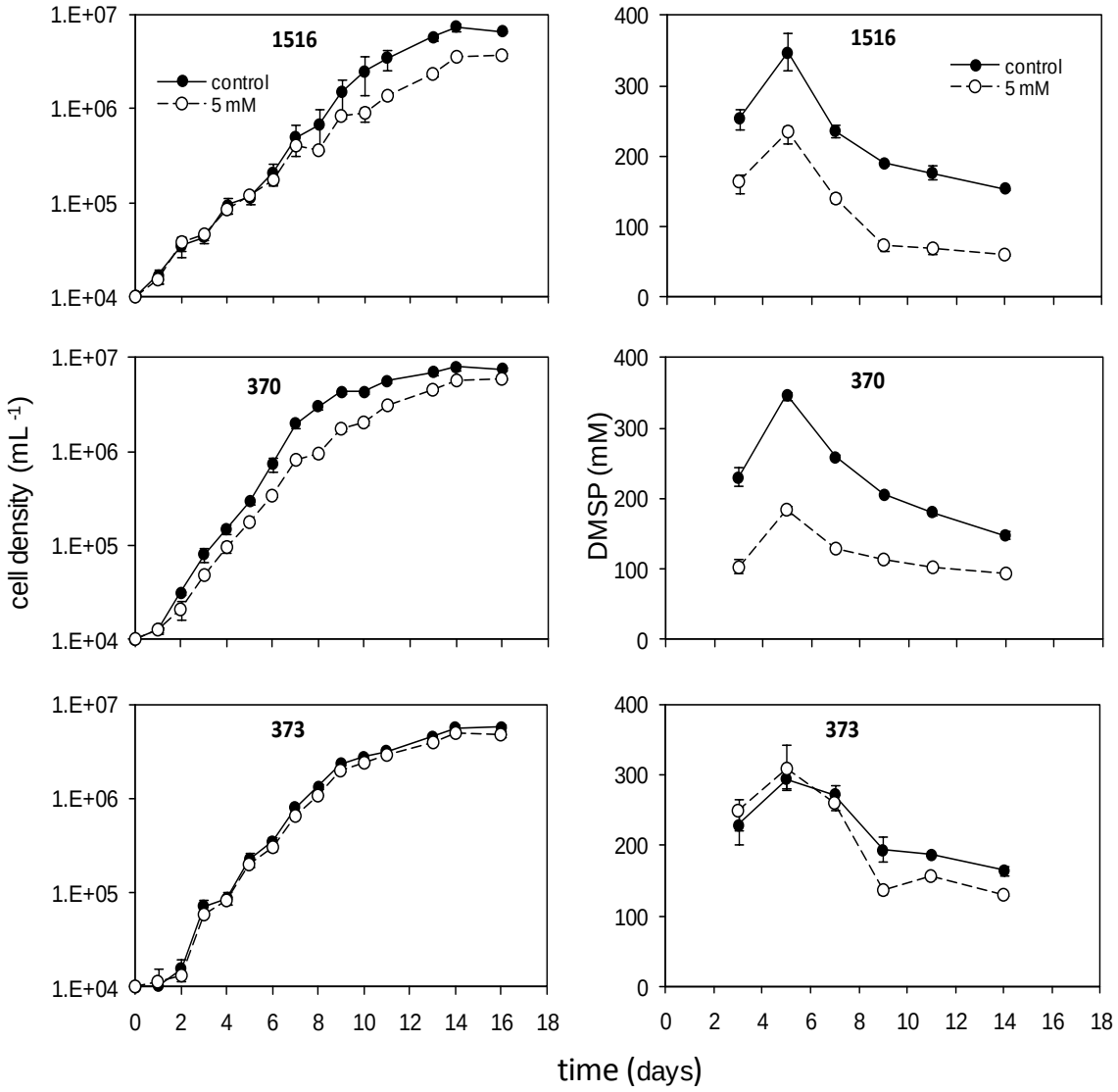

Figure 3.4 Changes in cell density (mL^{-1}) and intracellular DMSP concentration (mM) over the time course for *E. huxleyi* strains 1516, 370 and 373 grown in 25 mM and 5 mM SO_4^{2-} Results are shown as means ±standard deviation from 3 biological replicates.

3.3.3. Sulphate uptake

In plants and *C. reinhardtii* a typical response to sulphate starvation is an increase in sulphate uptake capacity (Takahashi et al. 2011). Therefore we analysed the effect of low sulphate concentration on its acquisition by *E. huxleyi* using incubation with $^{35}SO_4^{2-}$. The sulphate uptake was tested in 4 different scenarios:

(i) control culture incubated in control medium (25 in 25);

(ii) control culture incubated in low SO_4^{2-} medium (25 in 5);

(iii) low SO_4^{2-} culture incubated in control medium (5 in 25) and

(iv) low SO_4^{2-} culture incubated in low SO_4^{2-} medium (5 in 5).

The results from this experiment are presented in Figure 3.5. On the day of the incubation with radioactive sulphate the specific growth rates were 0.55 (±0.03) and 0.36 (±0.02) d^{-1} in the control and low S media, respectively. Cells grown in 5 mM SO_4^{2-} showed ~3-fold higher uptake capacity than control cells in both 25 mM and 5 mM incubation medium. The uptake was higher in 25 mM medium than in 5 mM medium for both types of culture indicating a very low affinity of the sulphate uptake system in *E. huxleyi*. These results are consistent with an increase in sulphate uptake in sulphur deficient plants and were corroborated by expression analysis showing induction of mRNA encoding for sulphate transporters upon sulphate limitation (see Chapter 4).

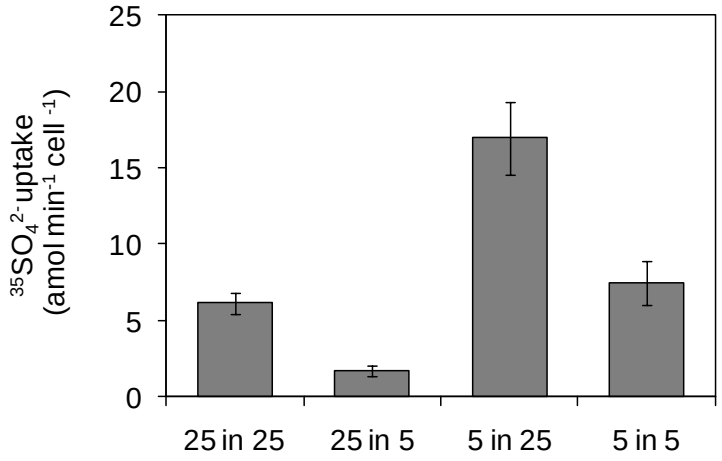

Figure 3.5 *E. huxleyi* sulphate uptake normalised to cell number. Labels on the x axis indicated 4 different experimental conditions for $^{35}SO_4^{2-}$ uptake: 25 in 25, cells grown and incubated in 25 mM SO_4^{2-}; 25 in 5, cells grown in 25 mM but incubated in 5 mM SO_4^{2-}; 5 in 25 cells grown in 5mM but incubated in 25 mM SO_4^{2-}; 5 in 5, cells grown and incubated in 5 mM SO_4^{2-}. Results are shown as means ±standard deviation from 3 biological replicates.

3.3.4. APS reductase activity

APS reductase (APR) activity is another indicator of sulphur status of plants as it is strongly induced by sulphate deficiency (Takahashi et al. 2011). Therefore the activity was measured over the time course of batch culture growth in control (25mM) and low sulphate (5mM) conditions (Figure 3.6). The time points when cells were harvested for the APR activity measurements corresponded to the different phases of *E. huxleyi* growth. At day 4 in the early stage of exponential growth, cells in control medium showed ~48% higher APR activity compared to S-limited cells (Student's t-test, $p<0.05$). By contrast, on day 7 when cultures were in mid-exponential stage, we observed no significant difference (Student's t-test, $p>0.05$) between control and low-S cultures (Figure 3.6). This was due to an increase in APR activity in S-limited cultures to ~40 nmol min^{-1} mg $protein^{-1}$ whereas APR activity in the controls stayed unchanged. This indicates that even with 5-fold lower SO_4^{2-} concentration, cells were able to maintain APR activity at a similar level to the control and that, in contrast to plants, in *E. huxleyi* the enzyme is not regulated by sulphate limitation. On day 9, APR activity dropped in both control and S-limited cultures and this coincided with a decline in the growth rate between day 8 and day 9 in all the cultures. At the following time points (day 11 and day 13) in the late exponential and early stationary growth phases activity was higher for all cultures than on day 9. Comparable levels of APR activity were measured on day 13 in both conditions, whereas there was ~2 fold lower intracellular DMSP concentration in the S-limited cultures (Figure 3.6, C and D). Interestingly, the level of enzyme activity we found in *E.huxleyi* was about 10-fold higher than usually measured in higher plants or green algae.

The results from these APR activity assays were consistent with transcriptome results (see Chapter 5) where mRNA encoding APS reductase was very abundant but not differently regulated in *E. huxleyi* grown under low S condition.

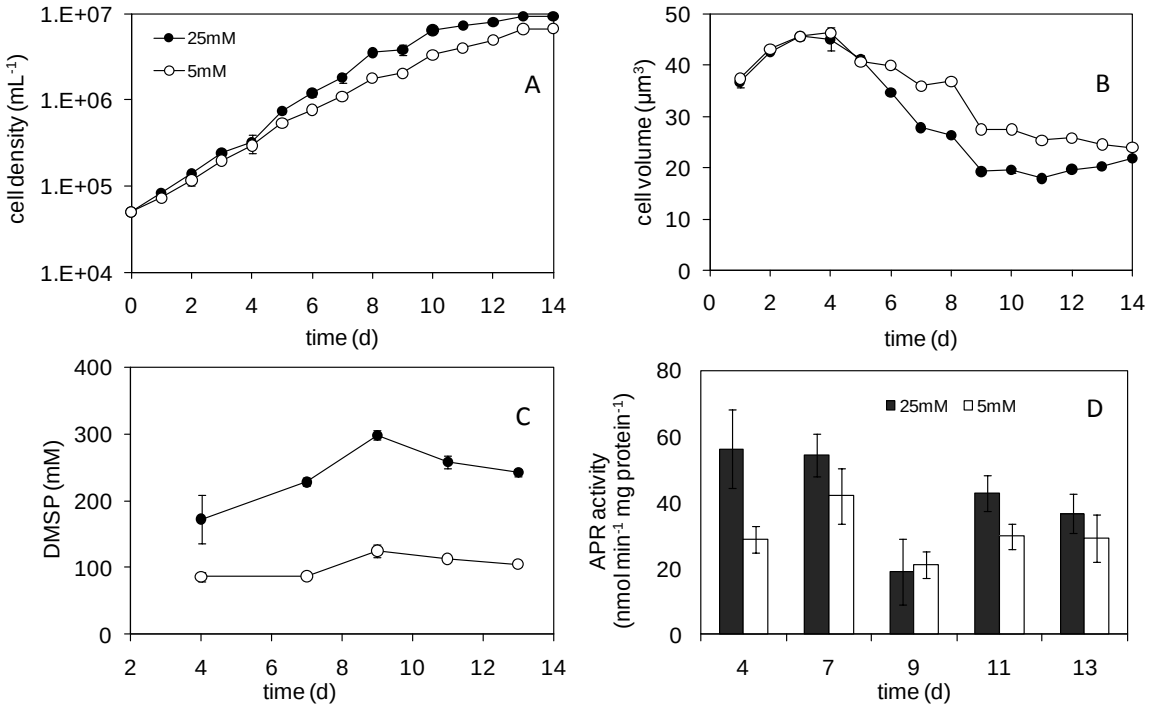

Figure 3.6 Changes in cell density (mL^{-1}) (A), cell volume (μm^3) (B), and intracellular DMSP concentration (mM) (C) and APR activity (nmol min^{-1} mg $protein^{-1}$) (D) over the time course of growth of *E. huxleyi* in 25 mM (black symbols) and 5 mM SO_4^{2-} (white symbols). Results are shown as means ±standard deviation from 3 biological replicates.

3.3.5. Thiol concentrations over the time course

The concentrations of cysteine (Cys) and glutathione (GSH) were measured in *E. huxleyi* cultures grown in 25 and 5 mM SO_4^{2-} (Table 3.2). Samples were taken at 3 different time points (days 3, 6 and 10) corresponding to mid-, late exponential and early-stationary phase. The specific growth rate and thiol content in these phases are shown in Table 3.2. The accumulation of cellular Cys declined markedly from 2.57 mM on day 3 to 0.79 mM on day 10. There was no significant difference in amount of Cys between control and low-S cultures over the time-course (Student's t-test, $p>0.05$). This suggests that, despite lowering the sulphate in the medium, *E. huxleyi* maintained the intracellular Cys homeostasis that is needed for synthesis of essential metabolites. GSH concentrations were in the same range as for Cys, however significant differences (Student's t-test, $p<0.05$) were observed between the 25 and 5 mM SO_4^{2-} cultures. GSH concentrations increased by about 20% between day 3 and day 10 in the control cultures (Table 3.2). By contrast, under low-S conditions, the GSH pool was similar to that of the control culture at day 3 but decreased to 50% of the control concentration at the end of the exponential phase (day 10).

Table 3.2 Specific growth rate and the concentrations (mM) of the thiols cysteine (Cys) and glutathione (GSH) in *E. huxleyi* grown under control (25 mM) and sulphate limited (5 mM) conditions. Values in brackets are standard deviation of biological triplicates.

	Control			Low S		
	Growth rate (d^{-1})	Cys (mM)	GSH (mM)	Growth rate (d^{-1})	Cys (mM)	GSH (mM)
Mid-log (day3)	0.63 (±0.07)	2.57 (±0.38)	2.71 (±0.17)	0.60 (±0.11)	2.70 (±0.36)	2.46 (±0.17)
Late-log (day 6)	0.58 (± 0.04)	0.97 (±0.05)	2.35 (±0.27)	0.38 (± 0.07)	1.08 (±0.05)	1.34 (±0.16)
stationary (day 10)	0.19 (±0.03)	0.79 (±0.05)	3.47 (±0.18)	0.25 (± 0.02)	0.75 (±0.05)	1.75 (±0.30)

3.3.6. *E. huxleyi* responses to sulphur re-supply

To confirm that sulphate indeed affects *E.huxleyi* growth we tested whether the slower growth at 5 mM sulphate can be restored after sulphate re-supply and two different experimental approaches were used for this. In the first approach, (Figure 3.7) the initial S-limited batch (5 mM SO_4^{2-}) was split into 2 duplicate sets. One set was supplemented with 20 mM SO_4^{2-}, whereas in another set the sulphate concentration was maintained. Adding sulphate to S-limited cultures resulted in ~20% increase in cell density compared to the unchanged cultures after 72 h (Figure 3.7, A). Similarly, the cell volume gradually decreased after re-supply of sulphate, although after 72 h the cells in 5+20 mM media were still larger than control cells (Figure 3.7, B). This was accompanied by a rapid increase in the intracellular DMSP pool which reached, within 72 h, the same level of DMSP (~250 mM) as in the control cultures (Figure 3.7, C).

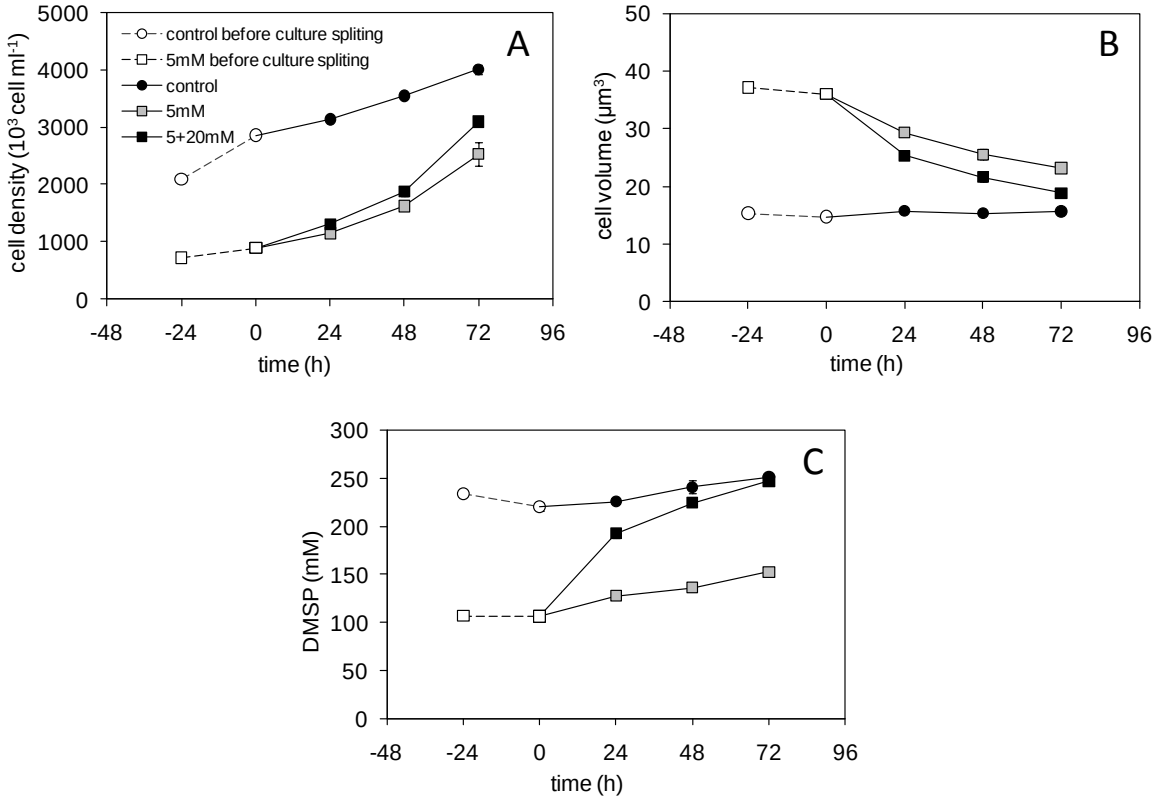

Figure 3.7 Effect of 20mM sulphate addition on the growth of S-limited *E. huxleyi* (A), cell volume (B) and intracellular DMSP (C). Dashed lines indicated before splitting and sulphate replenishment. Results are shown as means ±standard deviation from 3 biological replicates.

The second experimental approach also used triplicate batch cultures and confirmed the observations described above. The experiment started with cells that were in late exponential phase. At that time point (marked on the x-axis as 0, Figure 3.8) the S-limited cultures showed about 2 fold lower cell density and intracellular DMSP concentration compared to the sulphate sufficient controls. The addition of 20 mM SO_4^{2-} resulted in a rapid increase in the specific growth rate; 0.32 (±0.03) d^{-1} when sulphate was re-supplied compared with 0.15 (±0.01) d^{-1} in the sulphate-limited cultures. This increase was accompanied by a ~30% decrease in the cell volume which may indicate an enhancement of cell division capacity upon sulphate addition. Sulphate restoration enhanced DMSP accumulation with a dramatic increase within 72 h from 89 (± 8) to 238 (±6) mM (Figure 3.8, C). By the end of the experiment the DMSP concentration in the sulphate re-supplied cultures reached the level of sulphate–sufficient cultures. Unlike DMSP, APS reductase activity was not significantly different (Student's t-test, $p>0.05$) between cultures with different sulphate status, and after a decrease at 24 h it stayed within the same range of ~ 40 nmol min^{-1} mg protein $^{-1}$ over the time course (Figure 3.8, D).

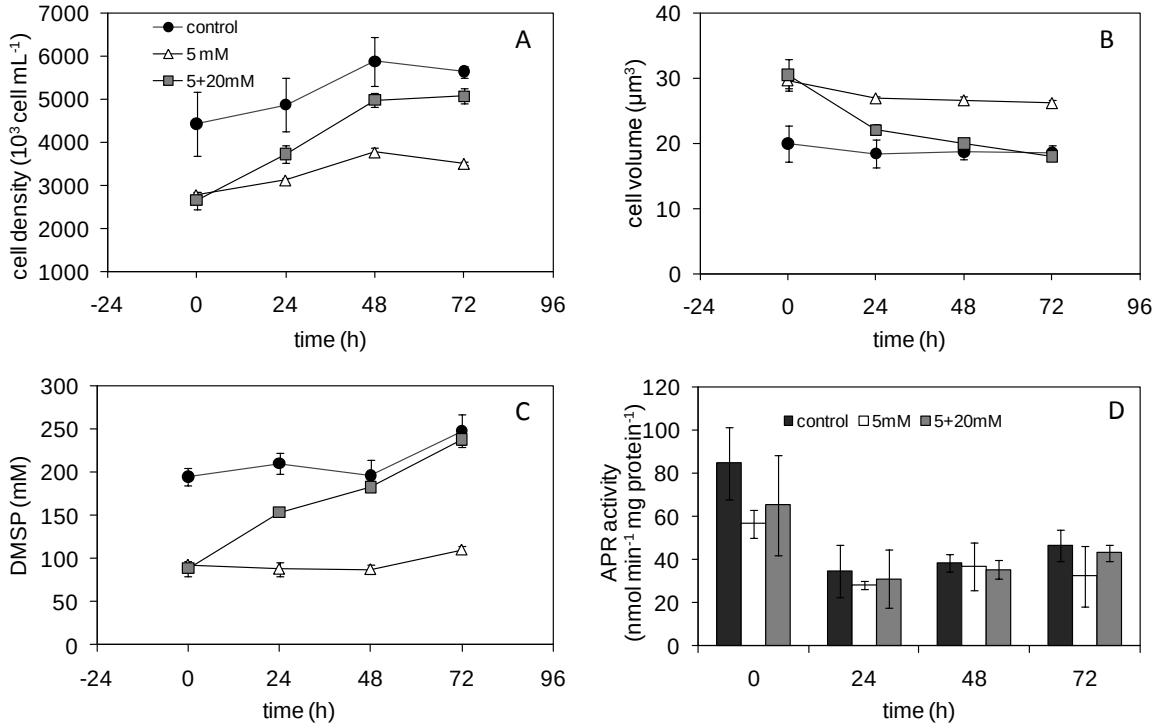

Figure 3.8 Effect of 20mM sulphate addition on S-limited *E. huxleyi* growth (A), cell volume (B) and intracellular DMSP (C) and APS reductase activity (D). Results are shown as means ±standard deviation from 3 biological replicates.

To compare the ability of different sulphur sources to restore growth of S-limited cells and their DMSP content we examined the response of S-limited *E. huxleyi* to cysteine (Figure 3.9) and methionine (Figure 3.10) additions. Culture growth, cell volume and DMSP concentration were unaffected by the addition of 0.2 mM Cys. On the other hand, the addition of 1 mM Cys was found to enhance the specific growth rate within 24h from 0.25 (±0.02) to 0.36 (±0.03). This concentration of Cys had a small, but significant (Student's t-test, $p<0.05$) effect on the increase in DMSP concentration.

Similarly to Cys, addition of 0.1 or 0.5 mM Met, which is a precursor of DMSP, to S-limited cultures had no clear effect on *E. huxleyi* growth and cell volume. After an initial (24 h) increase of DMSP in Met supplemented cultures its concentration dropped and stayed within the range of S-limited cultures until the end of the experiment.

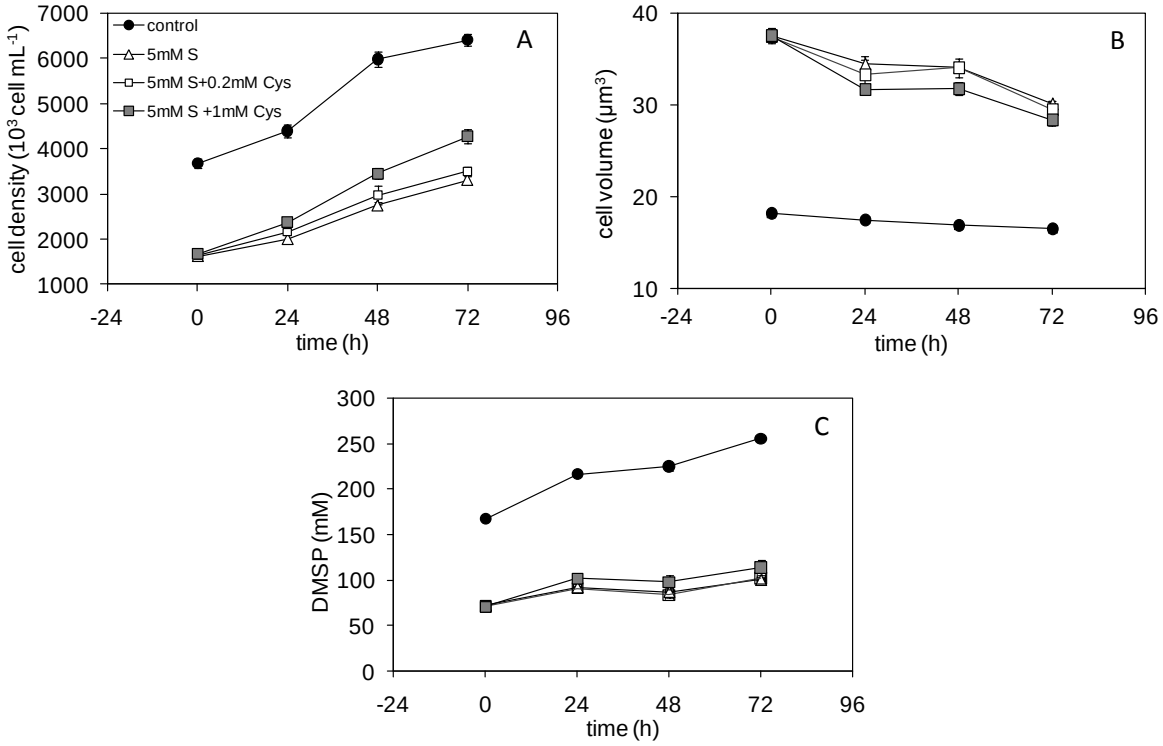

Figure 3.9 Effect of 0.2 and 1 mM Cys addition on S-limited *E. huxleyi* growth (A), cell volume (B) and intracellular DMSP (C). Results are shown as means ±standard deviation from 3 biological replicates.

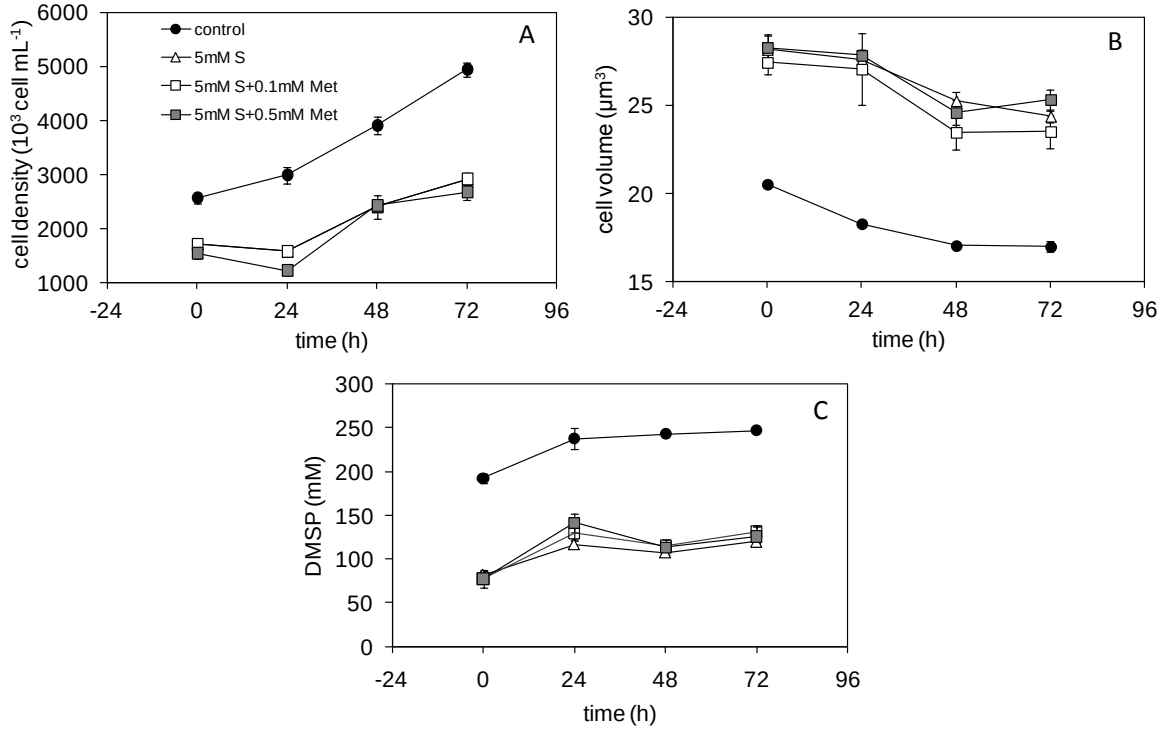

Figure 3.10 Effect of the 0.1 and 0.5 mM Met addition on S-limited *E. huxleyi* growth (A), cell volume (B) and intracellular DMSP (C). Results are shown as means ±standard deviation from 3 biological replicates

Equimolar S-compound resupply

To make a qualitative comparison between different S-sources we carried out the same experiment but adding equimolar (5 mM) concentration of sulphate, Cys and Met to triplicates of S-limited batch culture (Figure 3.11). In all 3 cases we observed continual increases of cell abundance and specific growth rate after S-compound addition. The specific growth rate measured after 48 h of incubation was higher in all S-supplemented cultures than in two controls: 25 and 5 mM SO_4^{2-},with the highest value (0.38 ±0.02 d^{-1}) following Met addition compared to 0.16 (±0.04) and 0.18 (±0.01) d^{-1} in 25 and 5 mM SO_4^{2-}, respectively. The addition of S-compounds did not result in a strong decrease in cell volume and the cells were ~50% bigger than those grown in control (Figure 3.11, B). Figure 3.11 C shows that upon addition of Cys, intracellular DMSP concentrations increased from 112 (±5) to 162 (±6) mM within 24 h. This suggests that the uptake of Cys was faster than the uptake of sulphate and Met. Seventy two hours after S-resupply the final DMSP concentration was similar in all 3 treatments and was ~25% higher than the 5 mM SO_4^{2-} culture and ~50% lower than the 25 mM SO_4^{2-} culture.

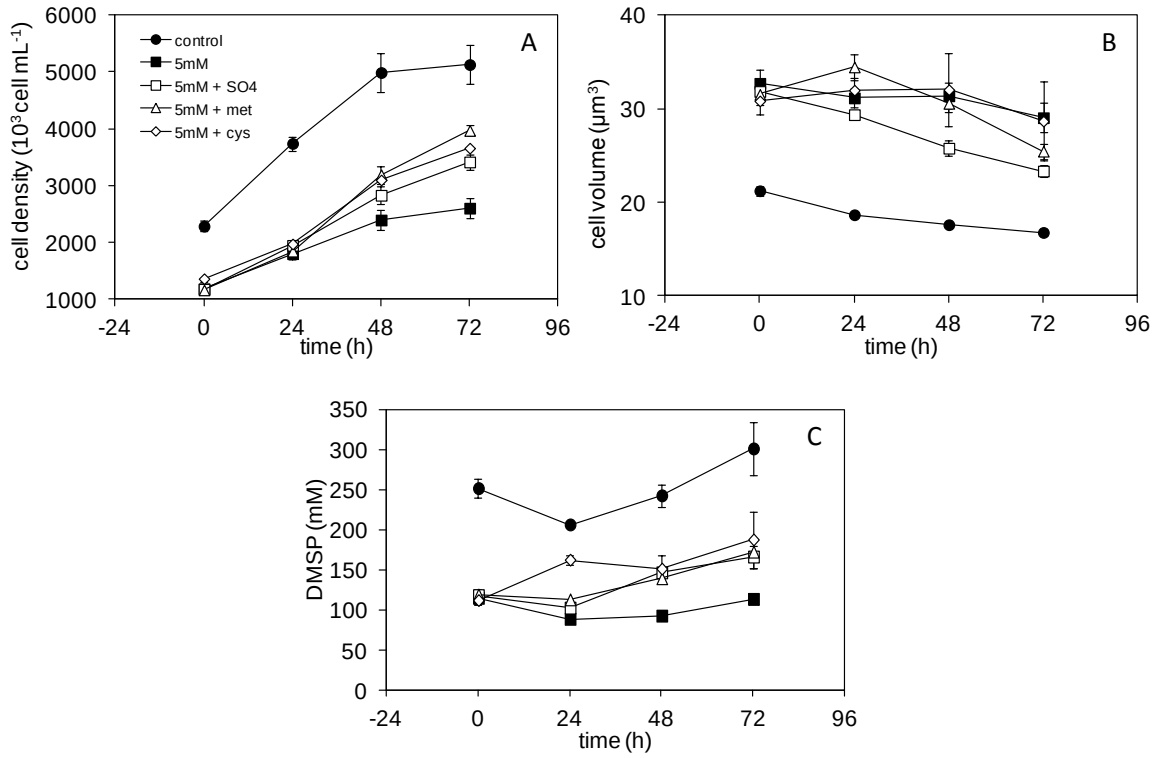

Figure 3.11 Effect of the 0.1 and 0.5 mM Met addition on S-limited *E. huxleyi* growth (A), cell volume (B) and intracellular DMSP (C). Results are shown as means ±standard deviation from 3 biological replicates.

3.3.7. Salinity down-shock

In this experiment we examined the effect of low salinity shock on the growth and intracellular DMSP concentration of *E. huxleyi* (Figure 3.12). The aim of this was to test whether lowering salinity by dilution, but keeping constant sulphate concentrations, had a comparable effect on growth and DMSP synthesis. To do this we used control (100%) and low-salinity (80 and 70%) ESAW media.

The specific growth rate measured when *E. huxleyi* cultures reached exponential phase markedly decreased under low-salinity from 0.72 (±0.05) to 0.66 (±0.01) and 0.61 (±0.00) in 80 and 70% ESAW dilutions respectively. Also cell number clearly decreased with decreasing salinity resulting in about 2-fold lower cell density in the 70% dilution culture than that in the control. The change of cell volume throughout the time course showed the same pattern in all 3 salinities, however the volume of algal cells grown in 70% dilute medium was ~10 μm^3 bigger than the total volume of algal cells grown in 100 and 80% salinity medium.

Low salinity had a clear effect on intracellular DMSP concentration (Figure 3.12, C). In the mid-exponential growth phase (day 4) DMSP concentration stayed the same level in both the 80 and 70% dilution cultures and was ~2-fold lower than the control. We observed a slight enhancement of DMSP during the experiment in salinity altered cultures, and the increase was significantly higher (Student's t-test, $p<0.05$) in cultures grown in less diluted medium. DMSP concentrations measured in the late exponential phase (day 8) were 224 (±5), 164 (±) and 121 (±7) in the 100, 80 and 70% ESAW dilutions respectively.

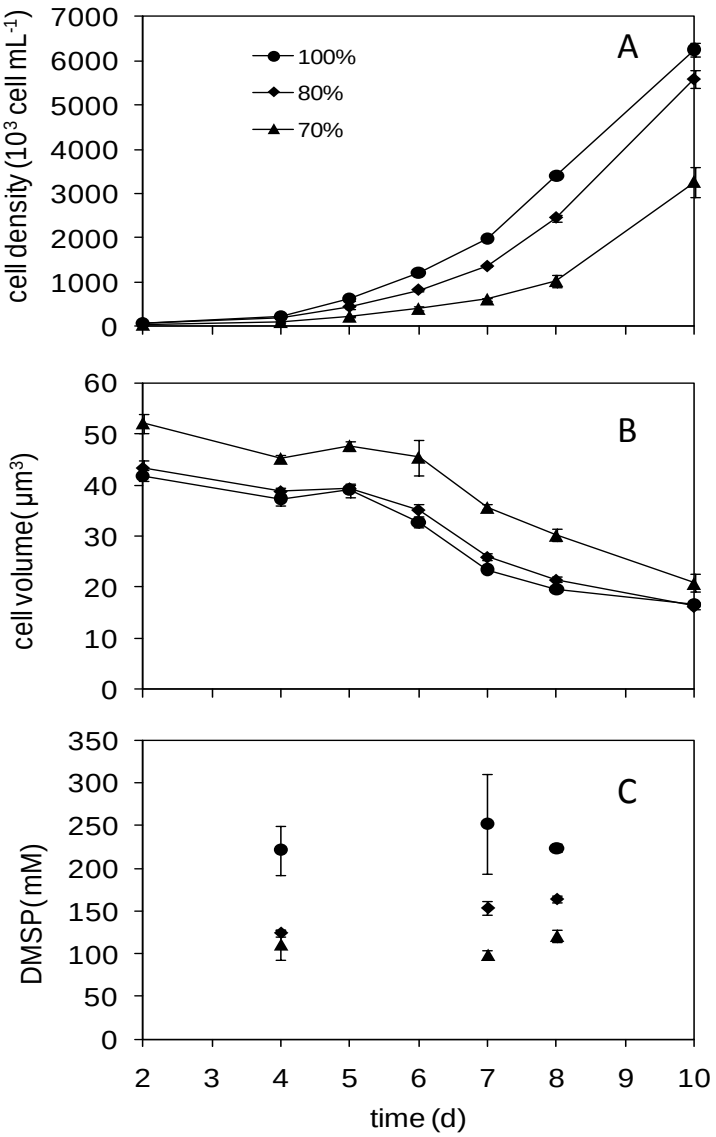

Figure 3.12 Effect of the salinity down-shock on *E. huxleyi* cell density (A), cell volume (B) and intracellular DMSP concentration (C). The medium salinity was expressed as the percentage of the standard ESAW salinity. Results are shown as means ±standard deviation from 3 biological replicates.

3.4. Discussion

Whilst sulphur forms part of many important molecules in marine algae, sulphur uptake and metabolism in these organisms is still rather poorly understood. The exception is the extensive work on DMSP since marine phytoplankton are the main producers of this S-metabolite. However even here there is very little knowledge of molecular mechanisms of the control of DMSP synthesis. This is particularly relevant as sulphate deficiency is one of the most studied environmental stresses in plant biology and so the lack of data makes comparisons between these groups difficult (Takahashi et al. 2011). In this chapter, therefore, we used various sulphate-limitation experiments as a tool to better understand sulphur metabolism in *Emiliania huxleyi.*

In the first experiment we compared growth and DMSP synthesis of this microalga under the range of low sulphate concentrations to test how it is affected by limited sulphate supply. At low sulphate levels *E. huxleyi* grew slower, with a decrease in growth rate observed below 10 mM SO_4^{2-} in the medium (Figure 3.2). These results are consistent with those published very recently by Ratti et al. (2011) who found that the growth rate of *E.huxleyi* dropped at 5 and 1 mM SO_4^{2-} below 0.40 d^{-1} but did not change above 10 mM. Our experiments showed clearly that *E. huxleyi* actually requires a high concentration of sulphate for optimal growth. The sulphate concentration of 5 mM that significantly limited *E. huxleyi* growth is 3 orders of magnitude higher than the concentration of sulphate that limits the growth of plants. Indeed , plants growth normally even at 5 µM sulphate (Hawkesford and De Kok 2006) whereas freshwater algae can adapt to environments with sulphate concentrations in the range of 0.01-1 mM (Giordano et al. 2005).
This high demand for sulphur supports the hypothesis that coccolithophorids, along with diatoms and dinoflagellates became dominant in the oceans when the sulphate concentration in seawater increased between Palaeozoic and Mesozoic times (Falkowski et al. 2004; Gill et al. 2007; Gill et al. 2011; Ratti et al. 2011). In addition to culture growth rate, sulphate limitation had an impact on cell morphology. In S-reduced cultures, cell size was larger than in the control which could indicate repressed cell division (Figure 3.2, C)

Interestingly, the photosynthetic efficiency did not show change at low sulphate with the exception of an initial decrease of Fv/Fm by ~25% at very low (1mM) SO_4^{2-} concentration, which then recovered within 2 days (Figure 3.2, C). Although, more experimental work is needed, this result combined with *E. huxleyi* transcriptome data indicating no change in expression of the genes involved in photosynthesis, suggests that

this process is unaffected by reduced sulphur availability. By contrast, sulphur limitation triggers down-regulation of photosynthesis in plants (Lunde et al. 2008) and green algae correlating with a reduction of ribulose-1,5- bisphosphate carboxylase/oxyganase (Rubisco) accumulation (Wykoff et al. 1998; Giordano et al. 2000). Since Rubisco requires reduced sulphur (Ferreira and Teixeira 1992) S may be reallocated to this protein from other sources in *E. huxleyi*. Indeed, we observed that the level of intracellular DMSP decreased concurrently with decreasing sulphate in the culture. This suggests that DMSP synthesis is regulated by sulphur availability, and that the change in the intracellular pool of DMSP could enable stored sulphur to be used for other metabolites. However, in order to prove this hypothesis, knowledge of the DMSP synthesis rate and turnover, rather than intracellular DMSP content is required. A similar but much weaker decrease of DMSP under S-deficiency was observed in the chlorophyte *Ulva pertusa* by Ito et al (2011). These authors measured ~30% reduction in DMSP content at 0.01 mM SO_4^{2-} compared to control alga (30 mM SO_4^{2-}). Surprisingly, Ratti et al. (2011) did not observe a significant change of DMSP in *E.huxleyi* (strain PML 92/11) at sulphate concentration between 5 and 20 mM. In their studies, intracellular DMSP per cell and cell volume was ~3 fmol $cell^{-1}$ and ~100 mM, respectively, which is within the range of our cultures grown under 1 mM SO_4^{2-}. This suggests that *E. huxleyi* strain PML 92/11 is a lower DMSP producer than the strain we used (1516) and so less affected by sulphate deprivation. However, to verify this hypothesis exactly the same experimental conditions should be applied to both strains. Since the 5 mM SO_4^{2-} culture responded with the greatest decrease in both growth rate (though still with a positive growth rate) and intracellular DMSP concentration (Table 3.1), we used this concentration as the S-limited baseline condition in the proceeding S-addback experiments. However, it has to be noted that while the growth of *E. huxleyi* decreased in 5 mM sulphate, typical sulphate concentration in plant growth media is 0.75 mM and it has to be diminished to under 0.02 mM to affect plant growth and metabolism.

To test the hypothesis that response to sulphate limitation may be linked to DMSP content we compared three *E. huxleyi* strains (CCMP 1516, 370 and 373) which have been previously shown to have distinctive intracellular DMSP content and DMSP-lyase activity (Steinke et al. 1998). These authors described strain 370 and 373 as having notably higher DMSP producer than strain 1516, but our results demonstrate that the latter has the highest DMSP content in sulphate replete conditions (Figure 3.4). The discrepancy between Steinke et al. and our study may be related to the method of cell size measurement, as we used a Coulter counter approach rather than microscopic enumeration; however there is no

direct evidence explaining these different values. Sulphate limitation induced a decrease in both cell density and intracellular DMSP concentration in strain 1516 and 370 but not in strain 373. A possible reason why this strain was not affected by sulphate depletion may be that its high DMSP-lyase activity could recycle sulphur from DMSP more efficiently and so increase the availability of sulphur-containing metabolites. Wolfe et al (2002) proposed that DMSP cleavage can maintain DMSP/DMS homeostasis and thereby help the cell to adjust to the environmental changes. Further work, e.g. measurement of DMSP lyase activity upon exposure to low S-conditions, would help to better understand the differences between these *E. huxleyi* strains.

One of the typical responses to sulphur depletion is an increase of exogenous sulphate uptake in plants (Clarkson et al. 1999; Koralewska et al. 2009) and green algae (Yildiz et al. 1994; Weiss et al. 2001; Koralewska et al. 2009; Pootakham et al. 2010). We assessed ^{35}S acquisition in *E. huxleyi* grown in low and replete sulphate conditions in both 5 and 25 mM sulphate. Similarly to green algae and plants, *E. huxleyi* responded to low-S condition by inducing the uptake rate ~4 fold (Figure 3.5). Although no dedicated attempt to characterise sulphate uptake in *E. huxleyi* was performed, the fact that the uptake rate was more than two-fold higher at 25 mM sulfate than at 5 mM sulphate shows that uptake is not saturated at 5 mM sulphate. This suggests that the uptake is in the low affinity range with a K_M higher than 5 mM. This is significantly higher than the *Arabidopsis* low affinity transporters SULTR2;1 and -2;2 which have KM values of 0.41 mM and 1.2 mM, respectively (Takahashi et al. 2001) and in agreement with a study of marine red alga *Rhodella maculate* which has a sulphate uptake system with K_M of 21.9 mM (Millard and Evans 1982).

The increase in sulphate uptake activity correlated with an induction of the expression of sulphate transporter genes detected in S-limited *E. huxleyi* (see Chapter 5). This is consistent with the responses of plants and green algae (Maruyama-Nakashita et al. 2006; Pootakham et al. 2010) and may suggest that as in these organisms, sulphur molecules have a signalling function in sulphur metabolism in *E. huxleyi*. However, our results differ from those presented by Ratti and co-workers (2011) where *E.huxleyi* (strain PML 92/11) grown at 5 mM SO_4^{2-} exhibited lower sulphate uptake rate compare to cells grown under ambient sulphate. Thus, there seems to be substantial variation in response to sulphate limitation between different *E. huxleyi* strains, as also seen in the different regulation of DMSP content (Figure 3.4).

In contrast to the sulphate uptake results, S-limitation did not lead to the up-regulation of APR activity in *E. huxleyi* (Figure 3.6, D). Moreover, we observed that the activity of this enzyme was lower in S-limited cultures relative to the control during the early log phase. The difference in APR activity measured with the time course between S-replete and S-deplete cultures was not straightforward. Conversely, the withdrawal of sulphate from the environment is usually associated with an induction of transcript abundance and APR activity in plants (Takahashi et al. 1997; Hopkins et al. 2004; Kopriva 2006; Koralewska et al. 2008). Although we did not notice a strong effect of S-limitation on APR, its observed activity *in E. huxleyi* was an order of magnitude higher than the activity measured in *A. thaliana*. (Vauclare et al. 2002) and *C. reinhardtii* (Ravina et al. 2002). In addition, the *APR* mRNA was one of the most abundant in the *E. huxleyi* transcriptome (see Chapter 4) and Gao and colleagues (2000) demonstrated relatively high APR activity in marine phytoplankton species *Enteromorpha intestinalis* that produce DMSP. This may be related to substantial requirements for reduced sulphur in these species compare to low/non-DMSP producers; however we did not find a correlation between intracellular DMSP concentration and APR activity. Neither was a strong correlation observed in *E. intestinalis* (Gao et al. 2000).

We induced sulphate limitation to examine the changes not only in DMSP concentration but also other important S-metabolites: Cys and GSH. These thiols are very important for S-metabolism. Cys is the final product of S-assimilation and it gives rise to various metabolites (e.g. GSH) which in turn is considered (similarly to DMSP) as an important antioxidant (Polle and Rennenberg 1992; Foyer and Noctor 2005). Like DMSP, GSH concentration was down-regulated in *E. huxleyi* under sulphate limitation (Table 3.2). GSH down-regulation under S deficiency was also described in plants (Nikiforova et al. 2003; Lunde et al. 2008). Conversely, Cys concentration was not affected by S-limitation in the same way reported in plants (Nikiforova et al. 2003; Kaur et al. 2011). Our transcriptomic analysis revealed the expression of genes involved in re-cycling GSH back to Cys in response to low sulphate conditions, indicating that *E. huxleyi* may re-allocate sulphur to other metabolites via Cys as a central point keeping thus its concentration constant.

Since S-limitation leads to a decline in cell abundance and intracellular DMSP levels in *E. huxleyi,* we intended to test whether S-resupply would restore growth and DMSP concentration in S-deplete cultures. Indeed, when 20 mM of sulphate was added back to 5 mM sulphate, within 2 days cultures regained previous levels of intracellular

DMSP and moved significantly toward their original cell density.(Figure 3.7 and 3.8). Our preliminary experiments providing different concentrations of Cys (0.2 and 1 mM) or Met (0.1 and 0.5 mM) into S-limited cultures, did not result in an increase of the growth and/or DMSP production compared with S-depleted cultures (Figure 3.9). Probably, the amount of sulphur taken up from these additional sources was not sufficient to fill the internal sulphur pools. Indeed, when higher concentration (5 mM) of SO_4^{2-}, Met or Cys was added, we observed a significantly higher cell counts and intracellular DMSP concentrations compared with the low S culture. However, this response was similar in all 3 addback experiments. An earlier study by Uchida et al. (1993) showed that when sulphate was replaced with 5 mM Cys or Met, growth of the heterotrophic dinoflagellate *Crypthecodinium cohni* was much better with Cys than Met, whereas intracellular DMSP levels were highest in the Met treatment, indicating that it is a closely coupled with the DMSP precursor. Unfortunately no information exists regarding the *E. huxleyi* transcriptomic profile after sulphate replenishment, as this information would greatly aid to the interpretation of our results.

As a compatible solute, intracellular DMSP concentration is known to alter in response to salinity changes (Vairavamurthy 1985; Van Bergeijk et al. 2002; Van Bergeijk et al. 2003). Low salinity experiments are usually conducted by mixing seawater with distilled water. In our experiment we tested whether previously observed DMSP decreases are the effect of salinity down-shock or simply the effect of sulphate dilution in the medium. To do so, we kept sulphate concentration constant in all low salinity media. Indeed, our results suggest that decrease of the cell density and DMSP is closely related to the salinity reduction. Niki et al (2007) revealed that salinity-down shock triggered rapid DMSP realised from dinoflagellate *Heterocapsa triquerta* and that it also instantaneously converted released DMSP to DMS. Based on their observations, they conclude that low salinity condition may increase algal DMS production and at the same time decrease bacterial DMSP consumption.

3.5. Conclusions

This chapter focussed on the effect of sulphate availability on physiology and sulphur metabolism in *E. huxleyi*. Low availability of sulphate reduced the growth rate and yield, the intracellular concentration of the S-metabolites DMSP, GSH and Cys, whilst inducing the sulphate uptake rate. We showed that the response to S-limitation was strain specific in respect to growth and DMSP concentration. Although *E. huxleyi* was affected by sulphate limitation the response is different to that reported for higher plants and green algae. We observed substantially higher APS reductase activity compared to plants and freshwater algae, and in *E. huxleyi* the activity of this enzyme was not regulated by sulphur availability. We suggest that this is most likely due to sulphur metabolism having evolved in a different way in the seawater environment compared to terrestrial and freshwater habitats where organisms are more likely to face sulphur deprivation.

Whilst our approach does not allow us to fully explain DMSP biosynthesis and breakdown, our data show that by altering the sulphur pool available in the growth medium one can regulate intracellular DMSP levels, at least in *E. huxleyi*. We have demonstrated a clear effect of salinity on DMSP concentration, and for future work combining salinity changes with altered sulphate availability would provide more information about the role of DMSP and its regulation in marine microalgae.

More detailed studies will be needed to improve our understanding of S metabolism in marine algae. The results presented here led to an in-depth analysis of the effects of sulphate limitation in *E. huxleyi* at the molecular level and this is presented in Chapter 5.

4. Diurnal variation of sulphur metabolism in *Emiliania huxleyi*

4.1. Introduction

The photosynthetic machinery uses light energy, ATP and an electron donor to convert the inorganic molecules carbon dioxide and water into energy-rich carbohydrates and the by product oxygen. In nature the variation in light intensity is usually linked to the light:dark cycle and this determines physiological and metabolic changes in living organisms, especially photosynthetic organisms. Although, sulphur does not directly act in photosynthesis it is an important molecule for the photosynthetic apparatus as a constituent of the amino acids methionine (Met) and cysteine (Cys) and important co-factors of photosynthetic proteins such as iron sulphur centres. Apart from being a part of structure of photosynthetic proteins, sulphur in form of Cys, Met, glutathione (GSH) and dimethylsulphoniopropionate (DMSP) are essential for cellular antioxidant defence mechanism (Schupp and Rennenberg 1988; Sunda et al. 2002; Møller et al. 2007). All organisms need to eliminate reactive oxygen species (ROS); in the case of plants and algae ROS are also generated by light-dependent processes associated with photosynthesis and photorespiration. This is a particular issue under high light intensities or nutrient stress (Sunda et al. 2002). In this way S-metabolites that act as antioxidants might be expected to vary across the light:dark cycle.

There are very few studies showing diurnal changes of S-compounds in marine microalgae. Culture and field studies by Dupont and co-workers (2004) revealed that GSH concentration in the coccolithophore *Emiliania huxleyi* and diatom *Thalassiosira pseudonana* varied during the light/dark cycle reaching the highest values during light periods. In addition, Bucciarelli et al. (2007) recently showed that DMSP concentration is also affected by the diurnal rhythm in *E. huxleyi*. Unfortunately, the different methodological approaches e.g. light regime used in the experiments make the comparison between these two investigations difficult.

Here we describe diel oscillations in growth parameters and concentrations of the S-metabolites Cys, GSH and DMSP. Moreover, since it was shown that in vascular plants APS reductase (APR) activity is modulated by light:dark cycle (Kopriva et al. 1999), we also tested whether the same is true for *E. huxleyi*. A parallel experiment was carried out by Nicola Hockin (University of East Anglia and John Innes Centre) on *T. pseudonana* which allowed direct comparison between these two species. In addition, a further diurnal experiment was performed to study the effect of the light on the recovery of S-limited cultures of the *E. huxleyi*.

4.2. Materials and Methods

Triplicate batch cultures of *Emiliania huxleyi* were grown in 2 L conical flasks containing 1.5 L of ESAW medium. The experimental setup was prepared by inoculation the media with exponentially growing stock cultures to give an initial cell density of ~5 x 10^4 cells mL^{-1}. Cultures were grown at 15^oC under a light:dark cycle of 14:10 hours as detailed in Chapter 2. The diurnal experiment commenced when cultures were in mid-exponential phase with a cell density ~1 x 10^6 cells mL^{-1}. The first samples were taken just before the dark to light transition and the subsequent samples were taken every 2 or 3 h over 29 h. At each time point cultures aliquots of 2, 10 and 20 mL were withdrawn for the measurement of intracellular DMSP concentration, APR activity and the analysis of thiol concentrations (Cys and GSH) respectively. Aliquots for DMSP and thiol measurements were gently filtered by hand vacuum pump (< 10 cm Hg) through 25mm Whatman GF/F filters (nominal pore size 0.7 µm, Whatman UK Ltd., Maidstone, U.K.). Similarly, aliquots for APR activity measurement were filtered through 25 mm Nucleopore™ track-etched polycarbonate filters (nominal pore size 1.0 µm, Whatman UK Ltd., Maidstone, U.K.). Samples were stored and analysed according the procedures described in the chapter 2. The culture growth parameters cell number and cell volume were measured simultaneously at each sample collection point.

In the second experiment triplicate batch cultures were grown in 1 L conical flasks with 500 mL of ESAW medium with 25 or 5 mM SO_4^{2-}. When cultures reached exponential phase the experiment commenced by adding 20 mM SO_4^{2-} into one set of S-limited cultures and adjusting the ionic strength in S-limited and S-replete cultures. The growth parameter measurements and DMSP sample collections were done as described above. Again, further details can be found in Chapter 2.

4.3. Results and Discussion

4.3.1. Growth parameters

Figure 4.1 shows the diurnal cycle of the growth parameters and S-metabolites in *E. huxleyi* (strain CCMP 1516) grown in batch cultures under nutrient-replete conditions. The cell abundance did not change during the light period but there was a sharp increase in cell number during the night indicating that the cell division occurs in the dark phase (Figure 4.1, A). The same pattern was observed in *E. huxleyi* in previous studies (Paasche 1967; Bucciarelli et al. 2007). The cells exhibited a clear diurnal periodicity in cell size (Figure 4.1, B). The cell volume increased over the light period reaching the maximum value at the end of the light period and decreased in the dark period, reaching the minimum value at the end of the dark phase. The light:dark fluctuation in cell volume was responsible for the differing patterns observed for DMSP per cell and DMSP concentration i.e. normalised to cell volume (Figure 4.2, C and D). Intriguingly, in the diatom *T. pseudonana* grown under the same conditions the cell size was unchanged across the diurnal cycle (Nicola Hockin, University of East Anglia and John Innes Centre, personal communication).

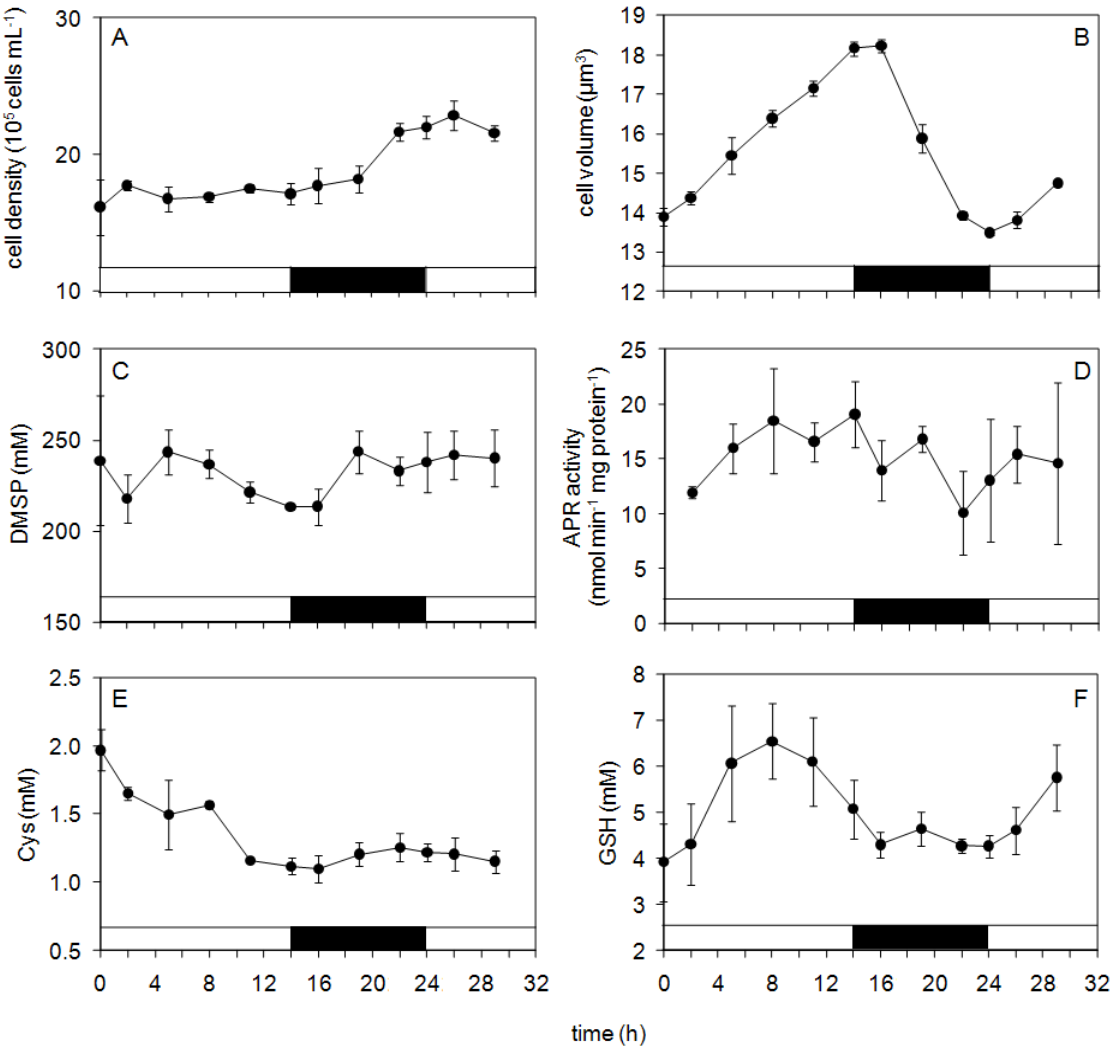

Figure 4.1 Effect of diurnal light variation on *E. huxleyi* cell abundance (A), cell volume (B), intracellular DMSP concentration (C), APS reductase activity (D), cysteine concentration (E) and glutathione concentration (F). The light:dark cycle is indicated by the white (light) or black (dark) bars. Time point 0 h corresponds to the beginning of the light period. Results are shown as means ± standard deviation of 3 replicates.

4.3.2. DMSP

The average intracellular DMSP concentration during the time-course experiment was 232 (±12) mM. There was no obvious trend in change of DMSP content expressed per cell volume over the light:dark period (Figure 4.1, C). Our results are in agreement with Rijssel and Gieskes (2002) who found that neither light regime nor light intensity affected DMSP concentration in *E. huxleyi* strain L. In contrast, Bucciarelli and co-workers (2007) reported a decrease in intracellular DMSP concentration during the light period and its increase in darkness in strain CCMP 374. Another diurnal pattern was revealed in low DMSP-producer *T. pseudonana* by Nicola Hockin (University of East Anglia and John Innes Centre, personal communication). She observed a continuous increase of intracellular DMSP during the day and its plateau at night. It is worth mentioning that the intracellular DMSP concentration in *T. pseudonana* was two orders of magnitude lower than this measured in *E. huxleyi*. Fairly constant level of DMSP over light:dark period should not rule out the potential for this molecule functioning in the cell antioxidant defence system as proposed by Sunda et al. (2002). According to these authors, DMSP is involved in an antioxidant cascade mechanism whereby the DMSP degradation products DMS and acrylate are even more effective in ROS scavenging than DMSP itself. In this system DMS could react with hydroxyl radicals (•OH) to form dimethylsulphoxide (DMSO). Keeping a high and constant level of intracellular DMSP might be the part of the cellular strategy for ensuring that the antioxidant system keeps running, especially since this multifunctional molecule is presumably involved in other physiological processes (see Chapter 1). However, to verify this hypothesis, DMSP synthesis rate data would be required.

4.3.3. Thiols

In addition to measuring intracellular DMSP we also examined diurnal variations in GSH and its precursor Cys as these thiols compounds are also involved in ROS detoxification. Cys concentration declined from ~2 to ~1 mM between the beginning and the end of the light period but we did not observed a diurnal cycle since after this initial decrease the concentration stayed at about the same level until the end of the experiment

(Figure 4.1, E). Nicola Hockin (personal communication) also found no fluctuation in Cys concentration in *T. pseudonana*.

The lack of Cys regulation by the diurnal cycle underlines the importance of this amino acid as central point mediating various metabolic pathways. Contrary to Cys, GSH concentration in *E. huxleyi* exhibited a clear diurnal pattern with the highest value of ~6 mM at 8 hours into the 14 hour light period and the lowest value of ~4 mM at the beginning the dark period. The concentration then stayed unchanged until the lights came on again (Figure 4.1, F). A similar diurnal cycle has been revealed for other marine algae including *E.huxleyi* strain CCMP 373 and *T. pseudonana* (Dupont et al. 2004; Nicola Hockin, personal communication), as well as in spruce needles (Schupp and Rennenberg 1988). Interestingly, the overall Cys and GSH concentrations in *E. huxleyi* strain CCMP 1516 were ~2 fold higher than in *T. pseudonana* (Nicola Hockin, personal communication).

The diurnal alteration in GSH concentration observed in these marine microalgae supports its role in oxidative stress response. GSH is the most abundant low-molecular-weight thiol a major electron donor to reduce oxidased ascorbate which is primary scavenger of H_2O_2 (Rouhier et al. 2008).

4.3.4. APS reductase

Although APS reductase (APR) activity regulation by light is well documented in plants (Neuenschwander et al. 1991; Kopriva et al. 1999) no information exists regarding diurnal variation in APR activity in marine microalgae. Here, we made an attempt to test APR activity variations in *E. huxleyi* under the light:dark cycle (Figure 4.1, D). The enzyme activity values varied between ~10 and ~19 nmol min^{-1} mg $protein^{-1}$ however the data are relatively noisy and there was no a clear difference (Student's t-test, $p>0.05$) between the light and dark period. A similarly lack of diurnal fluctuation was shown for *T. pseudonana* (Nicola Hockin, personal communication). On the other hand Kopriva and co-workers (1999) observed a diurnal rhythm of both APR activity and mRNA level in *Arabidopsis thaliana*. They found that enzyme activity was the highest during the light and the lowest at the beginning of the dark period. This discrepancy could indicate that sulphur assimilation is differently regulated in plants and marine algae. This might be related not

only to phylogenetic distance, but also to the very different habitats these organisms occupy in terms of sulphur-availability.

4.3.5. Diurnal variation in S-resupplied *E. huxleyi* cultures

In Chapter 3 we presented data that showed how cell abundance and DMSP concentration increased following sulphate re-supply to S-limited cultures. Here, we aimed to examine the dynamic of these increases in relation to the diurnal cycle (Figure 4.2). The experiment commenced 7 days after inoculation of the *E. huxleyi* cultures when intracellular DMSP concentration was ~35% lower in the S-limited (5 mM SO_4^{2-}) than in control (25 mM SO_4^{2-}) cultures (Figure 4.2, E). During the first 14 h light period, cell number and cell volume were the same in the 5 mM and S-resupplied (5+20 mM SO_4^{2-}) cultures (Figure 4.1, A & B). By contrast, at the end of the dark period there was a significant difference (Student's t-test, $p<0.05$) observed in cell number in that the cell density in the 5+20 mM cultures was ~33% higher than in 5 mM culture after 24 h (Figure 4.2, A). This increase was accompanied by a steeper drop in cell volume in the 5+20 mM culture compared to the 5 mM cultures (Figure 4.2, B).

During the light period the amount of DMSP per cell markedly increased in the 5+20 mM cultures from ~3 to ~5 fmol $cell^{-1}$, whereas there was far less variation in DMSP in the 5 mM cultures over the whole time-course (Figure 4.2, C). Since, during the first 14 h of the experiment the the cell volume changed at a similar rate in both the 5 mM and 5+20 mM cultures, the up-regulation in cellular DMSP content could be at least in part attributed to the light.

Intriguingly, intracellular DMSP in the S-limited *E. huxleyi* cultures exhibited a steady decrease from ~140 mM at the early light period down to ~80 mM at the early dark period and then small increase back to ~117 mM at the early light of the next day (Figure 4.2, C). This may suggest that, in contrast with S-replete conditions, in S-limited cultures the pool of antioxidant DMSP cannot be kept constant due to the insufficient sulphate supply from the external environment.

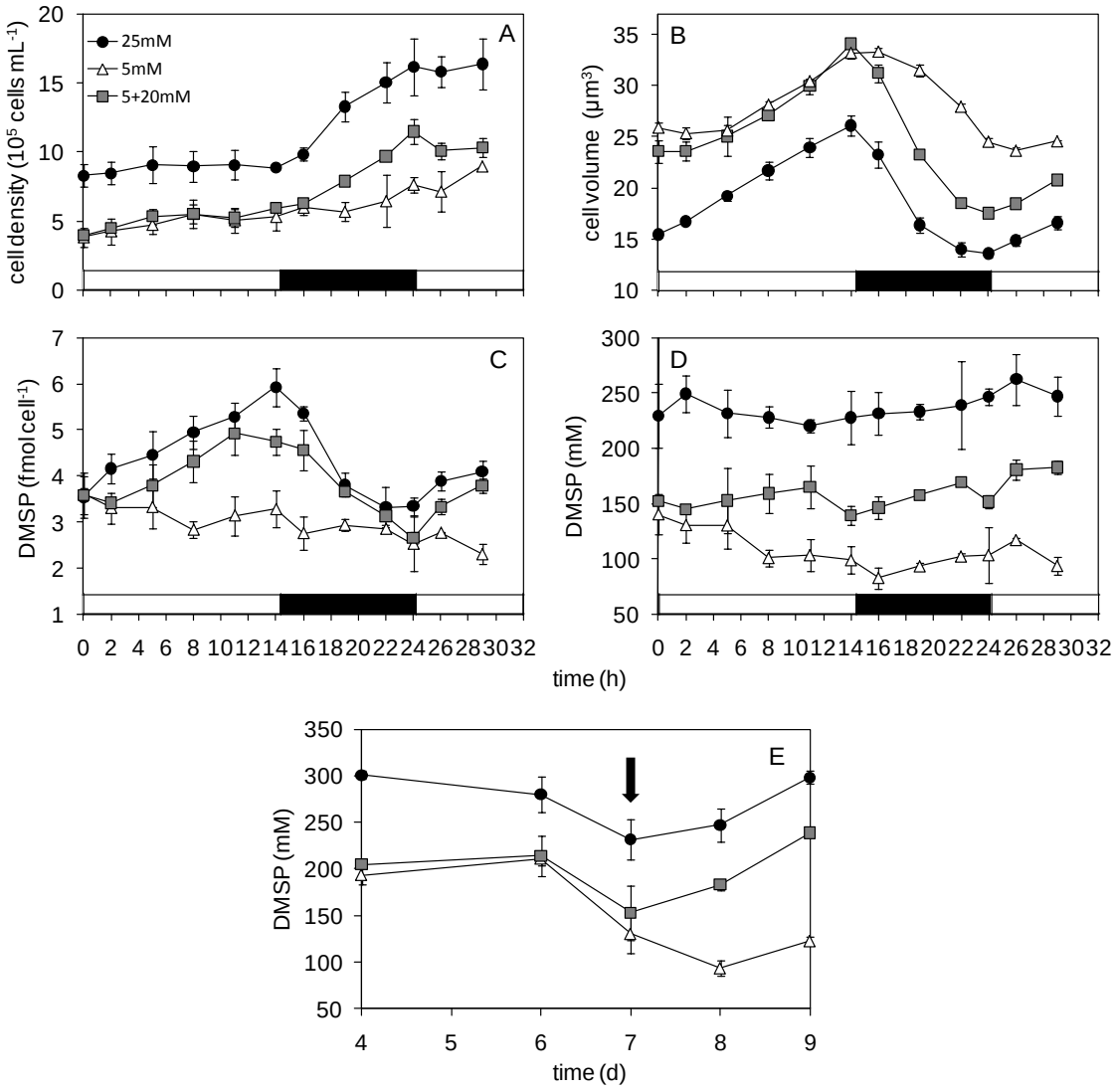

Figure 4.2 Effect of diurnal light variation on *E. huxleyi* under different sulphate status: 25 mM, S-replete; 5 mM, S-limited; 5+20 mM, S-restored cultures. The graphs show: cell abundance (A), cell volume (B), DMSP concentration per cell (C), intracellular DMSP concentration (D), intracellular DMSP concentration before and after the 29 h experiment (E). The light:dark cycle is indicated by the white (light) or black (dark) bars. Time point 0 h and black arrow in figure E correspond to the beginning of the light period. Results are shown as means ± standard deviation from 3 replicates.

4.4. Conclusions

In this chapter we examined the diurnal variation in growth and sulphur compounds in the marine microalga *E. huxleyi*. The temperature was constant during the experiments, so the main factor controlling these changes was the light. We demonstrated that the cell division takes place during the dark period and this process is preceded by an increase in the cell size during the light period when photosynthesis occurs.

Under control conditions intracellular DMSP concentration was maintained at a fairly similar level throughout the light:dark cycle, reflecting its modulation due to changes in cell volume. The high and relatively constant level of this S-molecule suggests that cells control the DMSP concentration quite tightly and/or that its various physiological roles, including that in ROS detoxification, do not have a substantial effect on DMSP concentration. In addition, light regulation of GSH concentration confirmed its function as ROS scavenger which when combined with the DMSP-DMS-DMSO antioxidant cascade may form an efficient ROS-scavenging mechanism in *E. huxleyi*.

While APR activity is altered by the light in plants, this seems to be not true for marine phytoplankton indicating that sulphate assimilation is differently regulated in these organisms.

The second experiment focused on the effect of the light:dark cycle on DMSP concentration in the *E. huxleyi* after sulphate restoration. Our results indicate that immediate and continuous increase in DMSP content in the light period is driven by the light, however this would need to be confirmed with more experiments e.g. looking at the affect of sulphate re-supply to S-limited cultures just before the dark period. To our knowledge, this was the first attempt to better understand DMSP regulation by sulphur availability and light status in marine algae. The results suggest that there is a synergistic regulation of DMSP by these environmental conditions, but further experiments are needed to better understand their relationship.

5. Transcriptome analysis of sulphur limitation in *Emiliania huxleyi* CCMP1516

5.1. Introduction

Sulphate deprivation is well known in the terrestrial soil and freshwater environments. This had led to substantial research on S-metabolism in higher plants such as *Arabidopsis thaliana* (Hirai et al. 2003; Maruyama-Nakashita et al. 2003; Nikiforova et al. 2003; Nikiforova et al. 2005a; Nikiforova et al. 2005b; Lewandowska and Sirko 2008; Kopriva et al. 2009) and the freshwater alga *Chlamydomonas reinhardtii* (Irihimovitch and Stern 2006; Gonzalez-Ballester et al. 2008; Nguyen et al. 2008; González-Ballester et al. 2010). Overall this body of research has revealed that removing sulphur from the external environment significantly decreases the level of various S-metabolites and this induces sulphate uptake transporters and key enzymes involved in the sulphate assimilation pathway. This stimulation was controlled primarily at the transcriptional level since genes encoding sulphate transporters, ATP sulphurylase and APS reductase are greatly up-regulated under low S-conditions.

In contrast to land and freshwater habitats, where S-metabolism is influenced by low sulphate conditions, the sulphate-rich ocean could possibly have influenced a different course in the evolution of S-metabolism in marine organisms. The biosynthesis of the S-molecule dimethylsulphoniopropionate (DMSP) by several phytoplankton groups (Keller et al. 1999a; Keller et al. 1999b) and the high ratio of sulpholipid to phospholipid in the marine cyanobacterium *Prochlorococcus* (Van Mooy et al. 2006) are good examples that illustrate the distinctive physiology of these organisms. Nevertheless, since sulphur is unlikely to ever be limiting in the sea, there are still many gaps in our understanding of S-metabolism in marine microalgae. Investigation of model marine microalgal species such the coccolithophore *Emiliania huxleyi* using novel sequencing approaches offers strong possibilities for filling these knowledge gaps.

E. huxleyi is a well studied and characterised eukaryotic phytoplankton species. It is very abundant which has implications not only for the ocean but also for the whole earth system, particularly the carbon and sulphur biogeochemical cycles. As such it has been used as a model organism to elucidate a range of complex and cross-linked environmental processes. Unfortunately, despite the continuing progress in *E. huxleyi* gene sequencing, there is still lack of valuable genomic resources for this microalga. Most of the gene expression studies in *E. huxleyi* were carried out with the expressed sequence tag (EST) analysis that can provides an expression profile for different environmental conditions. Wahlund et al. (2004) analysed 3000 ESTs generated under conditions that enhanced

coccolith formation with the aim of increasing the sequence database for *E. huxleyi* as well as the catalogue of genes potentially involved in calcification processes. As the result they obtained a unigene set of ~1523 ESTs with numerous transcripts related to the sexual reproduction and calcium homeostasis. More recent developments in molecular technologies have initiated further progress towards a better characterisation of coccolithophores. The draft genome of *E. huxleyi* CCMP 1516 released in 2006 by the International *E. huxleyi* Genome Sequencing Consortium and US Department of Energy Joint Genome Institute (http://www.jgi.doe.gov/) was a major step forward. The resulting, 168-megabases (Mb) draft genome was generated using a whole-genome shotgun approach, with 10 x coverage, followed by assembly of 7809 scaffolds. The genome was very difficult to sequence as *E. huxleyi* has high G+C content of 66%. To date, the *E. huxleyi* draft genome contains 39126 functionally annotated genes and gene models. Gene identifications and functional annotation was carried out based on more than 80000 EST/cDNA sequences generated under calcifying and non-calcifying conditions.

Besides the *E. huxleyi* nuclear genome sequenced, the complete plastid and mitochondrial genomes have also been sequenced and published (Sánchez Puerta et al. 2004; Puerta et al. 2005). The *E. huxleyi* chloroplast genome (cpDNA) consists of 105309 bp and it is much smaller than other cpDNAs from the red algal lineage. The analysis of *E. huxleyi* cpDNA suggests a close relationship between haptophyte plastid and the chl *c*-containing plastids from heterokonts and cryptophytes (Puerta et al. 2005).

With access to the genome of *E. huxleyi* high-throughput gene expression analysis became possible and a number of microarray experiments have been done. Quinn et al. (2006) used a cDNA microarray approach to characterise gene expression profiles in calcifying and noncalcifying *E. huxleyi* cultures grown in phosphate-limiting and phosphate-replete media, respectively. They detected 127 significantly different regulated genes out of 3000 transcripts, and these were mainly involved in cellular metabolism, ion channels, transport proteins, vesicular trafficking, and cell signaling.
In a different study, Rokitta et al. (2011) used microarray data to determine significant differences in gene expression between the haploid and diploid life –cycle stages of *E. huxleyi* Recently, the microarray-based technique was also employed to examine the transcriptome profile of virus-infected *E. huxleyi* during bloom progression (Pagarete et al. 2011). The authors observed a large change in transcriptome profile associated with amino acid and nucleotide metabolism, transcription and replication, as well as lipid metabolism.

To date explorations of the molecular features of *E. huxleyi* have mostly focussed on investigations on calcification and viral interactions, processes which make this coccolithophore a key player in numerous biogeochemical and ecological processes (Kegel et al. 2007; Richier et al. 2009; Von Dassow et al. 2009; Richier et al. 2010). Further characteristics such as high intracellular DMSP content and strain specific DMSP lyase activity suggest *E. huxleyi* could also be a model for studies of sulphur metabolism in marine organisms.

Measuring the expression of thousands of genes simultaneously under particular conditions has become possible thanks to the successful application of microarray technology and this is widely used for gene analysis. However, there are some limitations due to background noise, cross-hybridizations and ability to detect known sequences *a priori* (Forster et al. 2003; Russo et al. 2003). Novel Next-Generation Sequencing (NGS), approaches are high-throughput sequencing platforms that can overcome the problems often associated with microarrays. One of these commercially available technologies is the Solexa Illumina Gene Analyzer outlined by Morozova and Marra (2009). In brief, Illumina attaches specially designed adapters to the ends of previously prepared fragments from a library (Figure 5.1). Next, the DNA molecules are immobilized onto a solid surface called a flow cell using an adapter. A fixed single DNA fragment bends over to form a hybrid with the complementary linker and creates a "bridge" structure that can then serve as a template in the amplification step. The clusters formed in this way typically consist of ~1000 copies. With eight flow cell lines the instrument allows for several million clusters. Following this step, prepared single stranded amplification products undergo massive parallel sequencing-by-synthesis using a reversible terminate-based method. The nucleotides are modified with a fluorescently labelled terminator, which permits the incorporation of a single nucleotide into the growing DNA strand during each cycle. After recording its colour image, the terminator is cleaved off to allow incorporation of the next base in the following cycle. Although there are some limitations in form of short reads, 50 base pairs (bp) in this work, Illumina along with other NGS platforms, have become useful tools for pursuing transcriptome sequencing (RNA-seq).

The main goal addressed in this chapter was to investigate the role of sulphur in *E. huxleyi* at the molecular level using a transcriptomic approach. The results combined with the findings described in the previous chapters, served as an informative tool for comparing the different responses to S-availability amongst phylogenetically and ecologically distant organisms.

library preparation

cluster generation

sequencing

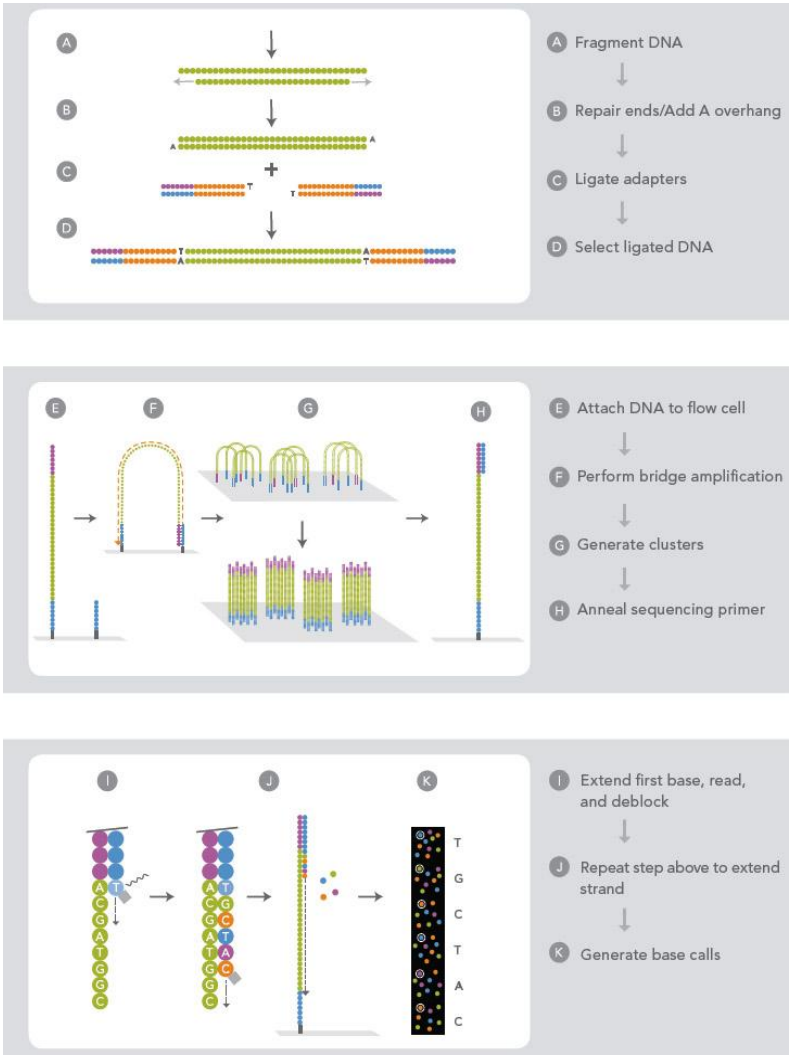

Figure 5.1 Schematic overview of the DNA and cDNA sequencing (RNA-Seq) workflow using Illumina's Genome Analyser. RNA is converted to a library of cDNA fragments attached with sequencing adaptors during library preparation. Using high-throughput sequencing technology a short sequence is obtained from each cDNA after cluster generation, and sequencing. Source: http://www.illumina.com/documents/products/brochures/brochure_genome_analyzer.pdf.

5.2. Methods

5.2.1. Growth conditions

Triplicate control and experimental batch cultures of *E. huxleyi* (CCMP 1516) were grown in 2 L conical flasks with 1L ESAW control medium (25 mM sulphate) or sulphur-limited (5 mM sulphate) as described earlier (see Chapter 2). The cell numbers were monitored on a daily basis. Samples for RNA extraction were collected when cultures entered mid-exponential phase. At this point, duplicate aliquots, 250 ml control and 350 ml experimental cultures were filtered onto 47-mm diameter 1.2 µm filters (Millipore™ Membrane Filter), placed into cryogenic vials, snap frozen in liquid nitrogen and stored at -80°C prior to RNA extraction. Along with RNA, samples from each biological replicate were taken for particulate DMSP analysis (see Chapter 2).

5.2.2. RNA isolation

Total RNA was extracted with TRI® Reagent (Sigma-Aldrich). After removing from the -80°C freezer, each filter was placed on a sterile Petri dish. Immediately, cells were washed from the filter with 800 µL of TRI® Reagent solution, transferred into 2 mL Eppendorf tubes and shaken for 15 min at room temperature to completely disrupt the cells. In order to precipitate DNA and proteins, 800 µl of chloroform was added, the shaking step was repeated and the tubes were centrifuged for 30 min at 9500 x g and 4°C. The supernatants were then transferred to new tubes and ice-cold isopropanol (vol:vol) was added. The nucleic acid precipitated during 20 min incubation at -20°C. Next, the centrifugation step was repeated. DNase digestion was carried out using the RNeasy® Plant Mini Kit (Qiagen) according to the manufacturer's protocol. After discarding the supernatant, the pellets were washed twice with 1 mL of ice-cold 75% ethanol and centrifuged for 2 min at 9500 x g and 4°C. Dry pellets were dissolved in 100 µL of RNase-free water. RNA concentrations were measured by absorbance at OD_{260} using a NanoDrop ND-1000 spectrophotometer (Thermo Scientific) and its purity was confirmed by measuring the ratios OD_{260}:OD_{280} and OD_{230}:OD_{260}. Prior to sending samples for Illumina deep-sequencing, RNA integrity was assessed by 1% agarose gel electrophoresis.

5.2.3. Illumina RNA-seq workflow

In this study, biological triplicates of control (25 mM SO_4^{2-}) and sulphur-limited (5 mM SO_4^{2-}) samples, each containing 5 µg of total RNA, were submitted to the GenePool research facility in Edinburgh, UK for sequencing on the Illumina Solexa GAIIx platform. Briefly, mRNA was obtained from total RNA using oligo-dT beads and converted into cDNA by random priming. The constructed cDNA library was loaded onto the flow cell and sequenced as 50-bp pair-end reads (Figure 5.1). Next, the sequences were aligned to the *E. huxleyi* reference transcriptome taken from the *E. huxleyi* CCMP1516 main genome assembly v1.0 using Mapping and Assembly with Qualities (MAQ) software set at a threshold of ≥ 30. This scoring system is based on two factors: singleness of the read and quality or mismatches of the read. In the case where a read matched at more than 2 locations, it was aligned randomly and a lower mapping quality was assigned. No more than 2 mismatches in the first 28 bp were allowed.

To identify functional categories, the transcripts were annotated against the Superfamily database 1.73 (http://supfam.cs.bris.ac.uk/SUPERFAMILY/). The superfamily/family description was attached to all genes with a domain assignment available. As part of their service, the Edinburgh GenePool generated the final data output with a raw read count of transcripts for each individual sample and provided these along with the read sequences and mapping statistics.

5.2.4. Data analysis

In order to investigate the difference in the gene expression pattern, the raw read counts were normalised in each library by dividing the number of reads by the total number of reads in the library. To identify which genes were up- or down-regulated in the low-S condition, the value of the normalised read counts from replicates (n=3) was averaged and a $\log_2$ ratio gene fold change was calculated using. Statistical comparison using the false discovery rate (FDR) was performed by Sam Mugford (John Innes Centre) according to Storey and Tibshirani (2003). The genes were considered to be differentially expressed when their q-values (proportion of false positives incurred when a particular test was called significant) were ≤ 0.05 and $\log_2$ ratios were either ≥1 or ≤-1.

5.2.5. Detection of differently expressed groups and iterative group analysis

To allow biological interpretation of changes resulting from S-deprivation, iterative group analysis was employed (Breitling et al. 2004). This is an automated procedure based on hypergeometric statistic that individually assigns a PC or Probability of Change value to each functional group. This highlights groups that have low absolute changes in expression despite their biological significance (Breitling et al. 2006). The enrichment was obtained separately for up- and down-regulated genes annotated to pathways from the Kyoto Encyclopedia of Genes and Genomes (KEGG) (Kanehisa and Goto 2000), the EuKaryotic Orthologous Group (KOG) (Tatusov et al. 2003) and the Gene Ontology (GO) terms (Ashburner et al. 2000). The lists of annotated genes were sorted by the descending (for up-regulated genes) or ascending (for down-regulated genes) S-limited/S-replete expression ratios. The significance threshold of each PC-value was calculated using an algorithm derived from the number of groups and the selected sensitivity.

5.2.6. Quantitative RT-PCR

To validate the transcriptomic data quantitative RT-PCR of selected genes from triplicate S-replete and S-limited cultures was performed. Total RNA was isolated from S-replete and S-limited cells as described above. A total of 1 µg of RNA was used for cDNA synthesis using a QuantiTec reverse transcription kit (Qiagen), which included a DNase treatment to ensure DNA-free RNA was obtained. No reverse transcription control was prepared to check for DNA contamination. The gene-specific primers were designed using Primer Premier 1.6 software (Premier Biosoft) (Table 5.1). The amplification efficiency was tested for each primer pair using a cDNA dilution series and this gave reaction efficiency values between 90 and 100%. The Q-PCR reactions were performed in 96-well plates. For each primer pair a 10 µM working stock was made using distilled water. The reaction mixture contained 4 µL of primer mix, 1 µL of cDNA template and 5 µL SYBR Green JumpStart *Taq* Ready Mix (Sigma-Aldrich). The reactions were run in the Opticon 2 continuous fluorescence detector (Bio-Rad, Hemel Hempstead, UK) for 4 min at 95^{o}C for initial denaturation, followed by 39 cycles of 15 sec of denaturation at 95^{o}C, 30 sec of annealing at 60^{o}C and 30 sec of elongation at 72^{o}C. Final dissociation was carried out for 10 min at 72^{o}C to ensure that each amplicon was a single product.

The *E. huxleyi* gene encoding actin (JGI protein ID 74049) was used as a reference and for each gene tested Ct values, defined as the PCR cycle number at which the fluorescence passes the threshold, were used to calculated relative expression values using comparative Ct method (Livak and Schmittgen 2001).

Table 5.1 Gene specific primers for quantitative RT-PCR analysis.

ID[a]	Product length (bp)	Forward primer (5'-3')	Reverse primer(5'-3')
450514	86	CTGTGCGGAGATCGACAAGGTG	CGACGAGGTCCGTGTTCCAGAT
452597	85	AGACCAACACCGACGACCTCTC	AACTTGAGCATCGCCAACGCAT
437926	91	GAGCACGGGCAACCTCATCTTC	CGACATGGCGACCTTGAATCCG
441761	127	TCGCCGAGGACAAGTACAACCT	CGCTGCTGGACGAGATGCTTT
454260	113	ACCGAAGACGGCACCACGAT	AGGTCGCACTCACGCTCGTT
440242	97	ATGCTGCCGATGGTGAACGAAG	AGCCGTAGCCGTACAGGAAGAC
442972	86	ATGAGGGACCGATGGGTATGGG	CAGCGAGTGAGCGAGTTGCT
74049[b]	85	AGTGCCATTCACCGCAAG	TGCTCGAGTACAAGCAGCAAG

[a]JGI protein accession number.
[b]Reference gene.

5.3. Results

5.3.1. Basic quantitative parameters

Previous experiments (see Chapter 3) have demonstrated that sulphur limitation induced a decrease in *E. huxleyi* cell growth, intracellular DMSP and GSH content while sulphate uptake increased. This suggested that these changes might be regulated on the transcriptional level. In order to examine the *E. huxleyi* transcriptome with respect to sulphur availability, RNA was obtained from replicate cultures that had been grown with 25 mM (control) and 5 mM (S-limited) sulphate. On the day of harvesting the average growth rate was 0.67 (± 0.04) day^{-1} and 0.46 (± 0.05) day^{-1} in control and S-limited cultures, respectively. Average intracellular DMSPp concentrations were 226 (± 5) and 103 (± 7) mM in control and treated cultures, respectively. In all cases the cell growth and intracellular DMSP were significantly different (Student's t-test; $p \leq 0.05$). Total RNA samples were further processed and analysed in the GenePool in Edinburgh (see section 5.2.3). Before sequencing, a cDNA library was prepared for each individual control (cont1, cont2 and cont3) and S-limited culture (S-limit1, S-limit2 and S-limit3) and the output for each sample was summarised in Table 5.2. The number of high-throughput paired-end sequences yielding reads ranged from 5 to 14.5 million per sample. Of these, approximately 70% could be mapped against the *E. huxleyi* CCMP1516 main genome assembly (v1.0). The remaining unmatched sequences were assembled *de novo* in the contigs. Apart from a few Illumina adapters (5 -10% are expected) no hit to contaminant sequences was found.

Subsequently, the generated transcripts were annotated with the Superfamily database 1.73. The total number of tags was 21.9 million and ranged from 1.8 to 5.2 million per sample (Table 5.2).

Table 5.2 Summary of sequencing output of the Illumina sequencing for control and sulphur-limited samples of *E. huxleyi.*

Sample	Read length (bp)	Reads number	Bases (Mb)	Paired end reads (PE)	Mapped PE reads
Cont1	50	1815582	90	4992234	3554470 (71%)
Cont2	50	4976244	249	13322358	9895842 (74%)
Cont 3	50	2654631	133	7040884	5124762 (73%)
S-limt1	50	5177502	259	14550654	10074492 (69%)
S-limit2	50	4207815	210	11482428	8151742 (71%)
S-limt3	50	3089598	154	8355714	6092740 (73%)
	Total	21921372	1095		

Altogether the RNA sequencing detected 27904 expressed genes. Most of these genes were found in at least one library each for control and sulphur-limited cultures. However, 404 genes were found only in the sulphur-limited samples while 10 were detected only in control ones. Out of these 27904 genes, 4945 differentially expressed genes were found at a False Discovery Rate (FDR) of 5%, including 4165 up-regulated genes and 780 down-regulated genes in the low sulphate condition. As shown in the gene expression histogram (Figure 5.2), the induction of gene expression ranged from 1.2 fold (log_2 ratio=0.3) to more than 32-fold (log_2 ratio>5), whereas the reduction of gene expression ranged from 0.9-fold change (log_2 ratio=-0.1) to less than 0.03 fold change (log_2 ratio<-5). Particularly, 2888 genes were up-regulated at least 2 fold (log_2 ratio≥1) including the 404 genes that were unique to the sulphur-limited libraries, while 236 genes were down-regulated at least 2 fold, including 10 genes uniquely expressed in the controls.

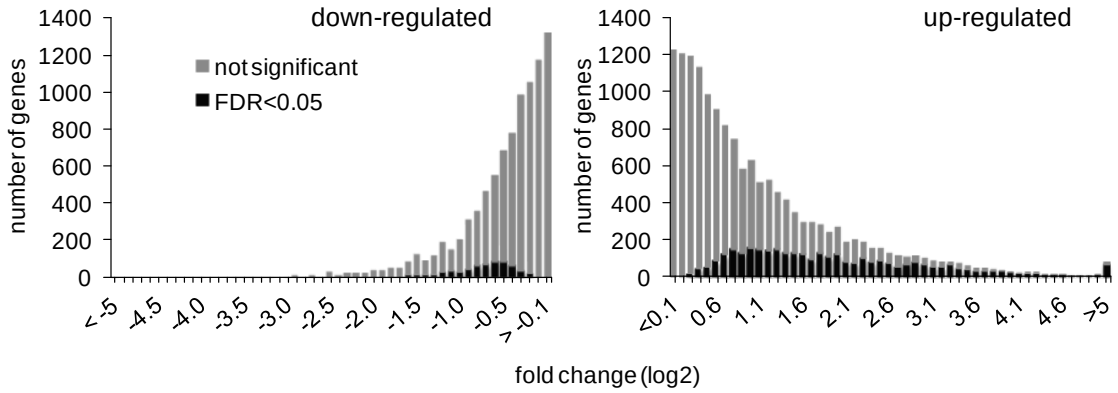

Figure 5.2 Histogram showing the distribution of observed fold changes in transcript expression with log_2 ratios for S-limited and S-replete *E. huxleyi* cultures.

The transcript expression patterns for the Illumina RNA-seq was verified by quantitative RT-PCR for seven differently regulated genes (FDR; q≤0.05) (Figure 5.3). For all the genes tested the direction of the change observed in the RNA-seq data was consistent with the qRT-PCR results (Table 5.3).

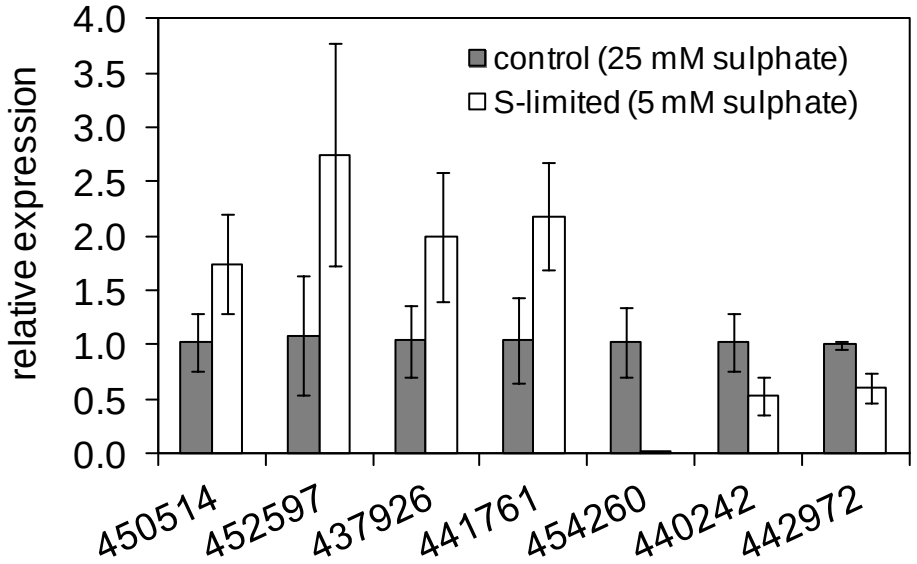

Figure 5.3 Transcript levels of the selected genes determined by quantitative RT-PCR for Illumina RNA-seq validation. Values are means ±SD from triplicate *E. huxleyi* cultures. All the values for the S-limited cultures were significantly different from S-replete controls (Student's t-test; p≤0.05).

Table 5.3 Comparison of the Illumina RNA-seq and quantitative RT-PCR.

ID[a]	function	Fold change (log2 values)	
		RNA-seq	qRT-PCR
450514	oxidoreductase activity	2.9	0.8
452597	aconitate hydratase	3.1	1.5
437926	acyl-CoA dehydrogenase activity	3.2	1.0
441761	predicted transmembrane sulphate ion transporter	3.3	1.1
454260	pseudouridine synthase activity	-3.5	-6.8
440242	putative 3-hydroxyacyl-CoA dehydrogenase	-2.1	-0.9
442972	hypothetical protein	-2	-0.7

[a]JGI protein accession number.

5.3.2. Analysis of general transcriptome response based on functional classification

To obtain information on the *E. huxleyi* biological processes affected by sulphur availability a transcriptome wide analysis was performed. Figure 5.4 shows the percentage share of KOG groups specifically assigned to significantly different genes (FDR; $q \leq 0.05$) with the $\log_2$ expression level either ≥ 1 or ≤ -1. This simplifies denoted 1422 versus 109 annotated genes in up- and down-regulated categories, respectively. In the up-regulated group, transcripts associated with 'cellular processes and signalling' were the most represented (40%), mainly by genes involved in signal transduction (12%), post-translational modification (10%) and cytoskeleton organization (8%). Although, the cytoskeleton organisation functional category was also represented in a major way in the down-regulated group (29%), the majority of genes were related to 'information storage and processing' (34%) mostly represented by genes involved in RNA processing (11%), transcription (5%) and translation (15%).

Interestingly, among 25 KOG groups enriched in up-regulation, 3 groups: 'carbohydrate transport and metabolism' (4%); 'cell cycle control, cell division, chromosome partitioning' (4%) and 'cell motility' (0.14%) were absent amongst the down-regulated genes, which could reflect the general metabolic changes triggered by S-deficiency.

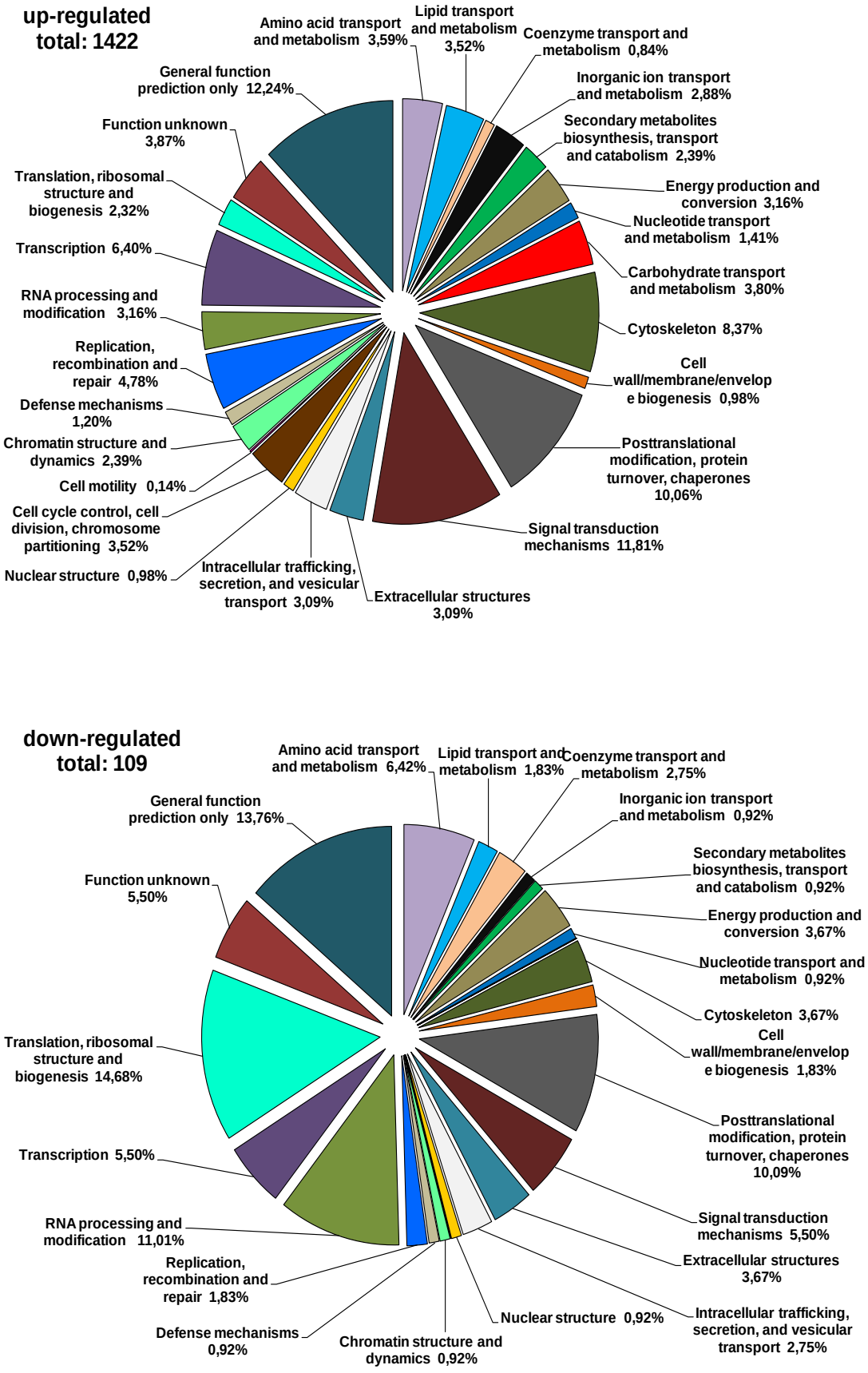

Figure 5.4 Pie chart showing a KOG functional classification comparison of up- and down-regulated genes for each functional class. Only significantly regulated genes ($q \leq 0.05$) with a fold change 2 or more were considered.

The iterative Gene Analysis (iGA) was another approach employed for transcription-wide analysis. Using the KEGG pathway classification, 2723 genes (from total of 27904) were annotated and clustered into 90 groups. To increase the number of KEGG groups, the higher sensitivity of the program was applied giving the PC-value a cut-off 0.055. Thus, 23 up-regulated and 30 down-regulated groups were identified and sorted by their statistical significance (Table 5.4). The first point to note is that 6 carbohydrate metabolism (a) and 5 lipid metabolism (c) groups are strongly represented in the up-regulated set. By contrast, the down-regulated set has no single prominent group but is rather equally represented by various KEGG classes. Most of the differentially expressed functional groups are assigned to the metabolism category, however other categories: genetic information processing (k) and environmental information processing (l) are also present among the down-regulated groups. Furthermore, 4 groups (pyrimidine metabolism, porphyrin and chlorophyll metabolism, folate metabolism and glycerolipid metabolism) were present in both up- and down-regulated lists. Interestingly, the degradation pathway for a range of xenobiotics was down-regulated under S depletion. Xenobiotics are foreign chemicals that are often detoxified by sulphur metabolites such as glutathione. Among the KEGG pathways triggered by low sulphur stress, there are groups known to be closely linked to sulphur metabolism. Glutathione metabolism was found among the up-regulated groups, whereas the methionine, thiamine and serine metabolic pathways were found among the down-regulated groups.

The iGA procedure was also used to do a KOG annotation (Table 5.5). Of the 27904 genes, 9947 were annotated and clustered into 2259 functional groups. The table shows 40 and 23 KOG groups enriched among the up- and down-regulated transcripts, respectively (PC-value ≤ 0.002). The KOG groups uniquely detected in the up-regulated list included 10 clusters assigned to the ‘Cytoskeleton’ class, 5 clusters assigned to the ‘inorganic ion transport and metabolism’ class and 1 cluster assigned to ‘energy production and conversion’, ‘nuclear structure’ and ‘function unknown’. In contrast, the groups appeared more evenly distributed throughout the down-regulated list, with 2 clusters uniquely assigned to ‘RNA processing and modification’ and 1 cluster assigned to ‘defense mechanism’ and ‘secondary metabolites’.

Interestingly, the ‘cytoskeleton’ class contains significantly up-regulated groups of genes encoding for kinesine and myosin motor proteins which are involved in numerous processes such as cell division, cellular transport and organelle relocation.

Sulphate depletion also resulted in an enrichment of the 'sulphate/bicarbonate/oxalate exchanger SAT-1 and related transporters (SLC26 family)' class, which is partially driven by strong expression of two sulphate transporter transcripts.

Results from iGA with both KEGG and KOG annotations were supported by using Gene Ontology (GO) annotations of the 'biological process' category. Of the 27904 genes, 3335 were annotated and clustered into 461 groups. Table 5.6 represents 31 up-regulated and 16 down-regulated groups enriched with a PC-value less than 0.01. GO analysis suggests an induction of cell signalling and DNA processes, accompanied by a reduction in RNA processing and protein biosynthesis at low-S. It is worth noting that whilst asparagine can accumulate in terrestrial plants due to S deficiency (Shewry et al. 2009), asparagine biosynthesis was down-regulated in *E. huxleyi*

To better visualise gene expression in the *E. huxleyi* global metabolic network , the Interactive Pathways Explorer (iPath2) was applied (Letunic et al. 2008). The general metabolic pathway (Figure 5.5) was designed by mapping the Enzyme Commission (EC) numbers of differently expressed genes that met the $\log_2 \geq 1$ (FDR; $q \leq 0.05$) criterion. For more accuracy further selection was applied to obtain enzymes with a unique identification (four-digit EC number). This displayed 222 up-regulated enzymes on the iPath2 metabolic pathway map.

This analysis revealed that low S-conditions triggered induction of the transcripts encoding enzymes associated with fatty acid biosynthesis and metabolism, as well as these for carbohydrate, amino acid and nucleotide metabolism over a number of others metabolic processes.

Table 5.4 An overview of metabolic responses to sulphur limitation in *Emiliania huxleyi* using enrichment in KEGG metabolic pathways identified by iGA. Only significantly regulated groups with Probability of Change (PC) value ≤ 0.056 are shown. The number of change versus total group members is given as a percentage. KEGG pathway classes: a: carbohydrate metabolism; b: energy metabolism; c: lipid metabolism; d: nucleotide metabolism; e: amino acid metabolism; f: metabolism of other amino acids; g: glycan biosynthesis and metabolism: h: metabolism of cofactors and vitamins; i: metabolism of other secondary metabolites; j: biodegradation of xenobiotics; k: translation; l: membrane translation.

KEGG groups	Members	Number changed	PC	%
Up-regulated				
Biotin metabolism (h)	2	2	0.003	100
Fatty acid metabolism (c)	19	16	0.004	84
Bile acid biosynthesis (c)	13	3	0.005	23
beta-Alanine metabolism (f)	4	1	0.007	25
Pyrimidine metabolism (d)	126	6	0.008	5
Sphingoglycolipid metabolism (c)	58	5	0.008	9
Glutamate metabolism (e)	23	13	0.008	57
Ascorbate and aldarate metabolism (a)	15	2	0.009	13
Purine metabolism (d)	122	8	0.011	7
Flavonoids, stilbene and lignin biosynthesis (g)	36	20	0.014	56
Tryptophan metabolism (e)	17	15	0.018	88
Butanoate metabolism (a)	15	2	0.023	13
Pyruvate metabolism (a)	23	10	0.023	43
Ubiquinone biosynthesis (h)	125	7	0.024	6
Prostaglandin and leukotriene metabolism (c)	13	12	0.029	92
Vitamin B6 metabolism (h)	7	5	0.032	71
Citrate cycle (TCA cycle) (a)	6	4	0.035	67
Glutathione metabolism (f)	35	8	0.039	23
Porphyrin and chlorophyll metabolism (h)	37	1	0.040	3
Folate biosynthesis (h)	84	14	0.046	17
Glycerolipid metabolism (c)	68	1	0.049	1
Aminosugars metabolism (a)	5	4	0.052	80
Galactose metabolism (a)	17	1	0.055	6
Down-regulated				
Fatty acid biosynthesis (path 1) (c)	25	2	0.000	8
Pantothenate and CoA biosynthesis (h)	16	16	0.005	100
Fructose and mannose metabolism (a)	29	3	0.005	10
Type III secretion system (l)	29	29	0.005	100
Arginine and proline metabolism (e)	33	30	0.007	91
Aminoacyl-tRNA biosynthesis (k)	43	34	0.008	79
Pyrimidine metabolism (d)	126	3	0.008	2
Glycolysis / Gluconeogenesis (a)	35	30	0.010	86
Alanine and aspartate metabolism (e)	8	7	0.013	88
Methionine metabolism (e)	13	9	0.014	69
Type II secretion system (l)	4	2	0.015	50
Nicotinate and nicotinamide metabolism (h)	86	82	0.018	95
N-Glycans biosynthesis (g)	36	10	0.019	28
Phenylalanine, tyrosine and tryptophan biosynthesis (e)	14	13	0.021	93
Selenoamino acid metabolism (f)	6	6	0.021	100
Glycerolipid metabolism (c)	68	5	0.022	7
Porphyrin and chlorophyll metabolism (f)	37	31	0.026	84
Fluorene degradation (j)	5	5	0.027	100
Folate biosynthesis (h)	84	21	0.027	25
Thiamine metabolism (h)	7	3	0.031	43
Carbon fixation (b)	15	13	0.031	87
Glycosaminoglycan degradation (g)	21	4	0.035	19
Sterol biosynthesis (c)	23	18	0.036	78
D-Arginine and D-ornithine metabolism (f)	17	14	0.037	82

Glycine, serine and threonine metabolism (e)	30	10	0.041	33
Nitorobenzene degradation (j)	2	2	0.042	100
Ethylbenzene degradation (j)	28	3	0.046	11
gamma-Hexachlorocyclohexane degradation (j)	11	8	0.050	73
Lipopolysaccharide biosynthesis (g)	22	21	0.051	95
Alkaloid biosynthesis II (i)	6	3	0.053	50

Table 5.5 An overview of metabolic responses to sulphur limitation in *Emiliania huxleyi* using enrichment in KOG functional classification identified by iGA. Only significantly regulated groups with Probability of Change (PC) value ≤ 0.002 are shown. The number of change versus total group members is given as a percentage.

KOG terms	Members	Number changed	PC	%
Up-regulated				
Ammonia permease	13	2	0.000	15
Kinesin (KAR3 subfamily)	8	3	0.000	38
DNA polymerase delta, catalytic subunit	2	2	0.000	100
GABA receptor	5	5	0.000	100
Putative zinc transporter	6	6	0.000	100
Beta tubulin	6	3	0.001	50
Alpha tubulin	9	4	0.001	44
Sulfate/bicarbonate/oxalate exchanger SAT-1 and related transporters (SLC26 family)	10	4	0.001	40
Myosin class II heavy chain	11	10	0.001	91
Vacuolar sorting protein VPS1, dynamin, and related proteins	4	4	0.001	100
Actin and related proteins	10	8	0.001	80
Cyclin B and related kinase-activating proteins	3	3	0.001	100
Cobalamin synthesis protein	20	2	0.001	10
Integral membrane protein	3	2	0.001	67
Phospholipase C	4	3	0.001	75
Predicted FAD-dependent oxidoreductase	3	1	0.001	33
Predicted signal transduction protein	4	4	0.001	100
Glutamate synthase	3	3	0.001	100
Dimethylglycine dehydrogenase precursor	4	4	0.001	100
Voltage-gated Ca2+ channels, alpha1 subunits	10	9	0.001	90
Kinesin-like protein	19	10	0.001	53
NADP/FAD dependent oxidoreductase	8	3	0.001	38
Helicase-like transcription factor HLTF/DNA helicase RAD5, DEAD-box superfamily	13	13	0.001	100
F-box protein JEMMA and related proteins with JmjC, PHD, F-box and LRR domains	2	2	0.001	100
Microtubule-binding protein involved in cell cycle control	2	2	0.001	100
K+/Cl- cotransporter KCC1 and related transporters	3	3	0.001	100
Ubiquitin-protein ligase	25	23	0.001	92
Centromere-associated protein NUF2	2	2	0.001	100
Structural maintenance of chromosome protein 1 (sister chromatid cohesion complex Cohesin, subunit SMC1)	2	2	0.001	100
Transcription factor TCF20	16	12	0.002	75
Predicted acyl-CoA dehydrogenase	2	1	0.002	50
Histone 2A	7	7	0.002	100
Transcription factor, Myb superfamily	33	7	0.002	21
Acetyl-CoA acetyltransferase	2	2	0.002	100
60S ribosomal protein L22	34	23	0.002	68

Beta-spectrin	2	2	0.002	100
WD40 repeat stress protein/actin interacting protein	3	3	0.002	100
Cysteine proteinase Cathepsin L	6	6	0.002	100
Rac1 GTPase effector FRL	21	1	0.002	5
Nucleolar GTPase/ATPase p130	36	9	0.002	25
Down-regulated				
Animal-type fatty acid synthase and related proteins	13	5	0.000	38
Triglyceride lipase-cholesterol esterase	3	3	0.000	100
Subtilisin-related protease/Vacuolar protease B	7	2	0.000	29
Molecular chaperones HSP70/HSC70, HSP70 superfamily	5	4	0.000	80
CAATT-binding transcription factor/60S ribosomal subunit biogenesis protein	3	2	0.001	67
Ribosome biogenesis protein - Nop58p/Nop5p	2	2	0.001	100
Ubiquitin and ubiquitin-like proteins	9	6	0.001	67
N-terminal acetyltransferase	6	5	0.001	83
Dual specificity phosphatase	15	9	0.001	60
rRNA processing protein	2	2	0.001	100
Ribosome biogenesis protein NIP7	2	2	0.001	100
Predicted panthothenate kinase/uridine kinase-related protein	2	2	0.001	100
Translation initiation factor 5 (eIF-5)	2	2	0.001	100
Trypsin	24	6	0.001	25
Palmitoyl protein thioesterase	5	2	0.001	40
tRNA-dihydrouridine synthase	10	6	0.002	60
WD40 repeat protein	15	4	0.002	27
FOG: TPR repeat	21	15	0.002	71
Aspartate aminotransferase/Glutamic oxaloacetic transaminase AAT1/GOT2	4	3	0.002	75
tRNA methyltransferase	2	2	0.002	100
Non-ribosomal peptide synthetase/alpha-aminoadipate reductase and related enzymes	7	7	0.002	100
ATP-dependent RNA helicase A	12	11	0.002	92
RNA polymerase I, second largest subunit	2	2	0.002	100

Table 5.6 An overview of metabolic responses to sulphur limitation in *Emiliania huxleyi* using enrichment in GO annotation identified by iGA. Only significantly regulated groups with Probability of Change (PC) value ≤ 0.011 are shown. The number of change versus total group members is given as a percentage.

GO terms	Members	Number changed	PC	%
Up-regulated				
microtubule-based movement	14	8	0.000	57
protein polymerization	14	8	0.000	57
microtubule-based movement	43	6	0.000	14
chromosome organization and biogenesis	16	4	0.000	25
nitrogen compound metabolism	7	6	0.002	86
cell organization and biogenesis	9	6	0.002	67
DNA replication	12	8	0.002	67
deoxyribonucleoside diphosphate metabolism	3	3	0.002	100
chromosome	7	2	0.003	29
DNA recombination	15	8	0.003	53
intracellular signaling cascade	11	5	0.004	45
small GTPase mediated signal transduction	24	21	0.004	88
signal transduction	15	9	0.004	60
glutamine biosynthesis	5	4	0.004	80
electron transport	27	20	0.004	74
DNA replication	19	9	0.004	47
immune response	5	2	0.005	40
DNA repair	25	11	0.005	44
'de novo' pyrimidine base biosynthesis	5	3	0.005	60
intracellular	35	2	0.006	6
response to antibiotic	10	8	0.006	80
ubiquitin-dependent protein catabolism	41	32	0.006	78
intracellular protein transport	27	22	0.007	81
transport	32	25	0.007	78
ubiquitin-protein ligase activity	6	4	0.008	67
DNA metabolism	14	7	0.008	50
calcium ion binding	3	2	0.008	67
G-protein coupled receptor protein signaling pathway	5	2	0.008	40
protein transport	29	23	0.008	79
cellular protein metabolism	37	23	0.009	62
ribonucleoside-diphosphate reductase complex	2	1	0.010	50
Down-regulated				
fatty acid biosynthesis	18	2	0.000	11
transcription	21	4	0.001	19
chromatin silencing	8	7	0.001	88
ribosome biogenesis and assembly	10	10	0.002	100
cytoplasm	6	6	0.003	100
protein biosynthesis	19	13	0.003	68
translational initiation	23	20	0.004	87
RNA processing	21	19	0.006	90
regulation of transcription	11	10	0.007	91
tRNA processing	11	8	0.007	73
heme biosynthesis	6	1	0.007	17
mismatch repair	3	1	0.007	33
regulation of translational initiation	4	2	0.008	50
tRNA aminoacylation for protein translation	36	26	0.008	72
asparagine biosynthesis	2	1	0.010	50
protein folding	27	26	0.010	96
cell adhesion	4	1	0.011	25

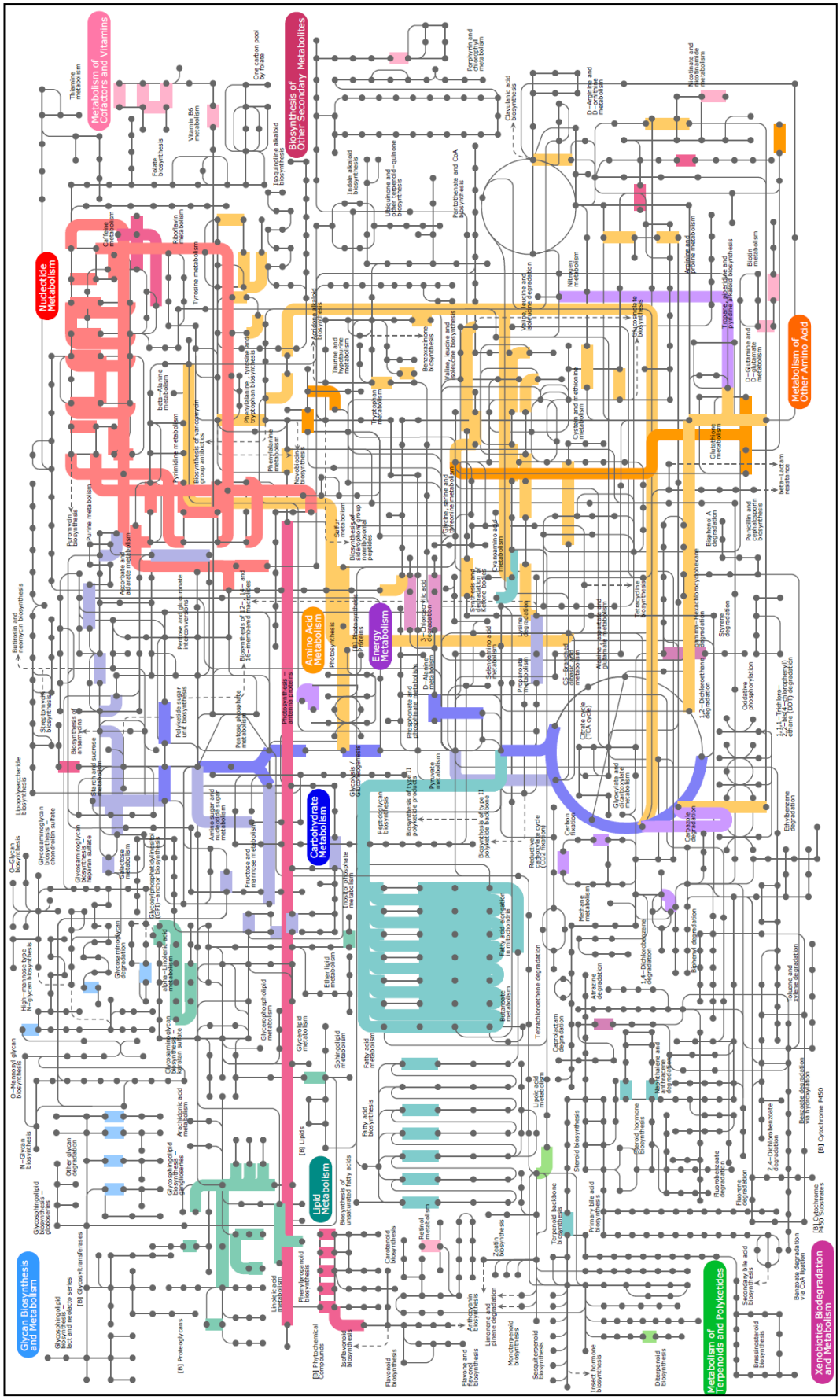

Figure 5.5 Metabolic pathways that were up-regulated in *E. huxleyi* under S-limited conditions highlighted using Enzymatic Commission (EC) queries.

5.3.3. Cross species comparison of the transcriptional response to sulphur requirement in *E. huxleyi*, *C. reinhardtii* and *A. thaliana*

The distant evolutionary relationships and different habitats occupied by *E. huxleyi*, *C. reinhardtii* and *A. thaliana* make the comparison of their transcriptome particularly interesting. We wanted to know whether the transcriptome response to sulphur limitation is similar in these species. To compare the gene expression profile we pooled the top 100 up-regulated genes from *E. huxleyi* (this study), *C. reinhardtii* (González-Ballester et al. 2010) and *A. thaliana* (Maruyama-Nakashita et al. 2006) and searched for their reciprocal homologues (Appendix Table A.1, A.2, A.3). For a more descriptive cross analysis of the most expressed genes from *E. huxleyi*, only proteins IDs with KEGG annotation were considered. Surprisingly, we got a different outcome according to the species analysed. For example, orthologs of *E.huxleyi* proteins were abidingly down-regulated in *C. reinhardtii* and not differentially expressed in *A. thaliana*. Only a few of the most up-regulated transcripts were found in all three organisms and these included some sulphur related genes (encoding S-transporters and serine acetyltransferase). This discrepancy might be due to differences in experimental setups dictated by the fact that all 3 species occur in distinct and different environments. Nevertheless, the different pattern in most induced genes may also reflect their evolutional and ecological distance.

5.3.4. Sulphur metabolism

In plants and green algae, sulphur limitation has a great impact on sulphate uptake, assimilation and the metabolism of S-molecules. Figure 5.6 shows the regulation of genes encoding enzymes involved in the metabolic pathway from sulphate acquisition to cysteine synthesis and the link to glutathione metabolism. To allow a rapid comparison with the well characterised species, the homologous transcripts of *C. reinhardtii* (González-Ballester et al. 2010) and *A. thaliana* (Maruyama-Nakashita et al. 2006) are included in the pathway. This analysis revealed significantly different regulation of the sulphate transport and cysteine formation steps. In *E. huxleyi* transcripts of three sulphate transporters: *STR2, STR3* and *STR4* responded to S-limitation by increasing their expression level 2, 10 and 15 fold, respectively. The same was observed in the other two model organisms. In *E. huxleyi* gene encoding STR4 was the most induced (~14 fold increase) by the S-limitation. This protein is most similar to the transporters up-regulated

by S-starvation in *C. reinhardtii* (SULTR2) and *A. thaliana* (SULTR 4.2). Similarly, the expression of genes involved in the last step of cysteine biosynthesis, encoding SAT1 and SAT2 isoforms of serine acetyltransferase and OASTL2 and OASTL3 for OAS thiollyase, increased under S-limited conditions (Figure 5.6). Expression analysis revealed the up-regulation of two genes encoding SAT1 and SAT2 enzymes that synthesise O-acetylserine (OAS), as well as up-regulation of two genes encoding OASTL2 and OASTL3 proteins that incorporate reduced sulphur into OAS to produce cysteine (Cys). A similar increase appeared in *C. reinhardtii* and *A. thaliana*. In contrast to *A. thaliana* and *C. reinhardtii*, genes coding for enzymes that catalyse the reduction of sulphate, ATPS, APR and SiR, showed no significant change in transcription level in response to low S conditions in *E. huxleyi*. It is important to note that the overall expression of ATPS2 and APR was very high placing the latter in the top 30 most expressed genes in the *E. huxleyi* transcriptome. In the two sequential steps of glutathione (GSH) synthesis only an increase in *GSH5* was observed in *E. huxleyi*. On the other hand, 2 out of 3 isoforms of γ-glutamyltranspepidase (*GTP1* and *GTP2*) were up-regulated indicating a higher degree of GSH degradation. The biosynthesis of the DMSP-precursor, methionine (Met) is a 4 step, 3 intermediate process (cysteine →cystathionine→ homocysteine→ methionine). In this pathway, two genes annotated as cystathionine γ-synthases did not respond to S-limitation. Moreover, the expression of mRNA involved in the synthesis of the intermediate product-homocysteine was not identified in the transcriptome. In the final step of methionine biosynthesis, transcripts encoding vitamin B12 dependent methionine synthase did not change significantly under S-deficiency. Also, the expression level of two transcripts encoding an enzyme that converts Met to *S*-adenosylmethionine (adenosylmethionine synthase; SAMS) did not change.

In Chapter 3 it was shown that S availability affects DMSP content in *E.huxleyi* cell However, as yet no genes associated with DMSP synthesis and degradation have been identified and this precludes a detailed analysis of DMSP metabolism. Interestingly, low S conditions triggered a significant up-regulation of two genes encoding proteins with JGI protein IDs 459683 and 470487 by 5 and 3 fold, respectively. These genes, predicted as Class III acyl CoA transferases, are homologues of the bacterial *DddD* (DMSP-dependent DMS production) gene which was proposed to convert DMSP into DMS and 3-OH-propionate (Todd et al. 2007; 2010). However, a phylogenetic analysis of these Class III acyl CoA transferases revealed a substantial evolutionary distance between the alga and bacterial lineages (Figure 5.7).

The abundance of mRNA for biotin synthase significantly increased with S-limitation. This enzyme requires two SAM molecules to serve as cofactors and these are recycled to Met during biotin production. Biotin can serve as a cofactor of acetyl-CoA carboxylase enzyme that is involved in fatty acids biosynthesis. Indeed, the gene (JGI protein ID 428897) encoding this enzyme was up-regulated by 5 fold in S-depleted *E. huxleyi* cells.

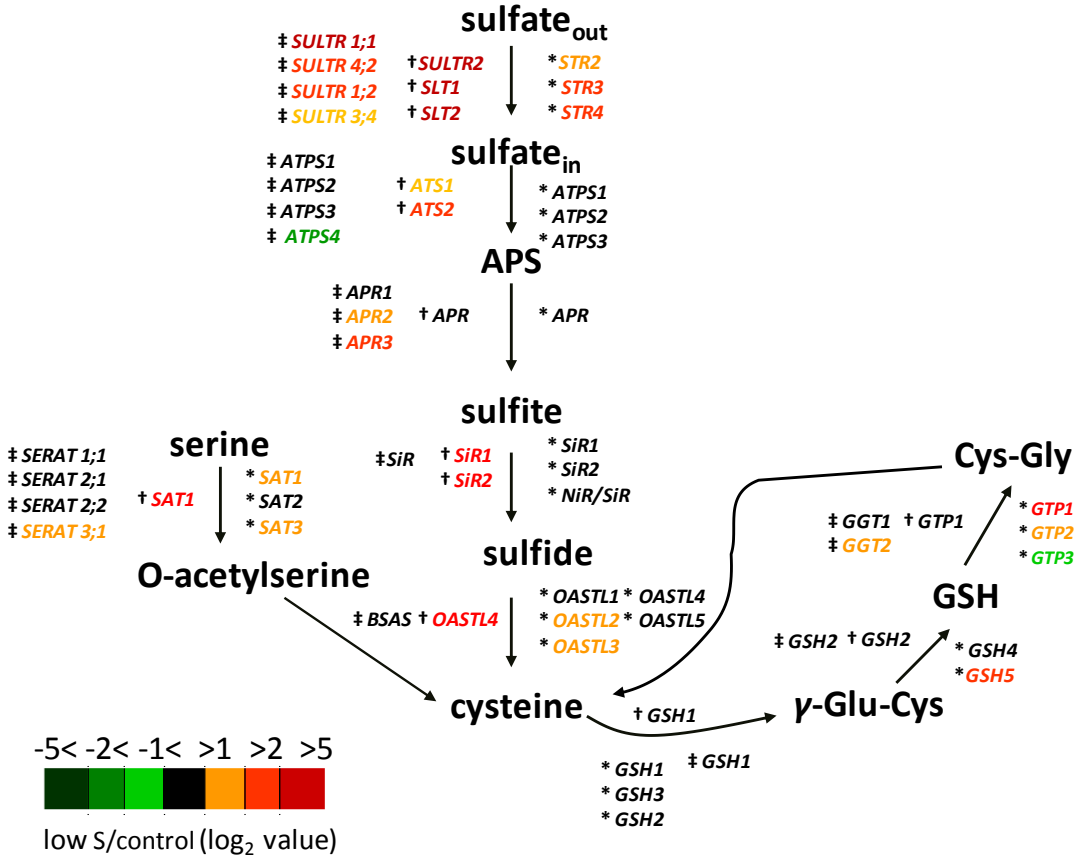

Figure 5.6 Sulphur metabolic pathway showing the genes that encode enzymes involved in the pathway. Gene expression was colour-coded according to their $\log_2$ value from the low S/control ratio. Asterisk, cross and double-cross indicate transcripts from *E. huxleyi* (this study); *C. reinhardtii* (González-Ballester et al. 2010) and *A. thaliana* (Maruyama-Nakashita et al. 2006), respectively.

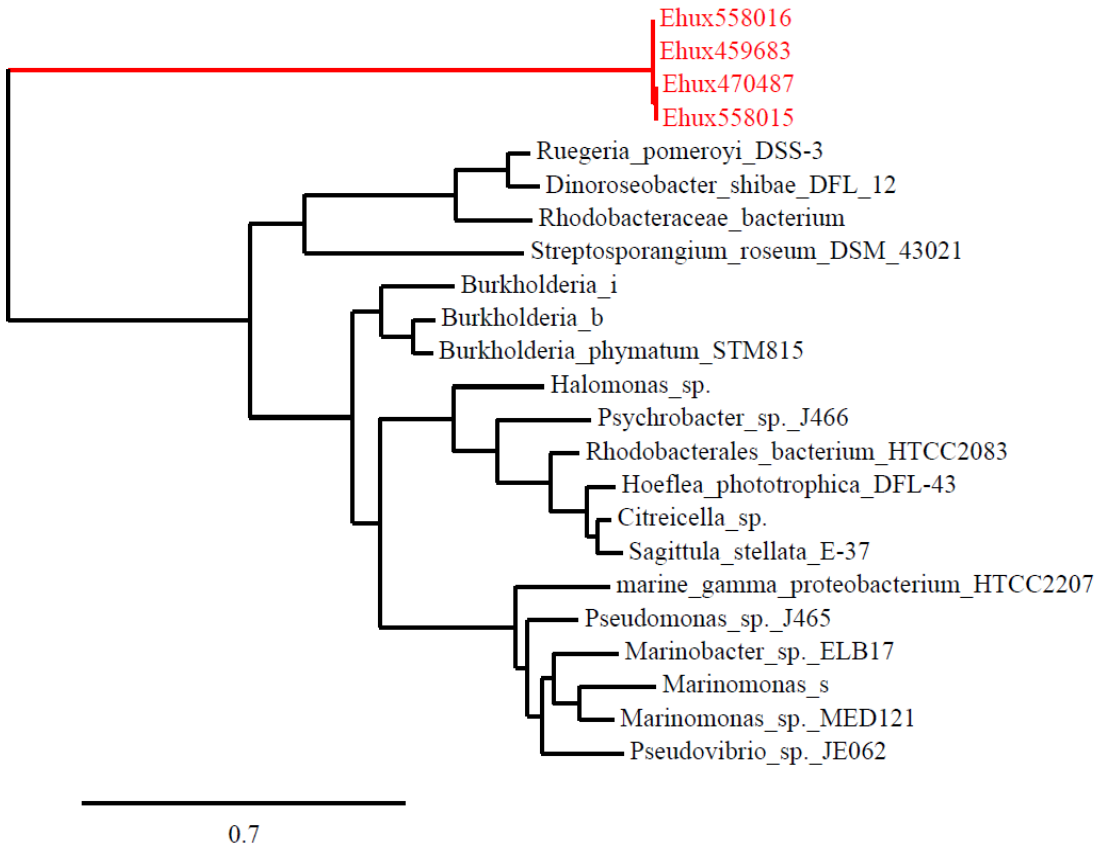

Figure 5.7 A phylogenetic tree of DddD proteins. Bacterial amino acids sequences were retrieved from the strains considered as DMS producers (J.D. Todd, personal communication). The tree was constructed using the Phylogeny.fr website (Dereeper et al. 2008). *E. huxleyi* proteins and their IDs are highlighted in red.

5.4. Discussion

5.4.1. Global transcriptome response to sulphur limitation

Transcriptome analysis of the sulphate starvation response has been undertaken in the model species for higher plants, *Arabidopsis thaliana* (Nikiforova et al. 2003; Maruyama-Nakashita et al. 2006) and fresh water green algae *Chlamydomonas reinhardtii* (Nguyen et al. 2008; González-Ballester et al. 2010). However, no such information exists, for marine organisms, and particularly phytoplankton. Our analysis of the marine microalga *Emiliania huxleyi* (CCMP 1516) fills this gap and provides the first insights into its response to S-limitation. Whilst sulphate has not been considered to limit the growth of marine phytoplankton (Giordano et al. 2005b) cultivating *E. huxleyi* in artificial seawater with 5 times less sulphate compare to ambient conditions, significantly decreased growth and intracellular DMSP biosynthesis (see Chapter 3). Therefore, even marine organisms are susceptible to sulphur deficiency and this opens a way to compare the response to this condition in organisms with a large evolutionary distance that are from very different environments. As transcriptomic data sets exist for *A. thaliana* and *C. reinhardtii*, we also analysed the effects of S-starvation on the *E. huxleyi* transcriptome. The method of choice was the Illumina RNA sequencing platform and this provided genome-wide transcript data. Here, it should be noted that *E. huxleyi* genome was made accessible as 'draft' assemblies whose quality is uncertain and more complete assembly has to be done to encompass full genome and the individual genes. Nonetheless, the current *E. huxleyi* genome sequence can still facilitate molecular analysis of this species and help shed light on sulphur metabolism in marine phytoplankton.

Using a stringent criterion for detecting the gene expression differences, 2888 up-regulated and only 236 down-regulated transcripts were identified. This indicates remarkable changes in gene transcription in *E. huxleyi* due to sulphur availability. The number of differentially regulated transcripts in *E. huxleyi* reached ~10% of detected transcripts. We used a range of annotations (KEGG, KOG and GO) available through the JGI *E. huxleyi* genome website to find which biological processes are affected by, and therefore probably important for, the response of *E. huxleyi* to low sulphate stress. The fundamental difference in the response to sulphate limitation in *E. huxleyi* compare to *A. thaliana* and *C. reinhardtii* is the ratio between up-regulated and down-regulated genes. The general response to prolonged sulphate limitation is a slowing down of metabolism

and shortening of life cycle (Hoefgen and Nikiforova 2008). Accordingly, in *A. thaliana* microarray experiments significantly more transcripts were repressed than induced by sulphate starvation (Hirai et al. 2003; Maruyama-Nakashita et al. 2003; Nikiforova et al. 2003). The same was true for *C. reinhardtii* were more than 2-fold transcripts were down-regulated than up-regulated by sulphate deficiency (González-Ballester et al. 2010) and for *D. salina* where sulphate deficiency resulted in decrease in Rubisco accumulation and PEP carboxylase and nitrate reductase activities (Giordano et al. 2000). In contrast, in *E. huxleyi* we found 2667 transcript were present only in sulphate deficient cells compared to 690 that were present only in the controls. Moreover, among transcripts detected in both conditions, greater than 10-fold more genes were up-regulated than down-regulated.

At the molecular level the responses to various stress conditions, such as sulphur limitation, are controlled through signal transduction pathways. Indeed, we observed induction of the genes involved in signal transduction and cytoskeleton reorganization in the cells exposed to the low sulphate condition (Table 5.5 and 5.6; Figure 5.4). The transcriptome profile also showed shifts in cell metabolism indicating an increase in fatty acid biosynthesis and metabolism under sulphur stress. Since the committing step in fatty acids biosynthesis involves carboxylation of acetyl-CoA to malonyl-CoA, one can speculate that there was an excess of acetyl-CoA which was converted to fatty acids for storage and thereby retained for the tricarboxylic acid cycle (TCA) in homeostasis. Interestingly we noticed a 5 fold up-regulation of a gene (JGI protein ID 471081) encoding acetyl-CoA carboxylase (ACCase) that catalyses this reaction. Under normal conditions, DMSP is an important sink for reduced carbon. Indeed, Matrai and Keller (1994) reported that more than 10% of the organic carbon can be allocated to DMSP in marine microalga such as *E. huxleyi.* Since one of the suggested functions of DMSP is a sink for excess carbon (Stefels 2000; Stefels et al. 2007), it is possible that a decrease in DMSP synthesis due to reduced availability of sulphate triggers an increase in fatty acid biosynthesis to store carbon from photosynthesis and tune the cell metabolic machinery. While in *A. thaliana* a decrease in S- supply significantly down-regulated the *SQD2* gene that encodes a sulpholipid biosynthesis enzyme (Nikiforova et al. 2003), we found that its orthologues in *E. huxleyi* were unaffected. Furthermore, the microalga RNA-seq revealed high transcript abundance. Interestingly we observed a 2 fold up-regulation of the genes encoding the sulpholipid sulfoquinovosyl diacylglycerol (SQDG) synthase. This sulphur-containing lipid is commonly present in photosynthetic organisms as it is an important structural and functional component of photosystem II (PS II) (Yu et al. 2002; Aoki et al.

2004; Zhang et al. 2004). Moreover, in marine algae it can contribute up to 50% of the total polar lipids (Dembitsky and Rozentsvet 1990; Dembitsky et al. 1990). Sugimoto et al. (2010) showed the increase of *SQD1* mRNA with induction of SQDG degradation in the green alga *C. reinhardtii* under S-starvation conditions. This increase was confirmed by González-Ballester et al (2010) who showed the up-regulation of the SQDG synthesis genes *LPB1, SQD1* and *SQD2* in S-deprived *C. reinhardtii* cells. Radiolabel experiments implemented for this organism by Sugimoto and al. (2007) suggested SQDG as a significant S-source and thus its synthesis and degradation is precisely regulated under low S-conditions. Since in marine microalgae such as *E. huxleyi*, DMSP is considered as the main S-reservoir, a similar approach could shed further light on sulphur regulation in these species.

As with carbon, excess nitrogen needs to be channelled during unbalanced growth due to sulphur deficiency. The enrichment of genes associated with amino acid metabolism and transport (Figure 5.4) in *E. huxleyi* grown in low S could be explained by a reduction in protein synthesis and in, consequence, an accumulation of amino acids (Kopriva and Rennenberg 2004). Also, there are indications that sulphur deficiency in plants induces catabolism of pyrimidine and purine (Nikiforova et al. 2005b). Pyrimidine catabolism may be due to a general decrease in metabolism and RNA content, whereas purine catabolism can be linked to drain excess nitrogen (Katahira and Ashihara 2002; Nikiforova et al. 2005b). In fact we also observed enrichment in transcripts involved in pyrimidine and purine metabolism (Table 5.4; Figure 5.4) that could reflect an analogous sulphur stress response in *E. huxleyi.*

Intriguingly, the elevated expression pattern in *E. huxleyi* under sulphate depletion have some similarity with this found recently in the haploid stage of *E. huxleyi,* strain RCC 1217 by Rokitta et al. (2011). The authors assessed the difference between gene expression in haploid and diploid cells of *E. huxleyi.* After assigning transcripts to KOG annotation, they reported an increase in haplont-specyfic transcripts related to amino acid transport and metabolism, cell cycle control, cytoskeleton and cell motility, lipid transport and metabolism, protein turnover. The similar gene expression observed in diploid life stage of *E.huxleyi*, strain CCMP 1516 under sulphate depletion (this study) may be attributed to physiological responses to change in sulphate concentration. In fact, in the natural environment, the haploid stage of coccolithophores may occupy low-nutrient and stratified regimes whereas their diploid stage may dominate in the nutrient-reach and mixed regimes (Houdan et al. 2006).

5.4.2. Sulphur metabolism

Growth of *E. huxleyi* under low sulphate conditions led to several changes in the expression of genes involved in sulphate acquisition and assimilation. For example, there was an increase in sulphate transporter mRNAs (*STR2, STR3,* and *STR4*) in treated cells. Sulphate transporters were also found to be induced in *C. reinhardtii* and *A. thaliana* in many S-deprivation experiments (Maruyama-Nakashita et al. 2006; González-Ballester et al. 2010). Interestingly, STR3 and STR4 transporters are ion co-transporters of the SLC26 family of proteins and this group was highlighted as being up-regulated in our iGA (Table 5.5). A protein Blast revealed homology of STR3 and STR4 with the high affinity H^+/SO_4^{2-} SULTR2 protein from *C. reinhardtii*, (Shibagaki and Grossman 2008; Pootakham et al. 2010) which suggests a similar sulphate transport response in S-limited *E. huxleyi*.
In contrast to the high up-regulation of sulphate transport genes we observed, we found no significant regulation of genes encoding enzymes involved in sulphate to sulphide reduction (Figure 5.6), indicating that they are not regulated by S availability in *E. huxleyi*. This difference in expression pattern compared to *A. thaliana* and *C. reinhardtii* could support the observation of Kopriva et al (2009) who suggested that plant/animal-like isoforms of ATP sulphurylase (ATPS), as are present in haptophytes and diatoms, contain a pyrophosphatase domain which can substantially increase the APS synthesis rate. Also, transcripts encoding APS reductase (APR) appear not to be regulated which is opposite to the situation in plants where APR is highly regulated by the demand for reduced sulphur (Takahashi et al. 1997; Leustek et al. 2000; Kopriva 2006). It is noteworthy that we found a high level of APR mRNA abundance that may also reflect an order of magnitude higher APS reductase activity compared to higher plants (see Chapter 3). While decreased sulphate did not stimulate SO_4^{2-} reduction to S^{2-}, we noticed a moderate induction of genes encoding serine acetyltransferase (SAT) and *O*-Acetylserine (thiol) lyase (*O*ASTL); components required for cysteine formation. A similar response was also reported for both *A. thaliana* and *C. reinhardtii* (Maruyama-Nakashita et al. 2006; González-Ballester et al. 2010). Furthermore, Ito et al. (2011) observed an increase in *O*ASTL activity in the seaweed *Ulva pertusa* following transfer to S-deficient medium.
Interestingly, Hopkins et al. (2005) argue that increases on *O*AS that occur under prolonged S-deficiency are the result of limited supply of sulphide and, thus disturbance in cysteine synthesis. Indeed in our experiment, cells were harvested after 5 days growth in a low sulphate medium when the cell growth already slowed.

Cys is a final product of assimilatory sulphate reduction and the precursor of many organosulphur metabolites such as glutathione (GSH). This small thiol compound attracted our attention because it plays an important role in neutralising reactive oxygen species (ROS) (Rennenberg 1980; Polle and Rennenberg 1992; Dupont et al. 2004) and it has been suggested that DMSP is also involved in scavenging ROS (Sunda et al. 2002). With the exception of *GSH5* which was up-regulated, there was no change in the expression of the genes involved in GSH synthesis in *E. huxleyi* (Figure 5.6). In contrast we observed up-regulation in genes encoding enzymes that recycle GSH back to Cys. This is consistent with a decrease in intracellular GSH in *E. huxleyi* grown under S-limitation (see Chapter 3). The increase in GSH catabolism may be linked to sulphur re-allocation in the cell triggered by the low S-condition, but a more detailed study is needed to verify this hypothesis.

One of the main motivations to characterise the transcriptional response in *E. huxleyi* to sulphur arose from previous experiments where we noticed a significant decrease in intracellular DMSP concentration induced by S-limitation (see Chapter 3). Despite the importance of DMSP and its high concentration in marine algae such as *E. huxleyi* (see Chapter 1), how DMSP synthesis and degradation is controlled at the biochemical and molecular level remains unclear. The observations we reported here shed some light on its regulation by sulphur availability. Although a DMSP synthesis pathway for algae was proposed by Gage at al. (1997) based on *in vivo* isotope labelling of the green macro-alga *Enteromorpha intestinalis* (since renamed *Ulva intestinalis*), the genes encoding the enzymes that catalyse DMSP synthesis are still unknown. Very recently, Ito at al. (2011) examined the effect of S-deficiency on DMSP production in *U. pertusa* and they speculate that the decline in DMSP synthesis may be due to Met being used for the synthesis of S-adenosyl-Met (SAM) and methionyl-tRNA rather than for DMSP. However, in our study on *E. huxleyi* this hypothesis was not confirmed by changes in the expression of transcripts encoding both S-adenosyl-Met synthetase and methionyl-tRNA synthetase. The regulation of DMSP precursor-Met synthesis, in *E. huxleyi* is more similar to that of plants rather than that of *C. reinhardtii* as the transcript levels for Met biosynthesis genes were not affected by sulphate deficiency, whereas they decreased in *C. reinhardtii* (González-Ballester et al. 2010). Interestingly, there was a significant increase in two genes (JGI protein ID 45983 and 470487) annotated to the type III acyl coenzyme A (CoA) transferase. These proteins are candidate orthologs of CoA transferase encoded by the *DddD* gene from the DMS-producing bacterium *Halomonas* HTNK1CoA (Todd et al.

2010). Todd et al (2007; 2010) predicted that the DddD enzyme would catalyse DMSP degradation by forming a DMSP-CoA thioester that can be cleaved to DMS and 3-hydroxypropionate. This suggests that a downshift in DMSP concentration in *E. huxleyi* could be driven by induction its catabolism rather than turnover and repression of synthesis. On the other hand, a phylogenetic analysis comparing the DddD proteins of a number of bacterial species with the *E. huxleyi* type III (CoA) transferases, revealed that the latter compose a distant cluster (Figure 5.7). To assess the potential for the type III (CoA) transferase to act as a DMSP catabolic enzyme in algae, additional genetic and biochemical studies are needed.

Extensive studies focus on transcription regulation by nutrient availability in marine phytoplankton; however they are restricted to the compounds that typically limit the cell growth in the natural environment such as carbon, nitrogen, phosphate, ion, etc. Since carbon dioxide is necessary for photosynthesis, the carbon transport and CO_2 accumulation is well described in many algae. Marine algae use various types of CO_2 concentrating mechanisms (CMMs) strategies to provide CO_2 on the active sites of RUBISCO-the enzyme incorporating CO_2 into organic carbon. The algal genome sequencing significantly advanced our knowledge about different strategies of CCMs in phytoplankton groups, e.g., CCM similar to plant C4 carbon fixation pathway in diatoms (Giordano et al. 2005a). For detailed information concerning CCMs mechanisms in algae we refer the reader to two reviews written by Giordano et al (2005a) and Reinfelder (2011). Also, the access to the whole genome sequence of two diatoms: *T. pseudonana* and *Phaeodactylum tricirnutum* resulted in discovery multiple transcripts for nitrate uptake and assimilation as well as for the transport of nitrite, ammonium, urea and other forms of organic nitrogen (Armbrust et al. 2004; Parker et al. 2008). Another recent fascinating discovery is the presence of animal-like urea cycle in these diatom species (Allen et al. 2011). The tight regulatory interactions between carbon, nitrogen and sulphur have been established in plants and these seem to be essential for normal growth (Kopriva et al. 2002). It is a challenge to future to understand this coordination in marine phytoplankton, therefore first we need to decipher sulphur metabolism in these organisms. Our work shed a light on S-metabolism in marine microalgae and can constitute a basis for further detailed investigations.

5.5. Conclusions

To the best of our knowledge this thesis contains the first transcriptome analysis of a marine microalga subjected to the sulphate limitation. The Illumina RNA-sequencing provided the transcriptome profile of both control and sulphur stressed *E. huxleyi* revealing numerous transcripts that responded to the S-limited condition. The KEGG, KOG and GO annotations enabled the identification of various changes in the *E. huxleyi* transcriptome and these changes suggest an orchestrated gene expression response to low sulphate concentrations. Special attention was paid to the expression of homologues of genes involved in sulphate uptake and the SO_4^{2-} to DMSP pathway. The patterns in transcript expression under the low S-condition are in good agreement with the metabolic changes in *E. huxleyi* discussed in Chapter 3. Both similarities and differences in sulphate assimilatory pathways appear to exist between *E. huxleyi*, *A. thaliana* and *C. reinhardtii* that highlight their phylogenetic and ecophysiological distance. Another important aspect of this work was that it has shed more light on DMSP metabolism in a marine microalga; a process that is currently rather poorly understood especially at the molecular level. The discovery of the up-regulation of mRNAs encoding Class III acyl CoA transferases in S-limited *E. huxleyi* cultures points us in a good direction for the future discovery of the DMSP lyase gene in this species and other DMSP-producing marine microalgae.

6. General discussion

6.1. Summary

Since sulphur is an essential nutrient for growth and through studying responses to changes in environmental conditions many aspects of sulphur metabolism have been revealed especially in the vascular plant *Arabidopsis thaliana* and the green algae *Chlamydomonas reinhardtii*. Whilst these model organisms are very noticeably different from one another, they derived from the primary endosymbiosis and had a common ancestor ~1.1 billion years ago (Gutman and Niyogi 2004). They are both representatives of green lineage of the Archaeplastida (Plantae) group within the tree of life as shown in Figure 6.1. That is why they are an excellent pair for studying sulphur metabolism in terrestrial environment. By contrast, *Emiliania huxleyi* is evolutionary much more distant species, which similarly to other marine eukaryotic algae, originated from secondary endosymbiosis. Unfortunately, sulphate assimilation and metabolism in marine microalgae has not attracted very much attention at all. This is probably largely due to the fact that sulphate is a very abundant anion in the ocean and given its ~28 mM concentration is seawater it probably never limits the growth of marine phytoplankton. Interestingly, an increase of the sweater sulphate level coincided with the evolutionary success of coccolithophorids that rose in Mesozoic ocean, where sulphate concentration rose from 13 and 27 mM (Ratti et al. 2011). This strongly suggests that sulphate was one of the major factors steering evolution of some marine microalgae. Despite its importance, to date studies of S-metabolites in marine eukaryotic algae have mostly related to DMSP and the products of its reactions and other aspects of sulphate metabolism have been largely ignored.

This PhD project aimed to address this gap in knowledge by better characterising the metabolism of S-compounds in marine microalgae. In order to do this, we chose to work on the haptophyte *Emiliania huxleyi* based on the following key characteristics:

- Phylogenetically distant from *A. thaliana* and *C. reinhardtii* (Figure 6.1).
- Cosmopolitan distribution in the ocean and ability to form conspicuous blooms mean that *E. huxleyi* is an important player in the global carbon cycle.
- Considered as a model species for the coccolithophore group.
- Biosynthesis of high intracellular concentrations of DMSP and thus a significant role in sulphur biogeochemical cycle.
- The availability of the recently sequenced genome of *E. huxleyi* CCMP 1516.

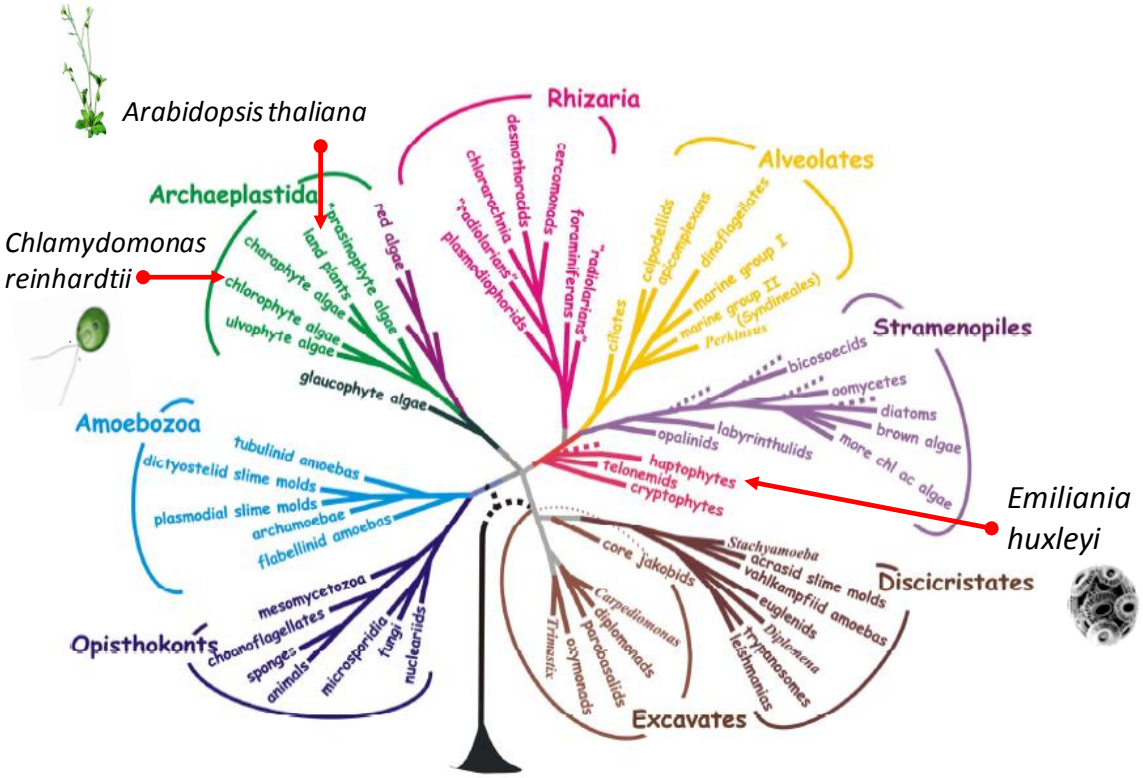

Figure 6.1 The position of *Emiliania huxleyi*, *Chlamydomonas reinhardtii* and *Arabidopsis. thaliana* in the eukaryotic tree of life which is a consensus phylogeny of eukaryotes based on molecular phylogenetic and ultrastructural data. Adapted from Baldauf (2008).

To achieve our goal we examined the physiological and molecular responses in *E. huxleyi* under various sulphate concentrations. In Chapter 3 we described the physiological responses of *E. huxleyi* to sulphur limitation and sulphur replenishment. In initial experiments we showed that sulphate availability affected cell growth and intracellular DMSP concentration. This response appeared to be strain-dependent in that, contrary to results for CCMP 1516 and CCMP 370, the DMSP content of the high DMSP-lyase strain CCMP 373 (Steinke et al. 1998) was not altered by S-limitation. We suggested that this different response pattern could be linked to differences in DMSP lyase activity. In future work it would be interesting to test whether, and if so to what extent, DMSP lyase activity is regulated by sulphate in these strains of *E. huxleyi*. Our further investigations revealed that sulphate re-supply back to S-limited cultures increased DMSP concentration and that this induction is likely to be associated with light conditions (Chapter 3 and 4).

Another important aspect of this work was to examine the changes in S-metabolites in *E. huxleyi* that have been previously been shown to be important in the sulphate assimilation pathways of *A. thaliana* and *C. reinhardtii*. Several studies have shown that the induction of sulphate uptake in plants and green algae is triggered by S-limitation conditions (Yildiz et al. 1994; Yoshimoto et al. 2007; Pootakham et al. 2010). In our experiments we showed the same positive effect of S-limitation on sulphate uptake in *E. huxleyi*, however our results suggest that this microalga has a lower affinity sulphate uptake system than *A. thaliana* and *C. reinhardtii.* This is likely to be due to the high and constant sulphate abundance in today's ocean. The same characteristic of seawater may, at least partly, explain the much higher level APS reductase activity we measured in *E. huxleyi* compared with activities seen in *A. thaliana* or *C. reinhardtii*. Furthermore from our observations it appears that, again contrary to plants and freshwater algae (Takahashi et al. 1997; Ravina et al. 2002), the APR activity in *E. huxleyi* is not regulated by sulphur demand. On the other hand, GSH and DMSP contents were regulated by sulphate availability in this microalga. Given that GSH is known to be a ROS scavenger , and this role has also been proposed for DMSP (Sunda et al. 2002), we examined the diurnal variation in these compounds and revealed that they are regulated in *E. huxleyi* by light (see Chapter 5).

Over recent years molecular biology and '–omics' technologies have substantially advanced our understanding of the role sulphur plays in living organisms. Indeed, *A. thaliana* and *C. reinhardtii* have both been well characterised through expression profiling of S-limited plants and cultures (Maruyama-Nakashita et al. 2006; González-Ballester et al. 2010). To enable the molecular comparison between the responses to sulphate deficiency of *E. huxleyi*, plant and green alga model systems, in Chapter 5 we used the RNA-seq Illumina platform approach. We analyse the whole transcriptome of *E. huxleyi* grown under sulphate limited conditions. We discovered that ~10% of the transcripts detected changed their expression level in low S-conditions. Consequently our results suggest that, as in plants and green algae, the expression of many *E. huxleyi* genes is modulated by sulphate availability. We showed that S-limitation triggered general responses to the stress condition through the up-regulation of genes involved in signalling transduction, cell structure organisation and fatty acid metabolism. We also gained insight into the expression of genes responsible for sulphur uptake and assimilation and compared this with the expression observed previously in *A. thaliana* (Maruyama-Nakashita et al. 2006) and *C. reinhardtii* (González-Ballester et al. 2010). Some transcripts such showed

the same expression pattern under S-limitation condition in all 3 species e.g. the induction of the genes encoding sulphur transporters and enzymes involved in Cys synthesis. On the other hand many other mRNAs from the sulphur metabolic pathway exhibited different expression pattern in *E. huxleyi.* For example, contrary to vascular plants, mRNA encoding APS reductase was very abundant but not differently regulated in S-limited *E. huxleyi*. High APR activity and high expression of *APR* gene, both may suggest that in sulphur rich marine environment some phytoplankton species evolved higher capacity for sulphate reduction than plants and freshwater green algae. This might also be attributed at least in part to high production of DMSP as reduced sulphur is required for DMSP synthesis.

In conclusion, we have shown that, despite being adapted to high sulphate concentrations in sea water, the marine microalga *E. huxleyi* still retains the genetic program to respond to artificial sulfate deficiency. Whereas the up-regulation of sulphate uptake and cysteine synthesis in *E. huxleyi* is in common with plants and freshwater algae, the global response significantly differs. Instead of slowing down photosynthesis and primary metabolism *E. huxleyi* responds to sulphate deficiency by up-regulation of genes involved in carbohydrate and fatty acid synthesis and appears to re-direct sulphur and carbon from DMSP into these alternative metabolite pools. Our findings could reflect the ecophysiological and phylogenetic distance between this coccolithophore and *A. thaliana* and *C. reinhardtii.*

6.2. Future perspectives

To get more novel insights into sulphur acquisition and metabolism in marine phytoplankton, further study is still needed. When taken as whole, this thesis put the foundation on general understanding of physiological, biochemical and molecular responses of *E. huxleyi* to sulphur availability. However the next steps should be a detailed measurement of sulphate uptake and sulphur distribution in *E. huxleyi* cells under both S-sufficient and S-deficient conditions.

In our experiment we demonstrated that similarly to plans and fresh water algae, sulphate uptake in *E. huxleyi* was enhanced by lowering external sulphate concentration. The next challenge is to determine kinetic parameters (K_M and V_{max}) of SO_4^{2-} uptake under different sulphate concentration in *E. huxleyi* grown at 25 and 5 mM SO_4^{2-}. Additionally, deciphering sulphur allocation in *E. huxleyi* should be experimentally determined.

[^{35}S]sulphate fluxes through the metabolic pathways and its incorporation into proteins, thiols and methionine has been successfully established in *A. thaliana* (Kopriva et al. 1999; Mugford et al. 2010). Similar approach could be potentially applied to reveal sulphur distribution in *E. huxleyi* S-sufficient, S-deficient and S-resupplied conditions. Using radioactive [^{35}S]sulphate labelling to study *E. huxleyi* S-metabolism in sulphate reach marine system, is technically challenging as high concentrations of this isotope is required. However, the use of the tracer technique with the ^{34}S stable isotope would be an alternative for evaluations of sulphur dynamics in the seawater environment. Applying ^{34}S tracer allows avoiding exposure to radioactivity. Moreover, since ^{34}S does not decay long time course experiments can be conducted and samples analysis delayed.

It is suggested that success o chlorophyll a+c algae such as *E. huxleyi* is related to high cellular sulphur content and the ability to produce DMSP (Giordano et al. 2005; Takahashi et al. 2011). Surprisingly, despite its importance, still little is known about algal DMSP metabolism. A current major challenge in DMSP research is to advance our understanding control of DMSP synthesis and cleavage especially on the molecular level. The bacterial genes involved in DMSP metabolism have only recently been identified (Todd et al. 2010; Vila-Costa et al. 2010) however, algal DMSP synthesis and cleavage genes still remain to be found and characterised. *E. huxleyi* is a good model phytoplankton for finding DMSP synthesis and cleavage genes given its high intracellular DMSP concentration. Altering the sulphate concentration in the medium provides an approach whereby a dramatic increase in intracellular DMSP concentration can be observed after sulphate replenishment, the logical next step would be the transcriptome profiling of S-limited *E. huxleyi* subjected to sulphate re-supply. In our RNA-seq dataset generated for S-limited cells, we have found two significantly up-regulated homologues of the bacterial *DddD* (DMSP dependent DMS production) genes involved in DMSP degradation to DMS and 3-hydroxypropionate. Detailed, functional characteristic of these two candidates could verify if they are genes encoding for DMSP lyase in *E. huxleyi*. Furthermore, analyses carried out on other *E. huxleyi* isolates suggested they were differently affected by low sulphate availability and expanding the study to additional strains should shed more light on DMSP metabolism. However, to better determine molecular mechanisms of sulphate-sensing and signalling and get more insights into *E. huxleyi* sulphur metabolism, it would be extremely advantageous to find the approach for knocking out genes in this microalga and thus allowing the genetic mutant screening.

Overall the physiological and molecular data for *E. huxleyi* in response to S-limitation presented in this thesis support each other and provide a foundation for further work on sulphur metabolism in the marine microalgae. Since sulphur metabolism is fairly well understood in plants and green algae, additional phenotypic data from marine algae should provide better insights into evolution and adaptation of plants and algae to their different environments.

Marine algal genomes are still in their relative infancy compared to those for higher plants and some green algae, but in the near future many more genomes should be available and they will lead us to a much improved understanding of the evolution of photosynthetic organisms.

Annotation of the whole genome sequence for *E. huxleyi* is currently processing. In addition to the information on gene expression, our *E. huxleyi* RNA-seq data for cells grown in control and S-limited conditions is promising for refining the *E. huxleyi* strain CCMP 1516 genome annotation and should help to decrease the number of genes assigned as ‘hypothetical’ or ‘unknown’ in the genome.

Appendix

Table 1A. Summary of the top 100 most up-regulated transcripts in S-limited *Emiliania huxleyi* with the best BLASTP hits (E-value cutoff of 1E-5) in *Chlamydomonas reinhardtii* and *Arabidopsis thaliana*. *E. huxleyi* genes descriptionws were retrieved from the Enzyme Commission (EC). E-value (expectation value) reflecting the number of hits expected to be found by chance

Emiliania huxleyi[a]				*Chlamydomonas reinhardtii*[b]			*Arabidopsis thaliana*[c]		
Protein ID[d]	Description	EC number	Fold Change (log_2)	Homolog ID[d]	E-value	Fold Change (log_2)	Homolog ID	E-value	Fold Change (log_2)
238059	Glycerol-3-phosphate dehydrogenase.	1.1.99.5	6.0	No			AT3G56840	1E-17	0.2
426799	Glutamate decarboxylase.	4.1.1.15	5.8	185104	2E-101	-0.7	AT5G43900	8E-129	0.3
455971	Sarcosine dehydrogenase.	1.5.99.1	5.8	205744	8E-07	0.1	AT5G67290	4E-11	0.4
458972	DNA-directed DNA polymerase.	2.7.7.7	5.6	No			No		
196679	Exo-alpha-sialidase.	3.2.1.18	5.5	No			No		
106050	Adenosinetriphosphatase.	3.6.1.3	5.2	171623	1E-23	-1.4	AT2G07690	1E-39	0.0
114117	Exo-alpha-sialidase.	3.2.1.18	5.1	No			No		
464628	Adenosinetriphosphatase.	3.6.1.3	5.1	152683	2E-45	-2.3	AT2G14050	1E-103	0.5
222150	Protein kinase.	2.7.1.37	5.1	113407	9E-20	-1.1	AT4G04740	9E-21	0.6
455696	DNA-directed DNA polymerase.	2.7.7.7	5.0	189721	6E-132	-1.3	AT5G63960	8E-146	0.2
42969	Ferredoxin--NADP(+) reductase.	1.18.1.2	4.9	195553	9E-92	-1.6	AT1G30510	1E-96	-0.3
198992	Acid--D-amino-acid ligases (peptide synthases).	6.3.2.-	4.7	194222	4E-51	-0.7	AT1G19880	7E-70	0.2
194351	Protein-methionine-S-oxide reductase. Peptide methionine sulfoxide reductase. Peptide Met(O) reductase.	1.8.4.6	4.6	187796	3E-09	0.4	AT5G61640	3E-15	0.4
441547	Acyl-CoA dehydrogenase.	1.3.99.3	4.6	118751	1E-92	0.2	AT3G06810	6E-179	0.3
457170	DNA-directed DNA polymerase.	2.7.7.7	4.6	177262	3E-69	-1.9	AT5G67100	6E-45	0.0
229721	DNA-directed RNA polymerase.	2.7.7.6	4.5	No			No		
417368	In phosphorous-containing anhydrides.	3.6.1.-	4.4	No			AT1G79890	3E-110	0.2
438851	6-phosphofructokinase.	2.7.1.11	4.4	196430	3E-12	-0.1	AT5G56630	8E-19	0.3
450278	Lanosterol synthase.	5.4.99.7	4.3	112249	5E-85	-2.2	AT5G25150	5E-28	0.4
450487	Acyl-CoA oxidase.	1.3.3.6	4.2	No			No		
426418	Palmitoyl-protein hydrolase.	3.1.2.22	4.2	131913	2E-24	0.0	AT3G60340	1E-28	0.2
236798	DNA-(apurinic or apyrimidinic site) lyase.	4.2.99.18	4.2	No			No		

452085	Adenosinetriphosphatase.	3.6.1.3	4.2	122561	7E-76	-1.6	AT3G09660	3E-140	0.3
456826	DNA-directed DNA polymerase.	2.7.7.7	4.1	140580	2E-75	-1.6	AT2G29570	2E-84	0.4
427020	Aldehyde dehydrogenase (NAD+).	1.2.1.3	4.1	135609	2E-81	0.3	AT3G24503	4E-92	0.4
433820	3-oxoacyl-[acyl-carrier protein] reductase.	1.1.1.100	4.1	127051	7E-27	0.7	AT1G24360	4E-32	0.3
233634	Adenosinetriphosphatase.	3.6.1.3	4.0	127671	5E-160	-2.0	AT4G02060	3E-80	-0.1
450336	Aldehyde dehydrogenase (NAD+).	1.2.1.3	4.0	135609	4E-108	0.3	AT3G48000	7E-112	0.3
233187	UDP-glucuronate decarboxylase.	4.1.1.35	4.0	135101	5E-08	-0.8	AT3G53520	7E-08	0.3
100060	DNA-directed DNA polymerase.	2.7.7.7	3.9	No			No		
52859	Adenosinetriphosphatase.	3.6.1.3	3.9	120667	3E-64	-1.8	AT1G72250	8E-66	0.5
101628	Hydrolases.	3.-.-.-	3.9	130834	7E-90	-1.1	AT5G26680		0.3
466973	Acid--D-amino-acid ligases (peptide synthases).	6.3.2.-	3.8	No			No		
212824	Ribonucleoside-diphosphate reductase.	1.17.4.1	3.8	185583	0	2.2	AT2G21790	0E+00	0.1
68124	DNA-directed DNA polymerase.	2.7.7.7	3.8	No			No		
468249	Peptidylprolyl isomerase.	5.2.1.8	3.8	205889	2E-45	-0.4	AT1G26940	8E-50	0.3
457592	Homogentisate 1,2-dioxygenase.	1.13.11.5	3.8	76437	1E-107	1.4	AT5G54080	1E-125	0.2
62542	Adenosinetriphosphatase.	3.6.1.3	3.7	152683	0E+00	-0.2	AT1G44900	0	0.3
416107	Hydroxymethylglutaryl-CoA lyase.	4.1.3.4	3.7	195057	5E-81	0.7	AT2G26800	1E-86	0.3
440231	Cyclopropane-fatty-acyl-phospholipid synthase.	2.1.1.79	3.7	191650	5E-26	-0.5	AT3G23530	2E-26	0.1
470226	Adenosinetriphosphatase.	3.6.1.3	3.7	120667	9E-31	-1.8	AT5G54670	1E-29	0.5
359119	Acid--D-amino-acid ligases (peptide synthases).	6.3.2.-	3.7	152270	1E-25	-1.5	AT5G65740		
415026	Mercury (II) reductase.	1.16.1.1	3.7	57890	3E-39	-0.3	AT1G48030	2E-40	0.4
451516	Acting on the CH-OH group of donors.	1.1.-.-	3.6	145585	2E-17	-1.3	AT4G09750	2E-17	0.3
96456	Acid--D-amino-acid ligases (peptide synthases).	6.3.2.-	3.6	No			No		
434807	Acetyl-CoA C-acyltransferase.	2.3.1.16	3.6	138637	4E-40	-1.3	AT1G04710	5E-39	0.5
205415	Alpha-N-acetylgalactosaminidase.	3.2.1.49	3.6	116873	2E-50	-0.7	AT3G56310	2E-56	0.5
249760	Plus-end-directed kinesin ATPase.	3.6.4.4	3.6	137882	3E-55	-1.4	AT2G37420	3E-59	0.
434017	Ubiquitin--protein ligase.	6.3.2.19	3.6	183594	8E-64	1.1	AT1G63800	5E-61	0.4
470988	Ribonucleoside-diphosphate reductase.	1.17.4.1	3.6	188785	5E-80	-1.3	AT3G23580	7E-94	0.2
95181	Glucan 1,4-alpha-glucosidase.	3.2.1.3	3.5	No			AT2G35630	2E-39	0.1
434961	Acting on the CH-OH group of donors.	1.1.-.-	3.4	56542	2E-13	0.0	AT1G24360	3E-17	0.3
457507	NAD(+) ADP-ribosyltransferase.	2.4.2.30	3.4	No			No		
52323	Glutamate--ammonia ligase.	6.3.1.2	3.4	No			No		

459854	NAD(+) ADP-ribosyltransferase.	2.4.2.30	3.4	No			AT4G02390	1E-86	0.8
413815	Dimethylaniline monooxygenase (N-oxide forming).	1.14.13.8	3.4	206143	3E-88	0.6	AT1G19250	4E-46	0.6
104811	Acrosin.	3.4.21.10	3.4	No			No		
454120	Aspartate-semialdehyde dehydrogenase.	1.2.1.11	3.4	148810	2E-63	-0.4	AT1G14810	9E-67	0.0
431876	Phosphotransferases with an alcohol group as acceptor.	2.7.1.-	3.3	113331	9E-31	-0.2	AT4G18700	1E-44	0.2
246026	Serine/threonine specific protein phosphatase.	3.1.3.16	3.3	95558	1E-14	0.1	AT5G53140	1E-13	0.3
225583	Phosphodiesterase I.	3.1.4.1	3.3	No			AT5G15170	1E-21	0.2
52656	Nucleotidyltransferases.	2.7.7.-	3.3	No			AT1G67320	1E-78	0.3
451556	Exo-alpha-sialidase.	3.2.1.18	3.3	No			No		
445028	Ceramidase.	3.5.1.23	3.3	No			No		
452428	Protein kinase.	2.7.1.37	3.2	178318	3E-17	0.2	AT4G35780	3E-14	0.1
113634	1-phosphatidylinositol 3-kinase.	2.7.1.137	3.2	196943	7E-28	0.3	AT1G60490	1E-28	0.2
437926	With other acceptors.	1.3.99.-	3.2	128289	1E-57	0.7	AT3G45300	2E-57	0.0
460965	Metalloendopeptidases.	3.4.24.-	3.2	152585	6E-41	-1.5	AT5G06680	1E-101	0.3
308857	Fructose-bisphosphate aldolase.	4.1.2.13	3.2	24459	1E-79	-0.3	AT2G21330	3E-17	-0.1
241574	Glucan 1,3-beta-glucosidase.	3.2.1.58	3.2	No			No		
349549	Tryptase.	3.4.21.59	3.2	No			No		
467665	DNA ligase (NAD+).	6.5.1.2	3.2	No			No		
220923	Beta-glucosidase.	3.2.1.21	3.2	No			AT1G02640	3E-52	0.4
225637	Plus-end-directed kinesin ATPase.	3.6.4.4	3.2	No			AT1G72250	7E-23	0.5
99551	DNA-directed DNA polymerase.	2.7.7.7	3.2	103391	1E-26	-1.5	AT2G42120	2E-37	0.3
198024	Pyruvate carboxylase.	6.4.1.1	3.2	112730	0	-1.5	No		
221716	DNA-directed DNA polymerase.	2.7.7.7	3.1	No			AT1G67630	5E-12	0.1
112261	Type I site-specific deoxyribonuclease.	3.1.21.3	3.1	No			No		
461771	Adenosinetriphosphatase.	3.6.1.3	3.1	38371	1E-55	-0.6	AT3G01610	1E-44	0.1
469045	Acid--D-amino-acid ligases (peptide synthases).	6.3.2.-	3.1	No			No		
65943	Methionyl aminopeptidase.	3.4.11.18	3.1	139416	6E-86	-2.0	AT3G51800	2E-88	0.1
443869	Succinate-semialdehyde dehydrogenase (NAD(P)+).	1.2.1.16	3.1	118012	2E-105	-0.1	AT1G79440	1E-128	0.1
216734	Serine endopeptidases.	3.4.21.-	3.0	No			No		
466584	DNA-directed RNA polymerase.	2.7.7.6	3.0	No			No		
110761	Metalloendopeptidases.	3.4.24.-	3.0	No			No		
369783	Orotate phosphoribosyltransferase.	2.4.2.10	3.0	116267	5E-14	-1.8	AT3G54470	2E-12	

212574	Tropine dehydrogenase.	1.1.1.206	3.0	128624	4E-52	-1.6	AT5G06060	3E-60	0.2
204876	Adenosine kinase.	2.7.1.20	3.0	No			No		
444614	Ubiquitinyl hydrolase 1.	3.4.19.12	3.0	182375	7E-62	-0.5	AT1G65650	2E-88	0.3
465841	In phosphorous-containing anhydrides.	3.6.1.-	2.9	145450	8E-93	-1.3	AT3G19210	4E-88	0.8
433512	Adenosine deaminase.	3.5.4.4	2.9	No			AT4G04880	2E-20	0.3
452782	DNA-directed RNA polymerase.	2.7.7.6	2.9	No			No		
68578	Phosphotransferases with an alcohol group as acceptor.	2.7.1.-	2.9	112765	4E-36	-0.2	AT5G01810	4E-34	0.4
450514	Succinate dehydrogenase (ubiquinone).	1.3.5.1	2.9	195972	0	-0.7	AT5G66760	0	0.2
100734	Metalloendopeptidases.	3.4.24.-	2.9	No			No		
467327	Protein kinase.	2.7.1.37	2.9	No			No		
223806	In phosphorous-containing anhydrides.	3.6.1.-	2.9	No			AT1G08600	6E-44	0.2
72956	Glutamate--ammonia ligase.	6.3.1.2	2.9	No			AT3G53180	2E-26	0.3
456336	Adenosylmethionine--8-amino-7-oxononanoate aminotransferase.	2.6.1.62	2.8	108892	1E-21	-1.2	AT5G57590	2E-23	0.4
468825	Acid--D-amino-acid ligases (peptide synthases).	6.3.2.-	2.8	No			No		

[a] this work
[b] González-Ballester et al. (2010)
[c] Maruyama-Nakashita et al. (2006)
[d] JGI protein accession number

Table 1B. Summary of the top 100 most up-regulated transcripts in S-limited *Chlamydomonas reinhardtii* with the best BLASTP hits (E-value cutoff of 1E-5) in *Emiliania huxleyi* and *Arabidopsis thaliana*. E-value (expectation value) reflecting the number of hits expected to be found by chance. Transcripts induced in all three species are highlighted in bold font

Chlamydomonas reinhardtii[a]			*Emiliania huxleyi*[b]			*Arabidopsis thaliana*[c]		
Protein ID[d]	Description	Fold Change (log_2)	Homolog ID[d]	E-value	Fold Change (log_2)	Homolog ID	E-value	Fold Change (log_2)
137329	ECP88, extracellular protein	13.4	No			No		
171504	Unknown	11.7	No			No		
130684	ECP76, extracellular protein	10.7	No			No		
205496	ARS1, arylsulfatase	10.5	No			No		
184479	LHCBM9, PSII light harvesting protein	10.0	No			AT2G05100	1E-96	0.8
						AT3G27690	3E-96	1.2
						AT1G29910	8E-92	0.8
109352		9.8	No			AT3G06380	4E-12	1.0
						AT5G18680	9E-12	1.2
						AT2G47900	1E-11	1.1
184282	Unknown	9.8	No			No		
175629	Unknown	9.3	No			No		
194201	ECP 56, extracellular protein	8.6	No			No		
119420	ECP 61, extracellular protein	8.5	No			No		
143696	HAP2, vanadium haloperoxidase	8.4	No			No		
192634		8.2	No			No		
55757	ARS2, arylsulfatase	8.2	No			No		
174935		8.2	No			No		
100022	Snf1 like Ser/Thr protein kinase	8.2	No			AT4G33950	3E-52	1.6
						AT1G60940	1E-51	1.1
						AT5G63650	7E-51	1.2
185846		8.1	No			No		

168785	HAP1, vanadium haloperoxidase	7.9	No			No		
205841	U6i,U6 snRNA	7.8	No			No		
156670		7.5	No			No		
205690	Unknown	7.4	No			No		
192633	Unknown, small RNA like	7.4	No			No		
196724	YEE3, membrane protein	7.3	No			No		
181230		7.3	No			No		
153934	Aldehyde dehydrogenase	7.3	No			No		
143415	Unknown	7.2	No			No		
182794	HAP3, vanadium haloperoxidase	7.1	No			No		
127464	TAUD1, taurine dioxygenase	7.1	No			No		
96408		7.0	No			No		
122211		6.9	No			No		
181679		6.9	No			No		
205502	SLT1, animal type sulfate transporter	6.9	No			No		
184415	Unknown, small RNA like	6.7	No			No		
167940	Unknown	6.6	No			No		
149078	Serine/threonine protein kinase	6.5	No			AT4G32830	3E-31	1.2
183469	Unknown, small RNA like	6.3	No			No		
205501	SLT2, animal type sulfate transporter	6.3	No			No		
170694		6.3	No			No		
190325	Unknown, small RNA like	6.3	No			No		
180502		6.2	No			No		
205514	PWR1 domain	6.2	No			No		
112775	HTB10,Histone H2B	6.2	No			AT5G59910	3E-41	1.2
						AT3G45980	3E-41	1.2
						AT3G46030	3E-41	1.2
180839	CLR2,predicted protein of CLR family	6.2	No			No		
141881		6.2	No			No		
181051		6.1	No			No		
189761		6.1	No			No		
174551		6.1	No			No		

205818	U5d,U5 snRNA	6.0	No			No		
181739	MOT29,predicted protein	5.9	No			No		
169360		5.9	No			No		
187819	Oxygenase like protein	5.7	No			AT1G35190	2E-69	1.4
						AT3G46490	2E-61	1.1
						AT3G46480	2E-46	2.3
192462	Unknown	5.6	No			No		
151478		5.6	No			No		
116259		5.6	No			AT3G02850	2E-05	0.5
150931	Unknown	5.5	No			No		
171929		5.4	No			No		
196871	UBL3,ubiquitin like protein	5.4	No			No		
184802		5.4	No			No		
182845	SBD1,selenium binding protein	5.4	No			AT4G14030	3E-156	2.0
						AT3G23800	1E-148	0.8
150514	**SULTR2, plant type sulfate transporter**	**5.3**	**453061**	**4E-48**	**3.9**	**AT5G13550**	**5E-133**	**1.9**
						AT3G12520	2E-131	6.2
						AT1G22150	2E-107	0.8
162607	CGL41 domain	5.2	No			AT4G04330	2E-17	8.5
143723		5.2	204049	1E-11	n/a	No		
77600	TAUD2, taurine dioxygenase	5.2	No			No		
115518	GDPD2,glycerophosphoryl diester phosphodiesterase family protein	5.2	No			AT1G74210	5E-66	1.3
						AT5G08030	7E-66	2.2
						AT5G58050	9E-15	1.2
179525		5.2	No			No		
171151		5.2	No			No		
153947	RDP1,Rhodanese domain phosphatase	5.2	No			AT5G03455	9E-05	1.2
196813	YEE1, membrane protein	5.2	No			No		
180559		5.2	No			No		
114955	**HTR17,Histone H3**	**5.1**	461181	6E-74	-0.4	AT4G40030	3E-59	1.1
			78924	5E-75	-0.6	AT3G27360	3E-59	1.2
			359333	**5E-75**	**1.3**	**AT1G75600**	**2E-56**	**7.4**

						AT1G13370	**3E-55**	**4.3**
205985	**SAT1a, serine acetyltransferase, (i. a)**	**5.1**	**248485**	**4E-41**	**1.5**	**AT5G56760**	**1E-60**	**1.2**
			234967	**3E-41**	**1.9**	**AT2G17640**	**8E-59**	**2.6**
			55024	1E-38	0.3	**AT1G55920**	**2E-52**	**1.3**
143258		5.1	No			No		
205806	U2f,U2 snRNA	5.1	No			No		
151243		5.1	No			No		
187821	SAT1b, serine acetyltransferase, (i. b)	5.1	No			as shown in SAT 1a		
144820	Unknown	5.1	No			No		
153054	Cysteine type endopeptidase	5.0	114918	3E-08	1.1	No		
196145	SelW2,Selenoprotein W2	5.0	No			No		
196834	CAH9, carbonic anhydrase, cyt.	5.0	No			No		
168671		5.0	No			No		
166553		4.9	No			No		
139591	Unknown	4.9	No			No		
185664		4.9	No			No		
196750	THB2,truncated hemoglobin	4.8	No			No		
184728	Major facilitate superfamily transporter	4.7	No			No		
151255		4.7	No			No		
143892	CDO1, cysteine dioxygenase	4.7	433165	9E-16	3.8	No		
166895		4.7	No			No		
162043		4.6	No			No		
154596		4.6	No			No		
147414		4.6	No			No		
112129		4.6	452712	1E-48	0.1	AT3G48750	5E-45	1.2
			433442	4E-45	3.7	AT3G14720	5E-43	1.2
			354761	7E-41	-0.3	AT3G18040	9E-43	1.3
169460		4.6	No			No		
161581		4.6	No			No		
186295	CLR21	4.6	No			No		
153996		4.5	No			No		

116001		4.5	459364	7E-21	1.5	AT5G16750	1E-14	0.9
			427427	1E-15	-0.5	AT1G11160	4E-14	1.2
			44132	9E-20	0.3	AT1G73720	1E-13	1.2
			99690	6E-12	-0.6			
121177		4.5	No			No		
166922		4.5	No			No		
96117		4.5	No			AT1G53270	2E-12	1.8
						AT2G36380	2E-11	1.3
98733	Serine/threonine protein kinase	4.5	56016	2E-17	0.6	AT4G32830	3E-16	1.2
			453419	1E-17	-0.6	AT2G25880	8E-16	1.1
			62403	2E-18	0.4	AT5G57630	1E-15	1.3

[a] González-Ballester et al. (2010)
[b] this work
[c] Maruyama-Nakashita et al. (2006)
[d] JGI protein accession number

Table 1C. Summary of the top 100 most up-regulated transcripts in S-limited *Arabidopsis thaliana* with the best BLASTP hits (E-value cutoff of 1E-5) in *Emiliania huxleyi* and *Chlamydomonas reinhardtii* E-value (expectation value) reflecting the number of hits expected to be found by chance. Transcripts induced in all three species are highlighted in bold font

Arabidopsis thaliana[a]			*Emiliania huxleyi*[b]			*Chlamydomonas reinhardtii*[c]		
Protein ID	Description	Fold Change (log_2)	Homolog ID[d]	E-value	Fold Change (log_2)	Homolog ID[d]	E-value	Fold Change (log_2)
AT2G44460	putative beta-glucosidase	8.0	68714	9E-102	-0.2	169029	2E-33	-0.8
			103655	2E-92	0.0	167861	2E-31	1.2
			74482	1E-75	0.9	No		
			107040	3E-31	0.7	No		
AT1G12030	hypothetical protein predicted by genefinder	7.6	No			No		
AT3G49580	putative protein ;supported by full-length cDNA: Ceres:26235.	6.5	No			No		
AT4G08620	**putative sulfate transporter; supported by cDNA: gi_14196242_dbj_AB018695.2_AB018695**	**6.5**	**453061**	**1E-37**	**3.9**	**150514**	**3E-115**	**5.3**
AT5G48850	putative protein similar to unknown protein (gb|AAC72543.1)	6.5	441761	5E-12	3.3	No		
AT5G26220	putative protein cation transport protein chaC, Escherichia coli, PIR:G64868	6.4	47921	8E-16	-0.4	142997	4E-41	0.3
			57918	8E-16	-0.6	No		
AT3G60140	beta-glucosidase-like protein several beta-glucosidases - different species; supported by cDNA: gi_10834547_gb_AF159376.1_AF159376	6.3	68714	1E-101	0.5	167861	5E-32	1.2
			103655	2E-91	0.0	169029	9E-30	-0.8
			439489	3E-22	0.6			
AT5G49590	putative protein similar to unknown protein (pir||T02348)	5.6	No			No		
AT3G05400	sugar transporter, putative similar to integral membrane protein GB:U43629 from [Beta vulgaris] (Plant Physiol.(1996) 110 (2), 511-520)	5.4	470505	9E-29	1.3	196325	2E-23	0.4
			432500	1E-27	1.2			

			41648	2E-26	-1.0			
AT1G23730	putative carbonic anhydrase	5.2	No			196245	5E-15	0.9
						133249	3E-10	0.5
						24552	5E-09	-2.2
AT3G29510	transposon related protein similar to retroviral-like transposon Tnt GI:20044 from [Arabidopsis thaliana]	4.7	No			No		
AT1G39430	putative replication protein A1	4.5	No			No		
---	hypothetical protein predicted by genscan and genefinder	4.5	No			No		
AT1G33960	AIG1 identical to AIG1 (exhibits RPS2- and avrRpt2-dependent induction early after infection with Pseudomonas) GB:U40856 [Arabidopsis thaliana] (Plant Cell 8 (2), 241-249 (1996)); supported by cDNA: gi_1127803_gb_U40856.1_ATU40856	4.5	249415	5E-17	1.6	No		
AT3G21830	SKP1/ASK1 (At8), putative similar to Skp1 homolog Skp1b GI:3068809, UIP2 GI:3719211 from [Arabidopsis thaliana]	4.5	434598	7E-32	0.3	128004	4E-31	-0.4
AT2G14300	putative helicase	4.5	No			No		
AT3G08860	putative aminotransferase similar to beta-alanine-pyruvate aminotransferase GB:BAA19549 [Rattus norvegicus], alanine-glyoxylate aminotransferase GB:Q64565 [Rattus norvegicus]; Pfam HMM hit: Aminotransferases class-III pyridoxal-phosphate	4.4	416568	2E-75	0.6	133057	1E-167	0.3
						205967	7E-52	2.2
						139007	1E-38	-0.4
AT1G72580	hypothetical protein predicted by genscan	4.3	No			No		
AT3G50160	putative protein some putative proteins - Arabidopsis thaliana and Oryza sativa	4.1	No			No		
AT3G52770	hypothetical protein emm32, Streptococcus pyogenes, EMBL:SPEMM32G	4.1	No			No		
AT5G24660	putative protein similar to unknown protein (emb CAB62461.1);supported by full-length cDNA: Ceres:268701.	4.0	No			No		
AT4G31330	predicted protein ; supported by cDNA: gi_15293232_gb_AY051050.1_	4.0	No			No		
AT4G18330	translation initiation factor eIF-2 gamma chain-like protein translation initiation factor eIF-2 gamma chain, Homo sapiens, PIR2:A53048;supported by full-length cDNA: Ceres:34867.	4.0	62317	2E-118	-0.3	126673	0	-1.3
AT4G03156	hypothetical protein	3.9	No			No		
AT3G42080	putative protein hypothetical proteins - Arabidopsis thaliana	3.9	No			No		
---	hypothetical protein	3.8	No			No		
AT1G75290	NADPH oxidoreductase, putative similar to GI:1708420 from [Arabidopsis thaliana] (J. Biol. Chem. 270 (44), 26224-26231 (1995))	3.8	No			132437	2E-06	-0.6

AT3G03410	calmodulin-like protein similar to calmodulin GB:P02599 [Dictyostelium discoideum], HMM hit: efhand	3.8	442625	2E-21	3.0	188144	1E-16	0.0
			443126	2E-21	2.2	9509	7E-10	0.2
AT5G26700	nectarin - like protein nectarin I precursor, Nicotiana plumbaginifolia, EMBL:AF132671; supported by full-length cDNA: Ceres: 14379.	3.8	No			No		
AT1G36120	putative reverse transcriptase	3.8	No			No		
AT5G27580	putative protein hypothetical proteins - Arabidopsis thaliana, weak similarity to MADS-box proteins	3.8	No			No		
AT2G23060	similar to hookless1 (HLS1)	3.7	No			No		
AT2G30220	putative GDSL-motif lipase/hydrolase similar to APG proteins; pFAM domain PF00657	3.7	No			No		
AT1G59850	hypothetical protein predicted by genemark.hmm	3.7	No			No		
AT5G37610	porin -like protein porin, Prunus armeniaca, EMBL:AF139498	3.7	No			No		
AT5G57730	unknown protein	3.6	No			No		
AT1G36035	putative gag-protease polyprotein	3.6	No			No		
AT1G30030	putative protein various reverse transcriptases and transposons	3.5	No			No		
AT5G28340	putative protein hypothetical protein T27I15_50 - Arabidopsis thaliana, PIR:T50517	3.5	No			114572	6E-07	0.1
AT3G21970	hypothetical protein contains Pfam profile: PF01657 Domain of unknown function	3.5	No			No		
AT2G19320	hypothetical protein predicted by genefinder	3.5	No			No		
AT1G45090	hypothetical protein predicted by genemark.hmm	3.5	No			No		
AT2G34800	hypothetical protein predicted by genscan	3.5	No			No		
AT1G21530	amp-binding protein, putative similar to amp-binding protein GB:X94625 GI:1903033 from [Brassica napus]	3.4	No			No		
AT2G44540	putative cellulase	3.4	No			142120	1E-49	1.0
						194521	2E-45	0.5
						194523	7E-45	0.3
AT5G44570	unknown protein	3.4	No			No		
AT5G53820	ABA-inducible protein-like ;supported by full-length cDNA: Ceres:24640.	3.4	No			No		
AT5G57240	oxysterol-binding protein-like	3.4	No			152242	6E-14	-1.0
						131777	2E-12	0.5
AT1G20530	hypothetical protein	3.4	No			No		
AT3G45250	hypothetical protein	3.4	No			No		
AT5G32590	putative protein various predicted proteins, Arabidopsis thaliana	3.4	No			No		
AT1G23600	putative OBP32pep protein	3.4	No			No		

AT2G14350	hypothetical protein predicted by genscan and genefinder	3.4	No			No		
AT1G26420	hypothetical protein similar to reticuline oxidase-like protein GB:CAB45850 GI:5262224 from [Arabidopsis thaliana]	3.4	No			No		
AT5G05840	putative protein strong similarity to unknown protein (emb|CAB81597.1)	3.4	No			No		
AT5G09340	ubiquitin-like protein ubiquitins - different species	3.3	354368	4E-12	-0.7	140045	4E-08	0.4
			358059	3E-12	1.2	196845	4E-08	-0.1
						195594	1E-07	-0.2
AT2G04310	Mutator-like transposase similar to MURA transposase of maize Mutator transposon	3.3	No			No		
AT3G47170	hypersensitivity-related protein-like protein hypersensitivity-related gene	3.3	No			No		
AT1G37063	hypothetical protein predicted by genemark.hmm	3.3	No			No		
AT4G28420	tyrosine transaminase-like protein tyrosine transaminase (EC 2.6.1.5)-rat, PIR1:XNRTY	3.3	424157	2E-64	0.4	206184	2E-19	-0.5
						118364	2E-17	-1.6
						136460	7E-16	-0.4
AT3G28560	hypothetical protein predicted by genemark.hmm	3.3	No			No		
AT5G28110	putative protein predicted resistance protein, Arabidopsis thaliana	3.3	No			No		
AT5G18430	putative protein proline-rich protein APG, Arabidopsis thaliana, PIR:S21961	3.3	No			No		
AT2G39820	putative translation initiation factor	3.3	62423	1E-83	0.0	188065	3E-85	-0.8
			114121	1E-83	0.6			
AT1G20290	hypothetical protein predicted by genemark.hmm	3.3	No			No		
AT3G26270	cytochrome P450, putative contains Pfam profile: PF00067 cytochrome P450	3.3	447375	2E-32	-0.3	196742	2E-24	-1.7
			72799	2E-22	2.0	196713	6E-18	1.3
AT2G19840	copia-like retroelement pol polyprotein	3.3	No			13035	3E-73	0.4
AT3G29030	expansin At-EXP5 identical to expansin At-EXP5 GB:AAB38071 from [Arabidopsis thaliana]; supported by cDNA: gi_1041703_gb_U30478.1_ATU30478	3.3				141251	2E-10	0.6
AT1G69100	aspartic protease, putative similar to aspartic protease precursor GI:951448 from [Lycopersicon esculentum]	3.3	356350	4E-45	0.8	128744	5E-36	2.5
			358471	1E-21	2.0			
AT2G18080	unknown protein possibly related to thymus-specific serine peptidase from Homo sapiens	3.3	62528	9E-21	0.3	No		
AT2G02670	hypothetical protein predicted by grail	3.2	No			No		
AT1G28135	unknown protein	3.2	No			No		
AT5G20340	beta-1,3-glucanase bg5	3.2	No			No		
AT1G34600	unknown protein similar to putative retroelement pol polyprotein GB:AAD20653 GI:4432801 from [Arabidopsis thaliana]	3.2	No			No		

AT1G37060	Athila retroelment ORF 1, putative similar to GB:CAA57397 from (Arabidopsis thaliana)	3.2	No			No		
AT3G46170	dehydrogenase -like protein alcohol dehydrogenase homolog, ripening-related, tomato, PIR:S39508	3.2	76705	1E-23	-0.5	128624	1E-20	-1.6
			64955	3E-25	-0.3	127051	6E-20	0.7
			433820	3E-20	4.1	114298	9E-20	-2.9
AT3G25200	hypothetical protein predicted by genemark.hmm	3.2	No			No		
AT3G30510	hypothetical protein predicted by genemark.hmm	3.2	No			No		
AT5G46260	disease resistance protein-like ; supported by cDNA: gi_16323098_gb_AY057653.1_	3.2	No			No		
AT3G19270	cytochrome P450, putative similar to cytochrome P450 GB:BAA37167 from [Arabidopsis thaliana];supported by full-length cDNA: Ceres:126144.	3.2	467235	4E-19	2.0	196674	2E-40	0.1
			454070	4E-19	1.6	196411	7E-28	-1.1
			458776	2E-15	2.3	196683	1E-27	-0.2
AT4G39610	putative protein predicted proteins, Arabidopsis thaliana;supported by full-length cDNA: Ceres:97747.	3.2	No			No		
AT3G32220	Athila ORF 1, putative similar to Athila ORF 1 GB:CAA57397 GI:806535 from [Arabidopsis thaliana]	3.2						
AT1G71420	hypothetical protein predicted by genscan	3.1	51716	3E-21	1.2	169792	3E-20	-0.2
AT1G63950	hypothetical protein predicted by genefinder	3.1	No			No		
AT3G42400	putative replication protein various predicted proteins, Arabadopsis thaliana	3.1	No			No		
AT2G11220	putative retroelement pol polyprotein	3.1	No			No		
AT2G06020	hypothetical protein predicted by genscan and genefinder	3.1	No			No		
AT5G37980	quinone oxidoreductase -like protein probable quinone oxidoreductase P1, Arabidopsis thaliana;supported by full-length cDNA: Ceres:116237.	3.1	75462	3E-26	0.2	174569	1E-18	-0.2
			115039	3E-27	0.6			
			462772	1E-28	1.9			
AT3G42930 AT5G30545	putative protein various predicted proteins, Arabidopsis thaliana	3.1	No			No		
AT2G12520	hypothetical protein similar to myosin-like protein GB:AAC28203	3.1	No			No		
AT1G17745	Expressed protein ; supported by cDNA: gi_15028272_gb_AY046051.1_	3.1	415674	3E-77	0.3	78757	2E-149	-1.4
			465676	2E-82	-0.5			
			440369	2E-38	0.2			
AT4G04330	hypothetical protein ; supported by cDNA: gi_15027850_gb_AY045782.1_	3.1	No			162607	3E-19	5.2

AT1G53690	RNA polymerase II, putative similar to GI:717186 from [Homo sapiens] (Mol. Cell. Biol. 15 (9), 4702-4710 (1995))	3.1	No			78868	7E-09	-1.0
AT5G36080	putative protein similar to unknown protein (emb|CAB88131.1)	3.1	No			No		
AT4G23310	serine/threonine kinase - like protein KI domain interacting kinase 1, Zea mays	3.1	No			No		
AT1G38340	retroelement pol polyprotein, putative	3.0	No			No		
AT1G58210	hypothetical protein predicted by genemark.hmm	3.0	No			No		
AT2G45130	hypothetical protein predicted by genscan	3.0	No			205638	2E-08	0.9
AT5G29090	putative protein	3.0	No			No		
AT4G36510	hypothetical protein	3.0	No			No		

[a]Maruyama-Nakashita et al. (2006)
[b] this work
[c] González-Ballester et al. (2010)
[d] JGI protein accession number

Abbreviations, Acronyms and Definitions

APR	APS reductase
APS	Adenosine 5’ phosphosulphate
CCMP	Center for culture of marine phytoplankton, Boothbay Harbor USA
cDNA	complementary DNA
Cys	Cysteine
DLA	DMSP lyase activity
DMS	Dimethylsulphide
DMSHB	4-dimethylsulphonio-2-hydroxybutyrate
DMSO	Dimethylsulphoxide
DMSP	Dimethylsulphoniopropionate
GC	Gas chromatography
GSH	glutathione
HPLC	high performance liquid chromatography
Met	Methionine
mRNA	messenger RNA
OAS	*O*-acetyl-serine
OASTL	*O*-acetyl-serine(thiol)-lyase, OAS(thiol)-lyase
RNA	ribonucleic acid
RNA-seq	transcriptome profiling using deep-sequencing technologies
ROS	Reactive oxygen species
SD	standard deviation

References

Aoki M, Sato N, Meguro A, Tsuzuki M (2004) Differing involvement of sulfoquinovosyl diacylglycerol in photosystem II in two species of unicellular cyanobacteria. European Journal of Biochemistry 271: 685-693

Armbrust EV, Berges JA, Bowler C, Green BR, Martinez D, Putnam NH, Zhou S, Allen AE, Apt KE, Bechner M, Brzezinski MA, Chaal BK, Chiovitti A, Davis AK, Demarest MS, Detter JC, Glavina T, Goodstein D, Hadi MZ, Hellsten U, Hildebrand M, Jenkins BD, Jurka J, Kapitonov VV, Kro?ger N, Lau WWY, Lane TW, Larimer FW, Lippmeier JC, Lucas S, Medina M, Montsant A, Obornik M, Parker MS, Palenik B, Pazour GJ, Richardson PM, Rynearson TA, Saito MA, Schwartz DC, Thamatrakoln K, Valentin K, Vardi A, Wilkerson FP, Rokhsar DS (2004) The genome of the diatom Thalassiosira Pseudonana: Ecology, evolution, and metabolism. Science 306: 79-86

Ashburner M, Ball CA, Blake JA, Botstein D, Butler H, Cherry JM, Davis AP, Dolinski K, Dwight SS, Eppig JT, Harris MA, Hill DP, Issel-Tarver L, Kasarskis A, Lewis S, Matese JC, Richardson JE, Ringwald M, Rubin GM, Sherlock G (2000) Gene ontology: Tool for the unification of biology. Nature Genetics 25: 25-29

Ayers GP, Cainey JM (2007) The CLAW hypothesis: A review of the major developments. Environmental Chemistry 4: 366-374

Baldauf SL (2008) An overview of the phytogeny and diversity of eukaryotes. Journal of Systematics and Evolution 46: 263-273

Barberon M, Berthomieu P, Clairotte M, Shibagaki N, Davidian JC, Gosti F (2008) Unequal functional redundancy between the two *Arabidopsis thaliana* high-affinity sulphate transporters SULTR1;1 and SULTR1;2. New Phytologist 180: 608-619

Baudoux AC, Noordeloos AAM, Veldhuis MJW, Brussaard CPD (2006) Virally induced mortality of Phaeocystis globosa during two spring blooms in temperate coastal waters. Aquatic Microbial Ecology 44: 207-217

Baumann KH (2004) Importance of size measurements for coccolith carbonate flux estimates. Micropaleontology 50: 35-43

Belviso S, Thouzeau G, Schmidt S, Reigstad M, Wassmann P, Arashkevich E, Stefels J (2006) Significance of vertical flux as a sink for surface water DMSP and as a source for the sediment surface in coastal zones of northern Europe. Estuarine, Coastal and Shelf Science 68: 473-488

Bentley R, Chasteen TG (2004) Environmental VOSCs - Formation and degradation of dimethyl sulfide, methanethiol and related materials. Chemosphere 55: 291-317

Berges JA, Franklin DJ, Harrison PJ (2001) Evolution of an artificial seawater medium: Improvements in enriched seawater, artificial water over the last two decades. Journal of Phycology 37: 1138-1145

Billard C, Inouye I (2004) What is new in coccolithophores biology? In Thierstein, H. R. & Young, J. [Eds.] Coccolithophores from Molecular Processes to Global Impact. Springer-Verlag, Heidelberg, Germany: 1-29

Bisson MA, Kirst GO (1995) Osmotic acclimation and turgor pressure regulation in algae. Naturwissenschaften 82: 461-471

Blomquist BW, Fairall CW, Huebert BJ, Kieber DJ, Westby GR (2006) DMS sea-air transfer velocity: Direct measurements by eddy covariance amd parameterizarion based on the NOAA/COAREgas transfer model. Geophysical Research Letters 33

Bork C, Schwenn JD, Hell R (1998) Isolation and characterization of a gene for assimilatory sulfite reductase from *Arabidopsis thaliana*. Gene 212: 147-152,153
Bown PR (1987) Taxonomy, evolution, and biostratigraphy of Late Triassic-Early Jurassic calcareous nannofossils. Palaeontological Association
Bradford MM (1976) A rapid and sensitive method for the quantitation of microgram quantities of protein utilizing the principle of protein dye binding. Analytical Biochemistry 72: 248-254
Breitling R, Amtmann A, Herzyk P (2004) Iterative Group Analysis (iGA): A simple tool to enhance sensitivity and facilitate interpretation of microarray experiments. BMC Bioinformatics 5: 34
Breitling R, Pitt AR, Barrett MP (2006) Precision mapping of the metabolome. Trends in Biotechnology 24: 543-548
Brown AD (1976) Microbial water stress. Bacteriological Reviews 40: 803-846
Brown CW, Yoder JA (1994) Coccolithophorid blooms in the global ocean. Journal of Geophysical Research 99: 7467-7482
Brunold C, Suter, M. (1990) Adenosine 5′-phosphosulfate sulfotransferase. Methods in plant biochemistry Lea P. (Ed), Academic Press, London 339-343
Bucciarelli E, Sunda WG (2003) Influence of CO2, nitrate, phosphate, and silicate limitation on intracellular dimethylsulfoniopropionate in batch cultures of the coastal diatom *Thalassiosira pseudonana*. Limnology and Oceanography 48: 2256-2265
Bucciarelli E, Sunda WG, Belviso S, Sarthou G (2007) Effect of the diel cycle on production of dimethylsulfoniopropionate in batch cultures of Emiliania huxleyi. Aquatic Microbial Ecology 48: 73-81
Buchner P, Takahashi H, Hawkesford MJ (2004) Plant sulphate transporters: Co-ordination of uptake, intracellular and long-distance transport. Journal of Experimental Botany 55: 1765-1773
Charlson RJ, Lovelock JE, Andreae MO, Warren SG (1987) Oceanic phytoplankton, atmospheric sulphur, cloud albedo and climate. Nature 326: 655-661
Clarkson DT, Diogo E, Amâncio S (1999) Uptake and assimilation of sulphate by sulphur deficient *Zea mays* cells: The role of O-acetyl-L-serine in the interaction between nitrogen and sulphur assimilatory pathways. Plant Physiology and Biochemistry 37: 283-290
Csonka LN, Hanson AD (1991) Prokaryotic osmoregulation -Genetics and physiology Annual Review of Microbiology 45: 569-606
Dacey JWH, Blough NV (1987) Hydroxide decomposition of dimethysulfoniopropionate to form dimethylsulfide. Geophysical Research Letters 14: 1246-1249
Danovaro R, Corinaldesi C, Dell'Anno A, Fuhrman JA, Middelburg JJ, Noble RT, Suttle CA (2011) Marine viruses and global climate change. FEMS Microbiology Reviews 35: 993-1034
Davies JP, Yildiz FH, Grossman A (1996) Sac1, a putative regulator that is critical for survival of *Chlamydomonas reinhardtii* during sulfur deprivation. EMBO Journal 15: 2150-2159
de Vargas C, Aubry, M. P., Probert, I. Young, J (2007) Origin and evolution of Coccolithophores: from coastal hunters to oceanic farmers. In Falkowski, P. G. Knoll, A. [eds.], Evolution of Primary Producers in the Sea. Academic Press 251-285
Dembitsky VM, Rozentsvet OA, Pechenkina EE (1990) Glycolipids, phospholipids and fatty acids of brown algae species. Phytochemistry 29: 3417-3421

Dereeper A, Guignon V, Blanc G, Audic S, Buffet S, Chevenet F, Dufayard JF, Guindon S, Lefort V, Lescot M, Claverie JM, Gascuel O (2008) Phylogeny.fr: robust phylogenetic analysis for the non-specialist. Nucleic acids research 36: W465-469

Dickson DMJ, Kirst GO (1986) The role of β-dimethylsulphoniopropionate, glycine betaine and homarine in the osmoacclimation of Platymonas subcordiformis. Planta 167: 536-543

Dupont CL, Goepfert TJ, Lo P, Wei L, Ahner BA (2004) Diurnal cycling of glutathione in marine phytoplankton: Field and culture studies. Limnology and Oceanography 49: 991-996

Dupont CL, Nelson RK, Bashir S, Moffett JW, Ahner BA (2004) Novel copper-binding and nitrogen-rich thiols produced and exuded by Emiliania huxleyi. Limnology and Oceanography 49: 1754-1762

Evans C, Malin G, Wilson WH, Liss PS (2006) Infectious titers of Emiliania huxleyi virus 86 are reduced by exposure to millimolar dimethyl sulfide and acrylic acid. Limnology and Oceanography 51: 2468-2471

Falkowski PG, Barber RT, Smetacek V (1998) Biogeochemical controls and feedbacks on ocean primary production. Science 281: 200-206

Falkowski PG, Katz ME, Knoll AH, Quigg A, Raven JA, Schofield O, Taylor FJR (2004) The evolution of modern eukaryotic phytoplankton. Science 305: 354-360

Ferreira RMB, Teixeira ARN (1992) Sulfur starvation in Lemna leads to degradation of ribulose-bisphosphate carboxylase without plant death. Journal of Biological Chemistry 267: 7253-7257

Flores J-A, Colmenero-Hidalgo E, Mejía-Molina AE, Baumann K-H, Henderiks J, Larsson K, Prabhu CN, Sierro FJ, Rodrigues T (2010) Distribution of large Emiliania huxleyi in the Central and Northeast Atlantic as a tracer of surface ocean dynamics during the last 25,000 years. Marine Micropaleontology 76: 53-66

Forster T, Roy D, Ghazal P (2003) Experiments using microarray technology: Limitations and standard operating procedures. Journal of Endocrinology 178: 195-204

Foyer CH, Noctor G (2005) Redox homeostasis and antioxidant signaling: A metabolic interface between stress perception and physiological responses. Plant Cell 17: 1866-1875

Frada M, Probert I, Allen MJ, Wilson WH, De Vargas C (2008) The "Cheshire Cat" escape strategy of the coccolithophore Emiliania huxleyi in response to viral infection. Proceedings of the National Academy of Sciences of the United States of America 105: 15944-15949

Fuhrman JA (1999) Marine viruses and their biogeochemical and ecological effects. Nature 399: 541-548

Fujiwara S, Tsuzuki M, Kawachi M, Minaka N, Inouye I (2001) Molecular phylogeny of the Haptophyta based on the rbcL gene and sequence variation in the spacer region of the RUBISCO operon. Journal of Phycology 37: 121-129

Gage DA, Rhodes D, Nolte KD, Hicks WA, Leustek T, Cooper AJL, Hanson AD (1997) A new route for synthesis of dimethylsulphoniopropionate in marine algae. Nature 387: 891-894

Gao Y, Schofield OME, Leustek T (2000) Characterization of sulfate assimilation in marine algae focusing on the enzyme 5 '-adenylylsulfate reductase. Plant Physiology 123: 1087-1096

Gill BC, Lyons TW, Saltzman MR (2007) Parallel, high-resolution carbon and sulfur isotope records of the evolving Paleozoic marine sulfur reservoir. Palaeogeography, Palaeoclimatology, Palaeoecology 256: 156-173

Gill BC, Lyons TW, Young SA, Kump LR, Knoll AH, Saltzman MR (2011) Geochemical evidence for widespread euxinia in the Later Cambrian ocean. Nature 469: 80-83

Giordano M, Beardall J, Raven JA (2005a) CO_2 concentrating mechanisms in algae: Mechanisms, environmental modulation, and evolution Annual Review of Plant Biology, pp 99-131
Giordano M, Norici A, Hell R (2005) Sulfur and phytoplankton: acquisition, metabolism and impact on the environment. New Phytologist 166: 371-382
Giordano M, Pezzoni V, Hell R (2000) Strategies for the allocation of resources under sulfur limitation in the green alga *Dunaliella salina*. Plant Physiology 124: 857-864
González-Ballester D, Casero D, Cokus S, Pellegrini M, Merchant SS, Grossman AR (2010) RNA-Seq analysis of sulfur-deprived chlamydomonas cells reveals aspects of acclimation critical for cell survival. Plant Cell 22: 2058-2084
Gonzalez-Ballester D, Pollock SV, Pootakham W, Grossman AR (2008) The central role of a SNRK2 kinase in sulfur deprivation responses. Plant Physiology 147: 216-227
Green JC, Course PA, Tarran GA (1996) The life-cycle of *Emiliania huxleyi*: A brief review and a study of relative ploidy levels analysed by flow cytometry. Journal of Marine Systems 9: 33-44
Greene RC (1962) Biosynthesis of dimethyl-beta-propiothetin. Journal of Biological Chemistry 237: 2251-2254
Grone T, Kirst GO (1992) The effect of nitrogen deficiency, methionine and inhibitors of methionine metabolisnm on the DMSP contents of *Tetraselmis subcordiformis* (Stein). Marine Biology 112: 497-503
Gutierrez-Marcos JF, Roberts MA, Campbell EI, Wray JL (1996) Three members of a novel small gene-family from Arabidopsis thaliana able to complement functionally an *Escherichia coli* mutant defective in PAPS reductase activity encode proteins with a thioredoxin-like domain and "APS reductase" activity. Proceedings of the National Academy of Sciences of the United States of America 93: 13377-13382
Gutman BL, Niyogi KK (2004) *Chlamydomonas and Arabidopsis*. A dynamic duo. Plant Physiology 135: 607-610
Hanson AD, Rivoal J, Paquet L, Gage DA (1994) Biosynthesis of 3-dimethylsulfoniopropionate in Wollastonia biflora (L.) DC. Evidence that S-methylmethionine is an intermediate. Plant Physiology 105: 103-110
Harrison PJ, Waters RE, Taylor FJR (1980) A broad spectrum artificial seawater medium for coastal and open ocean phytoplankton. Journal of Phycology 16: 28-35
Hatton AD, Darroch L, Malin G (2005) The role of dimethylsulphoxide in the marine biogeochemical cycle of dimethylsulphide. In: Gibson RN, Atkinson RJA (eds) Oceanography and Marine Biology, pp 29-55
Hawkesford MJ, De Kok LJ (2006) Managing sulphur metabolism in plants. Plant, Cell and Environment 29: 382-395
Heeg C, Kruse C, Jost R, Gutensohn M, Ruppert T, Wirtz M, Hella R (2008) Analysis of the *Arabidopsis* O-acetylserine(thiol)lyase gene family demonstrates compartment-specific differences in the regulation of cysteine synthesis. Plant Cell 20: 168-185
Hirai MY, Fujiwara T, Awazuhara M, Kimura T, Noji M, Saito K (2003) Gen expression profiling of sulfur-starved *Arabidopsis* by DNA macroarray reveals the role of O-acetyl-L-serine as a general regulator of gene expression in response to sulfur nutrition. Plant Journal 33: 651-663
Hoefgen R, Nikiforova VJ (2008) Metabolomics integrated with transcriptomics: Assessing systems response to sulfur-deficiency stress. Physiologia Plantarum 132: 190-198
Hopkins L, Parmar S, Błaszczyk A, Hesse H, Hoefgen R, Hawkesford MJ (2005) O-acetylserine and the regulation of expression of genes encoding components for sulfate uptake and assimilation in potato. Plant Physiology 138: 433-440

Hopkins L, Parmar S, Bouranis DL, Howarth JR, Hawkesford MJ (2004) Coordinated expression of sulfate uptake and components of the sulfate assimilatory pathway in maize. Plant Biology 6: 408-414

Houdan A, Probert I, Zatylny C, Véron B, Billard C (2006) Ecology of oceanic coccolithophores. I. Nutritional preferences of the two stages in the life cycle of Coccolithus braarudii and Calcidiscus leptoporus. Aquatic Microbial Ecology 44: 291-301

Irihimovitch V, Stern DB (2006) The sulfur acclimation SAC3 kinase is required for chloroplast transcriptional repression under sulfur limitation in *Chlamydomonas reinhardtii*. Proceedings of the National Academy of Sciences of the United States of America 103: 7911-7916

Ito T, Asano Y, Tanaka Y, Takabe T (2011) Regulation of Biosynthesis of dimethylsulfoniopropionate and its uptake in sterile mutant of *Ulva pertusa* (Chlorophyta). Journal of Phycology 47: 517-523

Jin G, Bierma TJ (2011) Guided-inquiry learning in environmental health. Journal of Environmental Health 73: 80-85

Kanehisa M, Goto S (2000) KEGG: Kyoto Encyclopedia of Genes and Genomes. Nucleic Acids Research 28: 27-30

Karsten U, Kirst GO, Wiencke C (1992) Dimethylsulphoniopropionate (DMSP) accumulation in green macioalgae from polar to temperate regions: interactive effects of light versus salinity and light versus temperature. Polar Biology 12: 603-607

Katahira R, Ashihara H (2002) Profiles of pyrimidine biosynthesis, salvage and degradation in disks of potato (*Solanum tuberosum* L.) tubers. Planta 215: 821-828

Kataoka T, Hayashi N, Yamaya T, Takahashi H (2004) Root-to-shoot transport of sulfate in Arabidopsis. Evidence for the role of SULTR3;5 as a component of low-affinity sulfate transport system in the root vasculature. Plant Physiology 136: 4198-4204

Kaur G, Chandna R, Pandey R, Abrol YP, Iqbal M, Ahmad A (2011) Sulfur starvation and restoration affect nitrate uptake and assimilation in rapeseed. Protoplasma 248: 299-311

Kawashima CG, Matthewman CA, Huang S, Lee B-R, Yoshimoto N, Koprivova A, Rubio-Somoza I, Todesco M, Rathjen T, Saito K, Takahashi H, Dalmay T, Kopriva S (2011) Interplay of SLIM1 and miR395 in the regulation of sulfate assimilation in Arabidopsis. The Plant Journal 66: 863-876

Kegel J, Allen MJ, Metfies K, Wilson WH, Wolf-Gladrow D, Valentin K (2007) Pilot study of an EST approach of the coccolithophorid *Emiliania huxleyi* during a virus infection. Gene 406: 209-216

Keller MD (1988) Dimethyl sulfide production and marine phytoplankton: the importance of species composition and cell size. Biological Oceanography 6: 375-382

Keller MD, Bellows WK, Guillard RRL (1989) Dimethyl sulfide production in marine phytoplankton. Saltzman ES, Cooper WJ eds, American Chemical Society, Washington DC

Keller MD, Kiene RP, Matrai PA, Bellows WK (1999) Production of glycine betaine and dimethylsulfoniopropionate in marine phytoplankton. I. Batch cultures. Marine Biology 135: 237-248

Keller MD, Kiene RP, Matrai PA, Bellows WK (1999b) Production of glycine betaine and dimethylsulfoniopropionate in marine phytoplankton. II. N-limited chemostat cultures. Marine Biology 135: 249-257

Kettle AJ, Andreae MO, Amouroux D, Andreae TW, Bates TS, Berresheim H, Bingemer H, Boniforti R, Curran MAJ, DiTullio GR, Helas G, Jones GB, Keller MD, Kiene RP, Leck C, Levasseur M, Malin G, Maspero M, Matrai P, McTaggart AR,

Mihalopoulos N, Nguyen BC, Novo A, Putaud JP, Rapsomanikis S, Roberts G, Schebeske G, Sharma S, Simo R, Staubes R, Turner S, Uher G (1999) A global database of sea surface dimethylsulfide (DMS) measurements and a procedure to predict sea surface DMS as a function of latitude, longitude, and month. Global Biogeochemical Cycles 13: 399-444

Kiene RP (1996) Production of methanethiol from dimethylsulfoniopropionate in marine surface waters. Marine Chemistry 54: 69-83

Kiene RP, Linn LJ (2000) Distribution and turnover of dissolved DMSP and its relationship with bacterial production and dimethylsulfide in the Gulf of Mexico. Limnology and Oceanography 45: 849-861

Kiene RP, Linn LJ, González J, Moran MA, Bruton JA (1999) Dimethylsulfoniopropionate and methanethiol are important precursors of methionine and protein-sulfur in marine bacterioplankton. Applied and Environmental Microbiology 65: 4549-4558

Kiene RP, Slezak D (2006) Low dissolved DMSP concentrations in seawater revealed by small-volume gravity filtration and dialysis sampling. Limnology and Oceanography-Methods 4: 80-95

Kocsis MG, Hanson AD (2000) Biochemical evidence for two novel enzymes in the biosynthesis of 3-dimethylsulfoniopropionate in *Spartina alterniflora*. Plant Physiology 123: 1153-1161

Kopriva S (2006) Regulation of sulfate assimilation in *Arabidopsis* and beyond. Annals of Botany 97: 479-495

Kopriva S, Büchert T, Fritz G, Suter M, Benda R, Schünemann V, Koprivova A, Schürmann P, Trautwein AX, Kroneck PMH, Brunold C (2002) The presence of an iron-sulfur cluster in adenosine 5'-phosphosulfate reductase separates organisms utilizing adenosine 5'-phosphosulfate and phosphoadenosine 5'-phosphosulfate for sulfate assimilation. Journal of Biological Chemistry 277: 21786-21791

Kopriva S, Fritzemeier K, Wiedemann G, Reski R (2007a) The putative moss 3'-phosphoadenosine-5'-phosphosulfate reductase is a novel form of adenosine-5'-phosphosulfate reductase without an iron-sulfur cluster. Journal of Biological Chemistry 282: 22930-22938

Kopriva S, Koprivova A (2004) Plant adenosine 5 '-phosphosulphate reductase: the past, the present, and the future Annual Meeting of the Society-for-Experimental-Biology. Oxford Univ Press, Edinburgh, SCOTLAND, pp 1775-1783

Kopriva S, Mugford SG, Matthewman C, Koprivova A (2009) Plant sulfate assimilation genes: Redundancy versus specialization. Plant Cell Reports 28: 1769-1780

Kopriva S, Muheim R, Koprivova A, Trachsel N, Catalano C, Suter M, Brunold C (1999) Light regulation of assimilatory sulphate reduction in *Arabidopsis thaliana*. Plant Journal 20: 37-44

Kopriva S, Rennenberg H (2004) Control of sulphate assimilation and glutathione synthesis: Interaction with N and C metabolism. Journal of Experimental Botany 55: 1831-1842

Kopriva S, Suter M, Von Ballmoos P, Hesse H, Krähenbühl U, Rennenberg H, Brunold C (2002) Interaction of sulfate assimilation with carbon and nitrogen metabolism in Lemna minor. Plant Physiology 130: 1406-1413

Kopriva S, Wiedemann G, Reski R (2007b) Sulfate assimilation in basal land plants - What does genomic sequencing tell us? Plant Biology 9: 556-564

Koprivova A, North KA, Kopriva S (2008) Complex signaling network in regulation of adenosine 5'-phosphosulfate reductase by salt stress in *Arabidopsis* roots. Plant Physiology 146: 1408-1420

Koralewska A, Buchner P, Stuiver CEE, Posthumus FS, Kopriva S, Hawkesford MJ, De Kok LJ (2009) Expression and activity of sulfate transporters and APS reductase in

curly kale in response to sulfate deprivation and re-supply. Journal of Plant Physiology 166: 168-179
Koralewska A, Stuiver CEE, Posthumus FS, Kopriva S, Hawkesford MJ, De Kok LJ (2008) Regulation of sulfate uptake, expression of the sulfate transporters Sultr1;1 and Sultr1;2, and APS reductase in Chinese cabbage (*Brassica pekinensis*) as affected by atmospheric H2S nutrition and sulfate deprivation. Functional Plant Biology 35: 318-327
Lana A, Bell TG, Simó R, Vallina SM, Ballabrera-Poy J, Kettle AJ, Dachs J, Bopp L, Saltzman ES, Stefels J, Johnson JE, Liss PS (2011) An updated climatology of surface dimethlysulfide concentrations and emission fluxes in the global ocean. Global Biogeochemical Cycles 25
Lee BR, Koprivova A, Kopriva S (2011) The key enzyme of sulfate assimilation, adenosine 5'-phosphosulfate reductase, is regulated by HY5 in *Arabidopsis*. Plant Journal 67: 1042-1054
Letunic I, Yamada T, Kanehisa M, Bork P (2008) iPath: interactive exploration of biochemical pathways and networks. Trends in Biochemical Sciences 33: 101-103
Leustek T, Martin MN, Bick JA, Davies JP (2000) Pathways and regulation of sulfur metabolism revealed through molecular and genetic studies Annual Review of Plant Biology, pp 141-165
Lewandowska M, Sirko A (2008) Recent advances in understanding plant response to sulfur-deficiency stress. Acta Biochimica Polonica 55: 457-471
Liang G, Yang F, Yu D (2010) MicroRNA395 mediates regulation of sulfate accumulation and allocation in *Arabidopsis thaliana*. The Plant Journal 62: 1046-1057
Lindberg P, Melis A (2008) The chloroplast sulfate transport system in the green alga Chlamydomonas reinhardtii. Planta 228: 951-961
Liu H, Aris-Brosou Sp, Probert I, de Vargas C (2010) A Time line of the Environmental Genetics of the Haptophytes. Molecular Biology and Evolution 27: 161-176
Livak KJ, Schmittgen TD (2001) Analysis of relative gene expression data using real-time quantitative PCR and the 2(-delta delta C(T)) method. Methods 25: 402-408
Lovelock JE, Margulis L (1974) Homeostatic tendencies of the Earth's atmosphere. Origins of Life 5: 93-103
Lunde C, Zygadlo A, Simonsen HT, Nielsen PL, Blennow A, Haldrup A (2008) Sulfur starvation in rice: the effect on photosynthesis, carbohydrate metabolism, and oxidative stress protective pathways. Physiologia Plantarum 134: 508-521
Malin G, Wilson WH, Bratbak G, Liss PS, Mann NH (1998) Elevated production of dimethylsulfide resulting from viral infection of cultures of Phaeocystis pouchetii. Limnology and Oceanography 43: 1389-1393
Marandino CA, De Bruyn WJ, Miller SD, Saltzman ES (2008) Open ocean DMS air/sea fluxes over the eastern South Pacific Ocean. Atmospheric Chemistry and Physics
Maruyama-Nakashita A, Inoue E, Watanabe-Takahashi A, Yamaya T, Takahashi H (2003) Transcriptome profiling of sulfur-responsive genes in *Arabidopsis* reveals global effects of sulfur nutrition on multiple metabolic pathways. Plant Physiology 132: 597-605
Maruyama-Nakashita A, Nakamura Y, Tohge T, Saito K, Takahashi H (2006) *Arabidopsis* SLIM1 is a central transcriptional regulator of plant sulfur response and metabolism. Plant Cell 18: 3235-3251
Matrai PA, Keller MD (1994) Total organic sulfur and dimethylsulfoniopropionate in marine phytoplankton: Intracellular variations. Marine Biology 119: 61-68
Medlin LK, Kooistra, W. H. C. F., Potter, D., Saunders, G. W. & Andersen, R. A. (1997) Phylogenetic relationships of the "golden algae" (haptophytes, heterokont

chromophytes) and their plastids. Plant Systematic Evolution. 11 Supplement: 187-219
Medlin LK, Sáez AG, Young JR (2008) A molecular clock for coccolithophores and implications for selectivity of phytoplankton extinctions across the K/T boundary. Marine Micropaleontology 67: 69-86
Melis A, Chen HC (2005) Chloroplast sulfate transport in green algae - Genes, proteins and effects. Photosynthesis Research 86: 299-307
Møller IM, Jensen PE, Hansson A (2007) Oxidative modifications to cellular components in plants Annual Review of Plant Biology, pp 459-481
Morozova O, Hirst M, Marra MA (2009) Applications of new sequencing technologies for transcriptome analysis Annual Review of Genomics and Human Genetics, pp 135-151
Moseley JL, Gonzalez-Ballester D, Pootakham W, Bailey S, Grossman AR (2009) Genetic interactions between regulators *Chlamydomonas* phosphorus and sulfur deprivation responses. Genetics 181: 889-905
Mugford SG, Lee B-R, Koprivova A, Matthewman C, Kopriva S (2010) Control of sulfur partitioning between primary and secondary metabolism. The Plant Journal 65: 96-105
Neuenschwander U, Suter M, Brunold C (1991) Regulation of sulfate assimilation by light and O-acetyl-l-serine in lemna minor L. Plant Physiology 97: 253-258
Nguyen AV, Thomas-Hall SR, Malnoë A, Timmins M, Mussgnug JH, Rupprecht J, Kruse O, Hankamer B, Schenk PM (2008) Transcriptome for photobiological hydrogen production induced by sulfur deprivation in the green alga Chlamydomonas reinhardtii. Eukaryotic Cell 7: 1965-1979
Niki T, Kunugi M, Otsuki A (2000) DMSP-lyase activity in five marine phytoplankton species: Its potential importance in DMS production. Marine Biology 136: 759-764
Niki T, Shimizu M, Fujishiro A, Kinoshita J (2007) Effects of salinity downshock on dimethylsulfide production. Journal of Oceanography 63: 873-877
Nikiforova V, Freitag J, Kempa S, Adamik M, Hesse H, Hoefgen R (2003) Transcriptome analysis of sulfur depletion in *Arabidopsis thaliana*: Interlacing of biosynthetic pathways provides response specificity. Plant Journal 33: 633-650
Nikiforova VJ, Bielecka M, Gakière B, Krueger S, Rinder J, Kempa S, Morcuende R, Scheible WR, Hesse H, Hoefgen R (2006) Effect of sulfur availability on the integrity of amino acid biosynthesis in plants. Amino Acids 30: 173-183
Nikiforova VJ, Daub CO, Hesse H, Willmitzer L, Hoefgen R (2005a) Integrative gene-metabolite network with implemented causality deciphers informational fluxes of sulphur stress response. Journal of Experimental Botany 56: 1887-1896
Nikiforova VJ, Kopka J, Tolstikov V, Fiehn O, Hopkins L, Hawkesford MJ, Hesse H, Hoefgen R (2005b) Systems rebalancing of metabolism in response to sulfur deprivation, as revealed by metabolome analysis of *Arabidopsis* plants. Plant Physiology 138: 304-318
Nishiguchi MK, Somero GN (1992) Temperature- and concentration-dependence of compatibility of the organic osmolyte β-dimethylsulfoniopropionate. Cryobiology 29: 118-124
Noctor G, Foyer CH (1998) Ascorbate and Glutathione: Keeping Active Oxygen under Control Annual Review of Plant Biology, pp 249-279
Okada H, Honjo S (1973) The distribution of oceanic coccolithophorids in the Pacific. Deep Sea Res 20: 355-374
Okada H, Honjo S (1975) Distribution of coccolithophores in marginal seas along the western Pacific Ocean and in the Red Sea. Marine Biology 31: 271-285

Otte ML, Wilson G, Morris JT, Moran BM (2004) Dimethylsulphoniopropionate (DMSP) and related compounds in higher plants. Journal of Experimental Botany 55: 1919-1925

Paasche E (1967) Marine plankton algae grown wiyh light-dark cycles. I. *Coccolithus huxleyi*. Physiologia Plantarum 20: 946-&

Paasche E (2001) A review of the coccolithophorid *Emiliania huxleyi* (prymnesiophyceae), with particular reference to growth, coccolith formation, and calcification-photosynthesis interactions. Phycologia 40: 503-529

Pagarete A, Le Corguillé G, Tiwari B, Ogata H, de Vargas C, Wilson WH, Allen MJ (2011) Unveiling the transcriptional features associated with coccolithovirus infection of natural *Emiliania huxleyi* blooms. FEMS Microbiology Ecology 78: 555-564

Parker MS, Mock T, Armbrust EV (2008) Genomic insights into marine microalgae Annual Review of Genetics, pp 619-645

Patron NJ, Durnford DG, Kopriva S (2008) Sulfate assimilation in eukaryotes: Fusions, relocations and lateral transfers. BMC Evolutionary Biology 8

Polle A, Rennenberg H (1992) Field studies on Norway spruce trees at high altitudes: II. Defence systems against oxidative stress in needles. New Phytologist 121: 635-642

Pootakham W, Gonzalez-Ballester D, Grossman AR (2010) Identification and regulation of plasma membrane sulfate transporters in *Chlamydomonas*. Plant Physiology 153: 1653-1668

Puerta MVS, Bachvaroff TR, Delwiche CF (2005) The complete plastid genome sequence of the haptophyte Emiliania huxleyi: A comparison to other plastid genomes. DNA Research 12: 151-156

Quinn P, Bowers RM, Zhang X, Wahlund TM, Fanelli MA, Olszova D, Read BA (2006) cDNA microarrays as a tool for identification of biomineralization proteins in the coccolithophorid *Emiliania huxleyi* (Haptophyta). Applied and Environmental Microbiology 72: 5512-5526

Raffi I, Backman J, Fornaciari E, Pälike H, Rio D, Lourens L, Hilgen F (2006) A review of calcareous nannofossil astrobiochronology encompassing the past 25 million years. Quaternary Science Reviews 25: 3113-3137

Ratti S, Knoll AH, Giordano M (2011) Did sulfate availability facilitate the evolutionary expansion of chlorophyll a+c phytoplankton in the oceans? Geobiology 9: 301-3012

Ravina CG, Barroso C, Vega JM, Gotor C (1999) Cysteine biosynthesis in *Chlamydomonas reinhardtii*. Molecular cloning and regulation of O-acetylserine(thiol)lyase. European Journal of Biochemistry 264: 848-853

Ravina CG, Chang CI, Tsakraklides GP, McDermott JP, Vega JM, Leustek T, Gotor C, Davies JP (2002) The sac mutants of *Chlamydomonas reinhardtii* reveal transcriptional and posttranscriptional control of cysteine biosynthesis. Plant Physiology 130: 2076-2084

Reinfelder JR (2011) Carbon concentrating mechanisms in eukaryotic marine phytoplankton. Annual review of marine science 3: 291-315

Rennenberg H (1980) Glutathione metabolism and possible biological roles in higher plants. Phytochemistry 21: 2771-2781

Richier S, Fiorini S, Kerros ME, von Dassow P, Gattuso JP (2010) Response of the calcifying coccolithophore *Emiliania huxleyi* to low pH/high pCO_2: from physiology to molecular level. Marine Biology: 1-10

Richier S, Kerros ME, De Vargas C, Haramaty L, Falkowski PG, Gattuso JP (2009) Light-dependent transcriptional regulation of genes of biogeochemical interest in the

diploid and haploid life cycle stages of *Emiliania huxleyi*. Applied and Environmental Microbiology 75: 3366-3369

Roelofs GJ, Lelieveld J, Ganzeveld L (1998) Simulation of global sulfate distribution and the influence of effective cloud drop radii with a coupled photochemistry-sulfur

Rokitta SD, de Nooijer LJ, Trimborn S, de Vargas C, Rost B, John U (2011) Transcriptome analyses reveal differential gene expression patterns between the life-cycle stages of *Emiliania huxleyi* (haptophyta) and reflect specialization to different ecological niches. Journal of Phycology 47: 829-838

Rouhier N, Lemaire SpD, Jacquot J-P (2008) The Role of Glutathione in Photosynthetic Organisms: Emerging Functions for Glutaredoxins and Glutathionylation. Annual Review of Plant Biology 59: 143-166

Russo G, Zegar C, Giordano A (2003) Advantages and limitations of microarray technology in human cancer. Oncogene 22: 6497-6507

Sánchez Puerta MV, Bachvaroff TR, Delwiche CF (2004) The complete mitochondrial genome sequence of the haptophyte Emiliania huxleyi and its relation to heterokonts. DNA Research 11: 1-10

Schmidt A (1973) Sulfate reduction in a cell free system of *Chlorella*. The ferredoxin dependent reduction of a protein bound intermediate by a thiosulfonate reductase. Arch. Mikrobiol. 93: 29-52

Schroeder DC, Oke J, Malin G, Wilson WH (2002) Coccolithovirus (*Phycodnaviridae*): Characterisation of a new large dsDNA algal virus that infects *Emiliania huxleyi*. Archives of Virology 147: 1685-1698

Schupp R, Rennenberg H (1988) Diurnal changes in the glutathione content of spruce needles (Picea Abies L.). Plant Science 57: 113-117

Shewry PR, Zhao FJ, Gowa GB, Hawkins ND, Ward JL, Beale MH, Halford NG, Parry MA, Abécassis J (2009) Sulphur nutrition differentially affects the distribution of asparagine in wheat grain. Journal of Cereal Science 50: 407-409

Shibagaki N, Grossman A (2008) The State of Sulfur Metabolism in Algae: From Ecology to Genomics. In: Hell R, Dahl C, Knaff D, Leustek T (eds) Sulfur Metabolism in Phototrophic Organisms. Springer Netherlands, pp 231-267

Stefels J (2000) Physiological aspects of the production and conversion of DMSP in marine algae and higher plants. Journal of Sea Research 43: 183-197

Stefels J, Steinke M, Turner S, Malin G, Belviso S (2007) Environmental constraints on the production and removal of the climatically active gas dimethylsulphide (DMS) and implications for ecosystem modelling. Biogeochemistry 83: 245-275

Steinke M, Malin G, Liss PS (2002) Trophic interactions in the sea: An ecological role for climate relevant volatiles? Journal of Phycology 38: 630-638

Steinke M, Malin G, Turner SM, Liss PS (2000) Determinations of dimethylsulphoniopropionate (DMSP) lyase activity using headspace analysis of dimethylsulphide (DMS). Journal of Sea Research 43: 233-244

Steinke M, Wolfe GV, Kirst GO (1998) Partial characterisation of dimethylsulfoniopropionate (DMSP) lyase isozymes in 6 strains of Emiliania huxleyi. Marine Ecology-Progress Series 175: 215-225

Storey JD, Tibshirani R (2003) Statistical significance for genomewide studies. Proceedings of the National Academy of Sciences of the United States of America 100: 9440-9445

Sugimoto K, Sato N, Tsuzuki M (2007) Utilization of a chloroplast membrane sulfolipid as a major internal sulfur source for protein synthesis in the early phase of sulfur starvation in *Chlamydomonas reinhardtii*. FEBS Letters 581: 4519-4522

Sugimoto K, Tsuzuki M, Sato N (2010) Regulation of synthesis and degradation of a sulfolipid under sulfur-starved conditions and its physiological significance in *Chlamydomonas reinhardtii*. New Phytologist 185: 676-686

Sukhanova IN, Flint MV (1998) Anomalous blooming of coccolithophorids over the eastern Bering Sea shelf. Oceanology 38: 502-505

Sunda W, Kieber DJ, Kiene RP, Huntsman S (2002) An antioxidant function for DMSP and DMS in marine algae. Nature 418: 317-320

Suttle CA (1992) Inhibition of photosynthesis in phytoplankton by the submicron size fraction concentrated from seawater. Marine Ecology Progress Series 87: 105-112

Takahashi H (2010) Regulation of sulfate transport and assimilation in plants International Review of Cell and Molecular Biology, pp 129-159

Takahashi H, Braby CE, Grossman AR (2001) Sulfur economy and cell wall biosynthesis during sulfur limitation of *Chlamydomonas reinhardtii*. Plant Physiology 127: 665-673

Takahashi H, Watanabe-Takahashi A, Smith FW, Blake-Kalff M, Hawkesford MJ, Saito K (2000) The roles of three functional sulphate transporters involved in uptake and translocation of sulphate in *Arabidopsis thaliana*. Plant Journal 23: 171-182

Takahashi H, Yamazaki M, Sasakura N, Watanabe A, Leustek T, De Almeida Engler J, Engler G, Van Montagu M, Saito K (1997) Regulation of sulfur assimilation in higher plants: A sulfate transporter induced in sulfate-starved roots plays a central role in *Arabidopsis thaliana*. Proceedings of the National Academy of Sciences of the United States of America 94: 11102-11107

Takahashi H, Yamazaki M, Sasakura N, Watanabe A, Leustek T, De Almeida Engler J, Engler G, Van Montagu M, Saito K (1997) Regulation of sulfur assimilation in higher plants: A sulfate transporter induced in sulfate-starved roots plays a central role in *Arabidopsis thaliana*. Proceedings of the National Academy of Sciences of the United States of America 94: 11102-11107

Tatusov RL, Fedorova ND, Jackson JD, Jacobs AR, Kiryutin B, Koonin EV, Krylov DM, Mazumder R, Smirnov S, Nikolskaya AN, Rao BS, Mekhedov SL, Sverlov AV, Vasudevan S, Wolf YI, Yin JJ, Natale DA (2003) The COG database: An updated vesion includes eukaryotes. BMC Bioinformatics 4

Taylor BF (1993) Bacterial transformations of organic sulfur compounds in marine environments. In: Oremland RS (ed) 10th International Symp on Environmental Biogeochemistry. Chapman & Hall, San Francisco, Ca, pp 745-781

Thierstein HR, Geitzenauer KR, Molfino B, Shackleton NJ (1977) Global synchroneity of late Quaternary coccolith datum levels Validation by oxygen isotopes. Geology 5: 400-404

Todd JD, Curson ARJ, Nikolaidou-Katsaraidou N, Brearley CA, Watmough NJ, Chan Y, Page PCB, Sun L, Johnston AWB (2010) Molecular dissection of bacterial acrylate catabolism - unexpected links with dimethylsulfoniopropionate catabolism and dimethyl sulfide production. Environmental Microbiology 12: 327-343

Todd JD, Rogers R, Li YG, Wexler M, Bond PL, Sun L, Curson ARJ, Malin G, Steinke M, Johnston AWB (2007) Structural and regulatory genes required to make the gas dimethyl sulfide in bacteria. Science 315: 666-669

Turner SM, Malin G, Liss PS, Harbour DS, Holligan PM (1988) The seasonal variation of dimethyl sulfide and dimethylsulfoniopropionate concentrations in nearshore waters. Limnology & Oceanography 33: 364-375

Vairavamurthy A, Andreae, M. O. and Iverson, R. L. (1985) Biosynthesis of dimethylsulfide and dimethylpropiothein by *Hymenomonas carterae* in relation to sulfur source and salinity variations. Limnol. Oceanogr. 30: 59-70

Van Bergeijk SA, Schönefeldt K, Stal LJ, Huisman J (2002) Production and consumption of dimethylsulfide (DMS) and dimethylsulfoniopropionate (DMSP) in a diatom-dominated intertidal sediment. Marine Ecology Progress Series 231: 37-46

Van Mooy BAS, Rocap G, Fredricks HF, Evans CT, Devol AH (2006) Sulfolipids dramatically decrease phosphorus demand by picocyanobacteria in oligotrophic marine environments. Proceedings of the National Academy of Sciences of the United States of America 103: 8607-8612

van Rijssel M, Gieskes WWC (2002) Temperature, light, and the dimethylsulfoniopropionate (DMSP) content of *Emiliania huxleyi* (Prymnesiophyceae). Journal of Sea Research 48: 17-27

Vauclare P, Kopriva S, Fell D, Suter M, Sticher L, Von Ballmoos P, Krähenbühl U, Op Den Camp R, Brunold C (2002) Flux control of sulphate assimilation in *Arabidopsis thaliana*: Adenosine 5'-phosphosulphate reductase is more susceptible than ATP sulphurylase to negative control by thiols. Plant Journal 31: 729-740

Vila-Costa M, Rinta-Kanto JM, Sun S, Sharma S, Poretsky R, Moran MA (2010) Transcriptomic analysis of a marine bacterial community enriched with dimethylsulfoniopropionate. ISME Journal 4: 1410-1420

Vogt M, Steinke M, Turner S, Paulino A, Meyerho?fer M, Riebesell U, LeQue?re C, Liss P (2007) Dynamics of dimethylsulphoniopropionate and dimethylsulphide under different CO2 concentrations during a mesocosm experiment. Biogeosciences Discussions 4: 3673-3699

Von Dassow P, Ogata H, Probert I, Wincker P, Da Silva C, Audic S, Claverie JM, de Vargas C (2009) Transcriptome analysis of functional differentiation between haploid and diploid cells of *Emiliania huxleyi*, a globally significant photosynthetic calcifying cell. Genome biology 10

Wahlund TM, Hadaegh AR, Clark R, Nguyen B, Fanelli M, Read BA (2004) Analysis of expressed sequence tags from calcifying cells of marine coccolithophorid (*Emiliania huxleyi*). Marine Biotechnology 6: 278-290

Weiss M, Haimovich Gal, Pick Uri (2001) Phosphate and sulfate uptake in the halotolerant alga *Dunaliella* are driven by Na+-symport mechanism. Journal of Plant Physiology 158: 1519-1525

Welsh DT (2000) Ecological significance of compatible solute accumulation by micro-organisms: From single cells to global climate. FEMS Microbiology Reviews 24: 263-290

Westbroek P, Brown CW, Bleijswijk Jv, Brownlee C, Brummer GJ, Conte M, Egge J, Fernández E, Jordan R, Knappertsbusch M, Stefels J, Veldhuis M, van der Wal P, Young J (1993) A model system approach to biological climate forcing. The example of *Emiliania huxleyi*. Global and Planetary Change 8: 27-46

Wingenter OW, Haase KB, Zeigler M, Blake DR, Rowland FS, Sive BC, Paulino A, Thyrhaug R, Larsen A, Schulz K, Meyerhöfer M, Riebesell U (2007) Unexpected consequences of increasing CO2 and ocean acidity on marine production of DMS and CH2ClI: Potential climate impacts. Geophysical Research Letters 34

Winter A, Jordan RW, Roth PH (1994) Biogeography of living coccolithophores in ocean waters. Coccolithophores: 161-177

Wolfe GV, Steinke M (1996) Grazing-activated production of dimethyl sulfide (DMS) by two clones of *Emiliania huxleyi*. Limnology and Oceanography 41: 1151-1160

Wolfe GV, Steinke M, Kirst GO (1997) Grazing-activated chemical defence in a unicellular marine alga. Nature 387: 894-897

Wolfe GV, Strom SL, Holmes JL, Radzio T, BradyOlson M (2002) Dimethylsulfoniopropionate cleavage by marine phytoplankton in response to mechanical, chemical, or dark stress. Journal of Phycology 38: 948-960

Wykoff DD, Davies JP, Melis A, Grossman AR (1998) The regulation of photosynthetic electron transport during nutrient deprivation in *Chlamydomonas reinhardtii*. Plant Physiology 117: 129-139

Yatusevich R, Mugford SG, Matthewman C, Gigolashvili T, Frerigmann H, Delaney S, Koprivova A, Flügge UI, Kopriva S (2010) Genes of primary sulfate assimilation are part of the glucosinolate biosynthetic network in *Arabidopsis thaliana*. Plant Journal 62: 1-11

Yildiz FH, Davies JP, Grossman AR (1994) Characterization of sulfate transport in *Chlamydomonas reinhardtii* during sulfur-limited and sulfur-sufficient growth. Plant Physiology 104: 981-987

Yoshimoto N, Inoue E, Watanabe-Takahashi A, Saito K, Takahashi H (2007) Posttranscriptional regulation of high-affinity sulfate transporters in Arabidopsis by sulfur nutrition. Plant Physiology 145: 378-388

Young JR, Henriksen K (2003) Biomineralization Within Vesicles: The Calcite of Coccoliths. Reviews in Mineralogy and Geochemistry 54: 189-215

Yu B, Xu C, Benning C (2002) *Arabidopsis* disrupted in SQD2 encoding sulfolipid synthase is impaired in phosphate-limited growth. Proceedings of the National Academy of Sciences of the United States of America 99: 5732-5737

Zhang Z, Shrager J, Jain M, Chang CW, Vallon O, Grossman AR (2004) Insights into the survival of *Chlamydomonas reinhardtii* during sulfur starvation based on microarray analysis of gene expression. Eukaryotic Cell 3: 1331-1348